

9-24-93
E-6566

NASA Technical Memorandum 103740

Interaction of Two Glancing, Crossing Shock Waves With a Turbulent Boundary-Layer at Various Mach Numbers

Warren R. Hingst
Lewis Research Center
Cleveland, Ohio

and

Kevin E. Williams
University of Washington
Seattle, Washington

September 1991



Interaction of Two Glancing, Crossing Shock Waves with a Turbulent Boundary-Layer at Various Mach Numbers

Warren R. Hingst

National Aeronautics and Space Administration
Lewis Research Center
Cleveland, Ohio 44135

Kevin E. Williams

University of Washington
Seattle, Washington 98195

ABSTRACT

A preliminary experimental investigation was conducted to study two crossing, glancing shock waves of equal strengths, interacting with the boundary-layer developed on a supersonic wind tunnel wall. This study was performed at several Mach numbers between 2.5 and 4.0. The shock waves were created by fins (shock generators), spanning the tunnel test section, that were set at angles varying from 4 to 12 degrees. The data acquired in this investigation are wall static pressure measurements, and qualitative information in the form of oil flow and schlieren visualizations. The principle aim of this study is two-fold. First, a fundamental understanding of the physics underlying this flow phenomena is desired. Also, a comprehensive data set is needed for computational fluid dynamic code validation. Results of this study indicate that for small shock generator angles, the boundary-layer remains attached throughout the flow field. However, with increasing shock strengths (increasing generator angles), boundary-layer separation does occur and becomes progressively more severe as the generator angles are increased further. The location of the separation, which starts well downstream of the shock crossing point, moves upstream as shock strengths are increased. At the highest generator angles, the separation appears to begin coincident with the generator leading edges and engulfs most of the area between the generators. This phenomena occurs very near the 'unstart' limit for the generators. The wall pressures at the lower generator angles are nominally consistent with the flow geometries (i.e. shock patterns) although significantly affected by the boundary-layer upstream influence. As separation occurs, the wall pressures exhibit a gradient that is mainly axial in direction in the vicinity of the separation. At the limiting conditions the wall pressure gradients are primarily in the axial direction throughout.

Nomenclature

α	Shock Generator Angle From The Tunnel Centerline
δ	Actual Boundary Layer Thickness
δ_{NOM}	Nominal Boundary Layer Thickness (2.54 cm)
δ^*	Displacement Thickness
θ	Momentum Thickness
M	Nominal Mach Number
M_{ACT}	Actual Mach Number
P	Local Wall Static Pressure
P_T	Total Pressure
P_{TS}	Average Tunnel Static Pressure
Re/m	Reynolds Number Per Unit Meter
T_T	Total Temperature
U	Local Velocity
U_e	Free Stream Velocity
X	Streamwise Coordinate Relative to the Wind Tunnel Nozzle Exit
X^*	Streamwise Coordinate Relative to the Inviscid Shock Crossing Location on the Tunnel Centerline
Y	Transverse Coordinate
Z	Spanwise Coordinate

INTRODUCTION

The shock wave/boundary-layer interaction phenomenon has long been recognized as a critical problem in fluid dynamics. The strong pressure gradients, three-dimensional flows, and flow separations associated with these interactions can have significant effects, both on the fluid dynamics and the bounding surface. In the flow, the shock wave/boundary-layer interaction can be the source of flow distortions leading to performance degradation of aerodynamic components such as inlets and nozzles. The interactions also result in high aeroacoustic and aerothermal loads that could be a design constraint on affected flow components. The high gradients in surface transport properties in the interaction region produce thermal stresses in the surface. These stresses, combined with the fluctuating pressures, can cause early failure of propulsion components. Therefore, the understanding of these phenomena is critical from both the aerodynamics and the structures standpoint.

One important class of shock/boundary-layer interactions is the glancing shock/turbulent boundary-layer interaction. These three-dimensional interactions occur in many practical applications and are at times referred to as fin interactions. These applications include supersonic inlets, nozzle flows and supersonic combustors. In addition to understanding the flow physics involved in these interactions, there is a need for data of sufficient detail and accuracy to validate computational fluid dynamic (CFD) methods. These oblique interactions, which are reviewed in reference [1], with their strong pressure gradients, transport property gradients and compressibility effects, are particularly difficult cases for computational techniques.

This investigation focuses on a particular class of the glancing sidewall interaction, that of the crossing shocks. Shown schematically in figure 1, this experimental configuration has the potential to provide good validation data for CFD methods. With a uniform approach boundary-layer, the boundary conditions are relatively simple and well defined. In addition, for equal shock strengths the flow has a plane of symmetry reducing the required calculation volume. By varying the shock strengths, the interaction can be varied from weak to strong enough to cause separation. The separated cases provide a particularly interesting test for CFD validation since the separation is not fixed by the geometry. Therefore, the CFD method must not only calculate separated flow but must be able to predict the location of the separation.

This crossing shock flow geometry was initially investigated at Mach 2.0 as reported in reference [2]. Additional experiments have been conducted at Mach 3.0 as reported in references [3] and [4]. In the present investigation data were obtained at Mach numbers of 2.5, 3.0, 3.5 and 4.0, and at Reynolds numbers per meter ranging from 1.3 to 1.7 million. Here, and in other locations in this report, the Mach numbers referred to will be nominal values. The actual Mach numbers of the test conditions are given in a table of run conditions. This investigation is restricted to equal shock strengths resulting in flow symmetry about the centerline. Shock generator angles investigated are in the range of 4 to 12 degrees. The shock generator angles referred to are the actual angle relative to the free stream flow, not an effective angle that attempts to include the effect of the boundary-layer buildup on the shock generator. These conditions represent shock strengths that would exist in typical supersonic inlet designs or adjacent struts in supersonic internal flows. This report presents data from an initial experimental investigation that include flow visualization and surface static pressure measurements. Subsequent investigations will extend these measurements to include unsteady surface pressures, surface transport and flow field surveys. These results will be presented in later publications.

EXPERIMENTAL APPROACH

Facility:

The experimental investigation was conducted in the NASA Lewis Research Center's 1'x1' supersonic wind tunnel. This continuous running wind tunnel has a Mach number range of 1.3 to 4.0. Tunnel total pressures can be varied from 1 to 3 atmospheres giving a unit Reynolds number of 1.2 to 2.4 million per meter. The tunnel test section, where the measurements are made, is 30.5 x 30.5 centimeters. A more detailed description of the tunnel is given in reference [5]. An illustration of the tunnel is shown in figure 2.

Experimental Configuration:

The crossing shock/boundary-layer experiment is configured by using two shock generator plates that span the tunnel test section. The 20.3 cm long shock generators, when at angle of attack to the free stream tunnel flow, produce oblique

shocks. The intersection of these shocks with the naturally occurring boundary-layer on the tunnel walls defines the experiment. The boundary-layer, which effectively begins at the nozzle throat, is not subjected to cross flow pressure gradients in the nozzle and can therefore be characterized as uniform and in equilibrium. In this respect the present investigation is more closely related to that of reference [2], which also used the tunnel wall boundary-layer. The experiment of references [3] and [4] mounted the shock generators in a box that generated new boundary-layers on the sidewalls. This configuration would result in thinner boundary-layers than using the tunnel sidewall boundary-layers.

A photograph of the experimental configuration mounted in the wind tunnel is shown in figure 3. Both shock generators shown in the photograph can be actuated to change the angle of attack while the tunnel is operating. The tunnel was started with the generators set at low angles and then the angles were increased to a given test condition. Therefore, the problems associated with starting the tunnel with significant blockage were eliminated. The influence of the expansion from the shock generators trailing edges effectively ends the simple interaction region. A more complicated multiple interaction problem continues downstream. This investigation focuses only on the simple interaction region. A second set of longer (25.4 cm) shock generators were not tested because of time limitations for this initial tunnel entry. These generators would have been suited for the higher Mach numbers, where the shock waves cross further downstream, and will be used for future investigations

Instrumentation and Experimental Technique:

This investigation utilizes both qualitative measurement techniques and quantitative instrumentation. The qualitative measurements included schlieren and surface oil flow visualization. Schlieren, which visually shows the flow density gradients, provides an integrated two-dimensional picture representative of the free stream flow. By contrast, the surface oil flow visualization indicates what is happening very close to the surface. The combination of these techniques is useful for diagnosing shock boundary-layer interactions.

The schlieren system in this wind tunnel facility is of conventional design. This system could be operated both with a knife edge for monochromatic or with a color band for color schlieren. The system was set up parallel to the Y axis, yielding a view 'down' on the shock generators. Schlieren from this view will not show shocks, compressions or expansions caused by the boundary-layer

interactions. Therefore, the primary function of these schlieren visualizations is to establish the behavior of the inviscid shocks.

The surface oil flow visualization utilized a petroleum based oil with a SAE viscosity rating of 140. This was mixed with a fluorescent dye. The resulting surface oil patterns were illuminated with UV light and photographed. This technique highlights the oil flow while suppressing the wall reflections. For this investigation, the oil was applied to the schlieren windows allowing the result of the visualization to be recorded either while the tunnel was running (by video camera) or after shutdown (by still frame camera). Some difficulty was experienced in maintaining the oil flow pattern where separation was present during tunnel shutdown due to the normal shock that swept past as the tunnel 'unstarted.' In these cases, the results were obtained from an on-line video recording and subsequent digitalization of specific frames of the video tape. A more detailed description of the oil flow technique is given in reference [6]. This technique is useful for determining the upstream influence of the interaction as well as indicating boundary-layer separations. However, these results can be misleading in determining the extent of the separation because the oil itself can influence the extent of separation. In addition, the oil flow technique gives no information of the unsteady behavior of the shock or separation. This technique indicates conditions and locations where other instrumentation should be used to provide more definitive measurements.

Quantitative measurements included surface static pressures, and upstream boundary-layer documentation. The surface static pressure measurements were done sequentially with an instrumented wall insert. This insert had 80 surface static taps. The static taps were distributed unsymmetrically on the insert and the insert was mounted off the midpoint of the tunnel sidewall. Therefore, by using a combination of four orientations of the tunnel sidewall and the instrumented insert, a total of 320 surface pressure locations were available. However, taps that were covered by or outside of the shock generators were not used, thus reducing the number of functional locations. The total number of functional taps varied depending on the shock generator angles. Since the tunnel flow conditions are well controlled between data surveys, the results of the four insert/sidewall orientations can be combined into a single representation of the flow phenomena. An illustration of the surface pressure measurement locations is shown in figure 4 for generator angles of 4 and 12 degrees.

The upstream boundary-layer was measured for each Mach number. The

wall static pressure was measured and combined with a series of Pitot pressure measurements taken from the wall into the free stream flow. The Pitot probe was electrically isolated from the tunnel wall. By using an electrical touch control, the distance of the Pitot probe from the tunnel wall was accurately determined. From these measurements, and assuming a temperature profile based on the adiabatic Crocco relation with a recovery factor of 0.89, the velocity profiles at a location 11.43 cm downstream of the nozzle exit (nominally 10.0 cm upstream from the shock generator leading edges) were determined for each flow condition.

EXPERIMENTAL RESULTS

Qualitative Results:

These results include the schlieren and surface oil flow visualization techniques. Figures 5(a) and (b) show the schlieren visualization results for Mach 3.5 and generator angles of 6 and 12 degrees. Although schlieren results were obtained at all conditions, these photographs are representative. In these photographs, the oblique shocks that originate at the leading edge of the shock generators are seen traversing across the windows of the wind tunnel test section. The two shocks cross on the tunnel centerline and exit downstream of the shock generators. The apparent broadening of the incoming shock is a result of the shock being affected by the boundary-layer on the windows.

Figure 6 shows the schlieren visualization result for Mach 2.5 and generator angles of 9 degrees. In this case, the shocks now intersect and then impinge on the generators. This appears to be closely related to the limiting case for maintaining supersonic flow between the shock generators. That is, any additional increase in the shock generator angles causes the model to 'unstart' and produces a normal shock ahead of the shock generators.

Unlike the schlieren results, the surface oil flow visualization was limited to Mach 3.5. The limited tunnel test time available for this initial investigation did not allow for extensive surface oil flow visualization. Figure 7 shows the surface oil flow for Mach 3.5 and a shock generator angles of 6 and 10 degrees.

In figure 7(a), the oil flow shows the shock/boundary-layer interaction for the shock generators at 6 degrees. Some migration of the oil toward the plane of symmetry is noted at this angle, although no separation is indicated. With the generators increased to 10 degrees, figure 7(b), the flow pattern indicates a

separation on the plane of symmetry and slightly downstream of the inviscid shock crossing location. From the on-line video of the oil visualization, oil was seen to be transported upstream in the separated region, indicating reversed flow.

Quantitative Results:

One of the objectives of this investigation is to provide data for CFD code validation. Therefore, in addition to the geometric information, the upstream boundary-layer conditions are presented to provide the inflow conditions to the computational domain. In figure 8, the initial boundary-layer profiles are presented for Mach numbers 2.5, 3.0, 3.5 and 4.0 respectively. Table 1 presents numerical information on the boundary-layers.

The majority of the quantitative data reported here consist of the tunnel wall static pressure distributions for the various test conditions. These conditions include Mach numbers of 2.5, 3.0, 3.5, and 4.0. Shock generator angles were varied from 4.0 degrees to 12.0 degrees. The maximum angle for each Mach number was determined by the model unstart characteristics. The tunnel conditions and shock generator geometry for each test condition are given in tables 2 and 3, respectively.

The results of these measurements are presented in figures 9 through 12 and in tabular form in table 4. These results are shown as both contour and surface plots of normalized wall pressures as a function of spatial location. The pressures were normalized with respect to the tunnel static pressure measured at the side walls upstream of the interactions. Therefore, a value of 1.0 would represent a normalized static pressure in undisturbed flow. The streamwise location is normalized with a nominal undisturbed boundary-layer thickness of 2.54 cm. The actual boundary-layer thickness for each case, which varied slightly with tunnel conditions, is given in table 1. In all cases the measurements are included at locations upstream and downstream of the shock generators.

Some general comments on the results can be made. For all Mach numbers and shock generator angles, the pressures are very symmetric about the tunnel centerline. This observation along with the apparent symmetry of the schlieren and oil flow visualizations indicates accurately matched generator angles and a well behaved interaction. For CFD validation, assumed flow symmetry is well supported by these results. Pressures also tended to be smooth and continuous even over combinations of different wall/insert orientations. This continuity

between surveys also indicates a well behaved interaction as well as repeatability of the experimental approach.

Figure 9 presents a detailed examination of the wall static pressure results for Mach number 2.5 test conditions. This includes shock generator angles of 4, 6, 8, and 9 degrees. The results for the 4 degree case, figure 9(a), show a pressure gradient that nominally follows the initial inviscid shock (indicated by the dot-dash line) but begins upstream of the inviscid shock due to the influence of the boundary-layer. These gradients merge at the centerline to produce an initial pressure rise substantially upstream of the inviscid shock crossing point. The pressure near the shock generators becomes relatively constant after the first shock but well upstream of the reflected shock, resulting in a lag behind the centerline pressures. Further downstream, the gradient near the shock generators increases until the pressure becomes near that of the centerline. At this point the pressure rise becomes more one-dimensional in appearance with little variation between the shock generators. This continues until the effect of the expansion waves from the trailing edges of the shock generators begins influencing the measurements, reestablishing two-dimensional gradients at the wall.

The results are similar for higher shock generator angles. However, the location where the pressure rise becomes nominally one-dimensional moves forward until at the 9 degree case, figure 9(g), the region has moved forward of the inviscid shock crossing point. The upstream influence of the interaction does not show substantial forward movement, with respect to the offset from the inviscid shock location, until the shock generators reach 9 degrees. From the results of the oil flow visualization, a substantial separation could be affecting the extent of upstream influence at this stronger interaction.

For the Mach 3.0 test condition presented in figure 10, the results are similar to those for Mach 2.5. However, for the 4 degree case, where the crossing point is further aft (due to increased Mach number) the effect of the expansion waves is evident before the pressure gradient becomes one-dimensional. As the shock generator angles are increased from 4 to 10 degrees, the pressure plots follow the trends seen in the Mach 2.5 plots. For the 11 degree case, figure 10(i), the one-dimensional pressure region has moved far forward and begins near the leading edge of the shock generators. For this condition, a severe separation appears to be present and influencing most of the flow between the generators. This would appear to be marginally stable with regard to unstarting the model. That is, any additional compression would trigger an unstart.

Looking at the results from an increase in Mach number to 3.5 in figure 11, the trends are similar to that of the Mach number of 3.0. At this Mach number the inviscid shock crossing occurs further aft relative to the shock generators (again due to the increased Mach number). The influence of the trailing expansion waves now has a more noticeable effect on the interaction. The one dimensional variation of the pressure is not observed at all until the shock generators are at 8 degrees. This continues to move upstream with increasing shock generator angle until again a limiting case is reached at 12 degrees, figure 11(i). Here the upstream influence on the pressure gradient has moved uniformly up to a line even with the leading edge of the shock generators.

The final Mach number condition tested was that of 4.0. These results are shown in figure 12. Comparing these results with those of Mach number 3.5, the two conditions look very similar. Increasing the Mach number from 3.5 to 4.0 did not allow an increase in the maximum shock generator angles before an unstart. The 12 degree case, figure 12(i), again moved the upstream influence of the shocks to the leading edge of the shock generators.

Figure 13 presents the centerline wall static pressures as a function of the distance from the inviscid shock crossing point. The centerline upstream influence moved upstream with increasing Mach number. In addition, a weaker dependence on shock generator angles is noted. In this case, the upstream influence decreases with increase in shock generator angle. This trend is more pronounced at the higher Mach number conditions. The centerline pressures for the maximum shock generator angles are conspicuous by the extent of their upstream influence. This is especially true for the 11 degree case at Mach number 3.0 and the 12 degree cases at Mach number 3.5 and 4.0 suggesting that substantial separations are responsible for these extreme influences. The pressure distributions in these latter cases have the characteristics of a two-dimensional shock/boundary-layer interaction with separation. That is, an initial pressure rise followed by a plateau region and a subsequent more substantial pressure rise.

On each plot the theoretical inviscid pressure after the crossing shocks is shown for a representative shock generator angle of 8 degrees. This shows that for the Mach number 2.5 conditions that the experimental value of static pressure peaks just at the theoretical. With increasing Mach number, the experimental value falls below the theoretical. This increasing difference is probably a result of the effect of the upstream influence of the expansion waves in the boundary-layer. Longer shock generators at the higher Mach numbers may negate this effect.

The results at Mach 2.5 compare well with those obtained at Mach number 2.0 in reference [2]. However, in none of the cases were any of the experimentally measured pressures substantially over the theoretical pressures as reported at Mach 3.0 in references [3] and [4]. This discrepancy may be due to the significantly different Reynolds numbers between experiments.

SUMMARY

A preliminary experimental investigation of two crossing sidewall shocks interacting with a supersonic tunnel wall boundary-layer was conducted over a Mach number range of 2.5 to 4.0. The investigation included a range of equal shock strengths produced by shock generators at angles from 4.0 to 12.0 degrees. The objective of the investigation was to understand the flow physics involved with these interactions and obtain data of sufficient detail and accuracy to validate computational fluid dynamic methods. The investigation utilized both qualitative and quantitative techniques to analyze the flow physics and to obtain data for computational fluid dynamic code validation. The qualitative techniques include both schlieren and surface oil flow visualization. For this preliminary investigation the quantitative measurements included documentation of the undisturbed upstream boundary-layer and wall static pressure distributions.

Results of the flow visualization show that the interaction is unseparated at the low shock generator angles. With increasing shock strength, the flow begins to form a separated region. This region grows in size and moves forward and eventually the model unstarts. The wall static pressures show a symmetrical compression that merges on the centerline upstream of the inviscid shock locations and becomes more one-dimensional downstream. The region of the one-dimensional pressure gradient moves upstream with increasing shock strengths until it coincides with the leading edge of the shock generators at the limit before model unstart. The data indicate that substantial separations are present at these limiting conditions.

Bibliography

- [1] Settles, G. S. and Dolling, D. S., "Swept Shock Wave/Boundary-Layer Interactions," in *AIAA Progress in Astronautics and Aeronautics: Tactical Missile Aerodynamics* (Hemsch, M. and Nielsen, J., eds.), pp. 297–379, AIAA, 1986.
- [2] Mee, D. J., Stalker, R. J., and Stollery, J. L., "Glancing Interactions Between Single and Intersecting Oblique Shock Waves and a Turbulent Boundary Layer," *Journal of Fluid Mechanics*, vol. 170, 1986, pp. 411–433.
- [3] Batcho, P. F., Ketchum, A. C., Bogdonoff, S. M., and Fernando, E. M., "Preliminary Study of the Interactions Caused by Crossing Shock Waves and a Turbulent Boundary Layer," Paper 89-0359, AIAA, 1989.
- [4] Poddar, K. and Bogdonoff, S. M., "A Study of Unsteadiness of Crossing Shock Turbulent Boundary Layer Interactions," Paper 90-1456, AIAA, 1990.
- [5] Skebe, S. A., *Experimental Investigation of Two Dimensional Shock Boundary Layer Interactions*. PhD thesis, Case Western Reserve University, Cleveland, Ohio, 1983.
- [6] Jurkovich, M. S., Greber, I., and Hingst, W. R., "Flow Visualization Studies of a 3-D Shock/Boundary Layer Interaction in the Presence of a Non-Uniform Approach Boundary Layer," Paper 84-1560, AIAA, 1984.

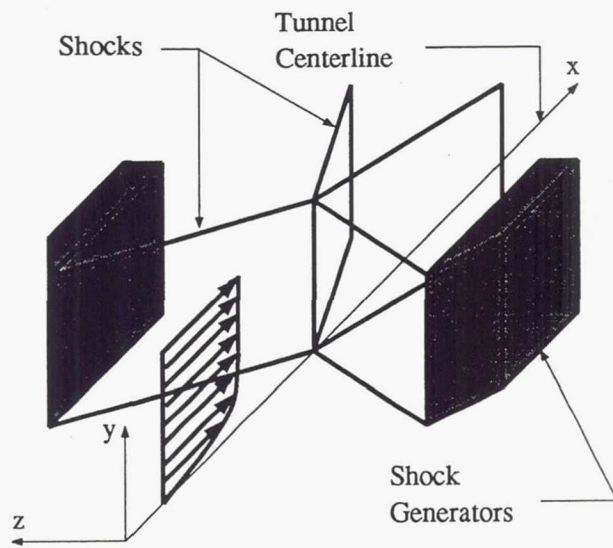


Figure 1. Shock interactions

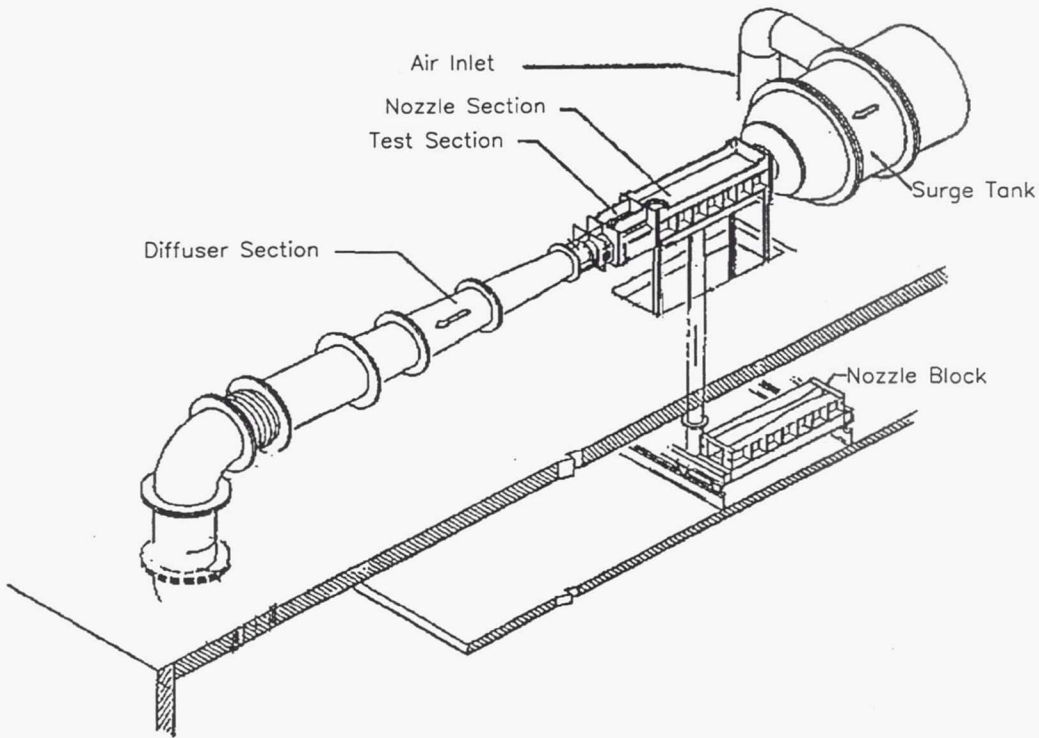


Figure 2. Tunnel schematics

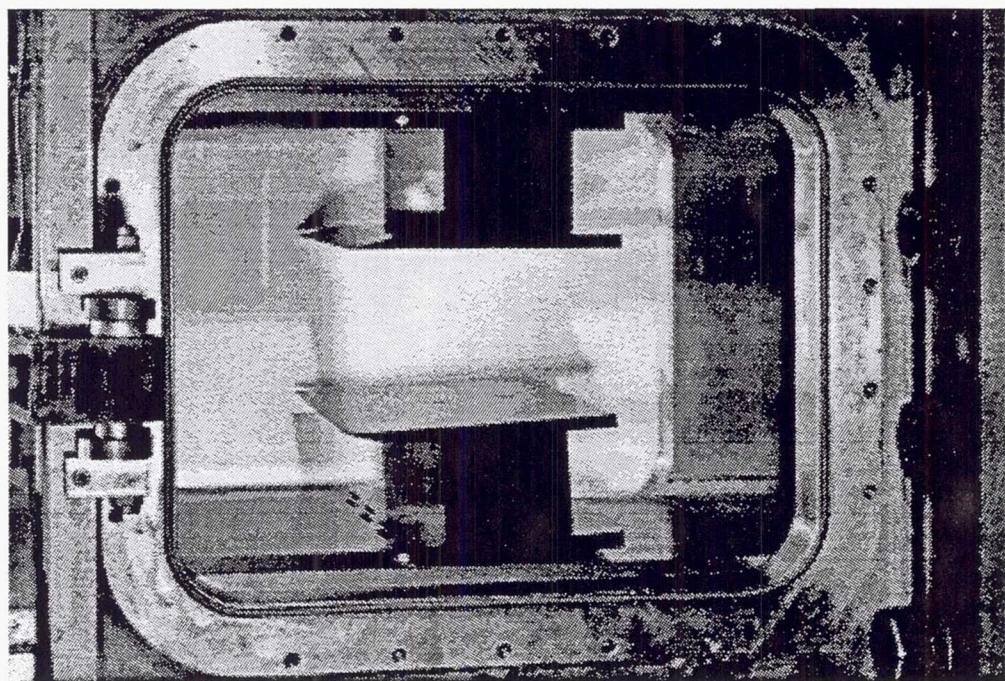
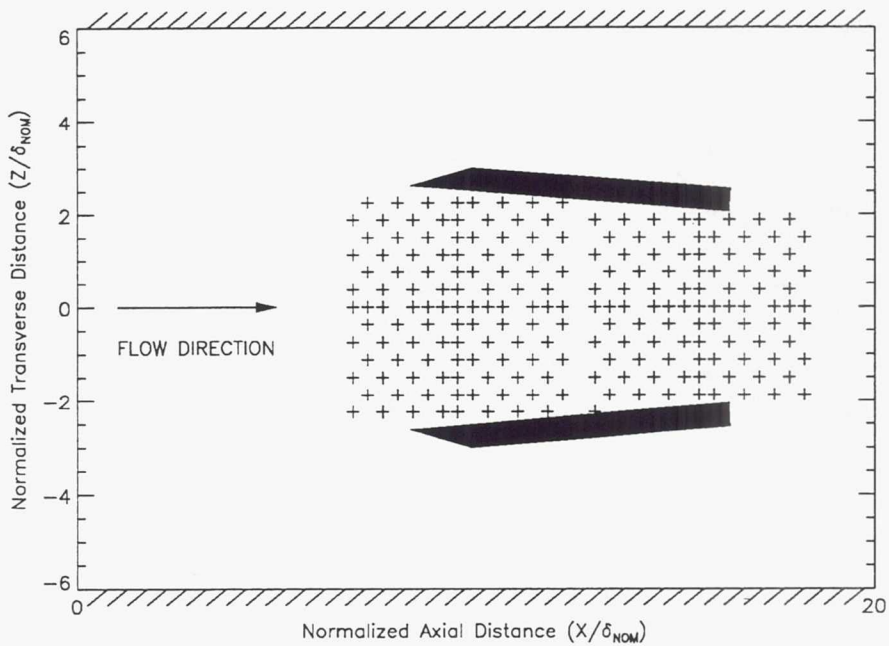
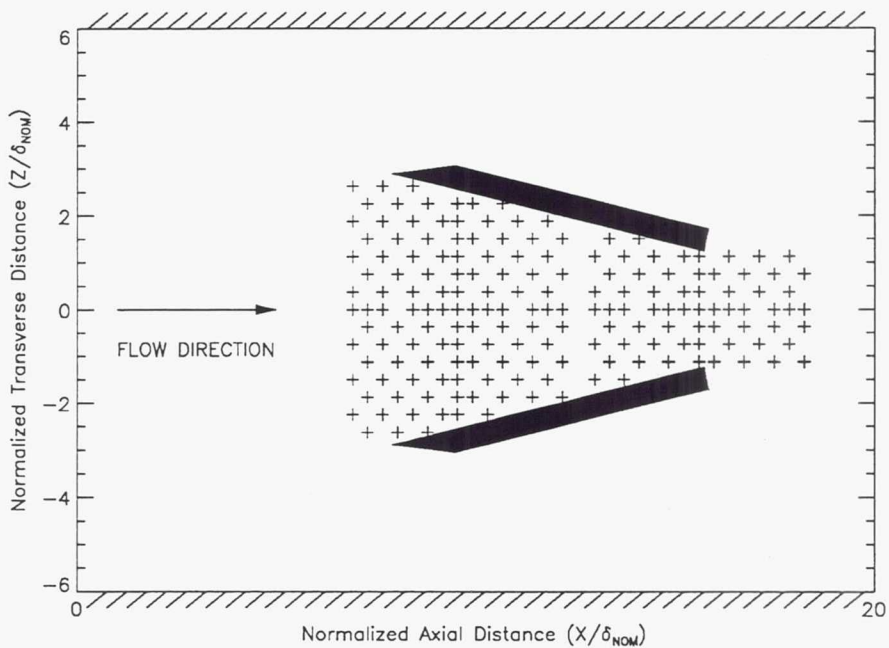


Figure 3. Tunnel test section

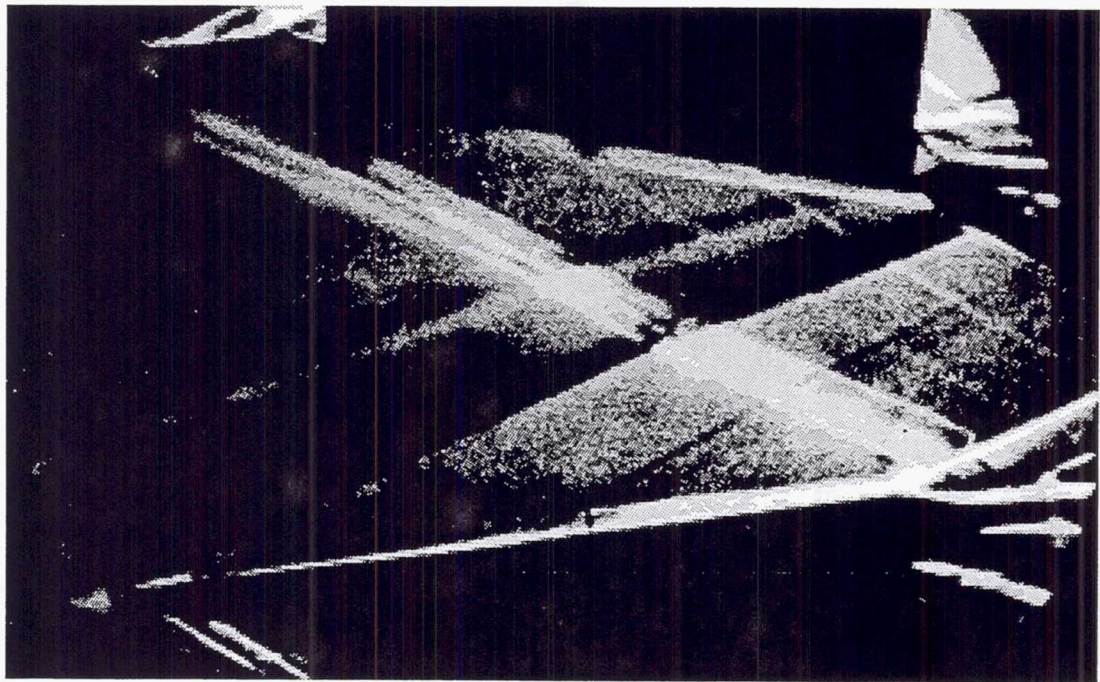


(a) Shock generator angle of 4 degrees

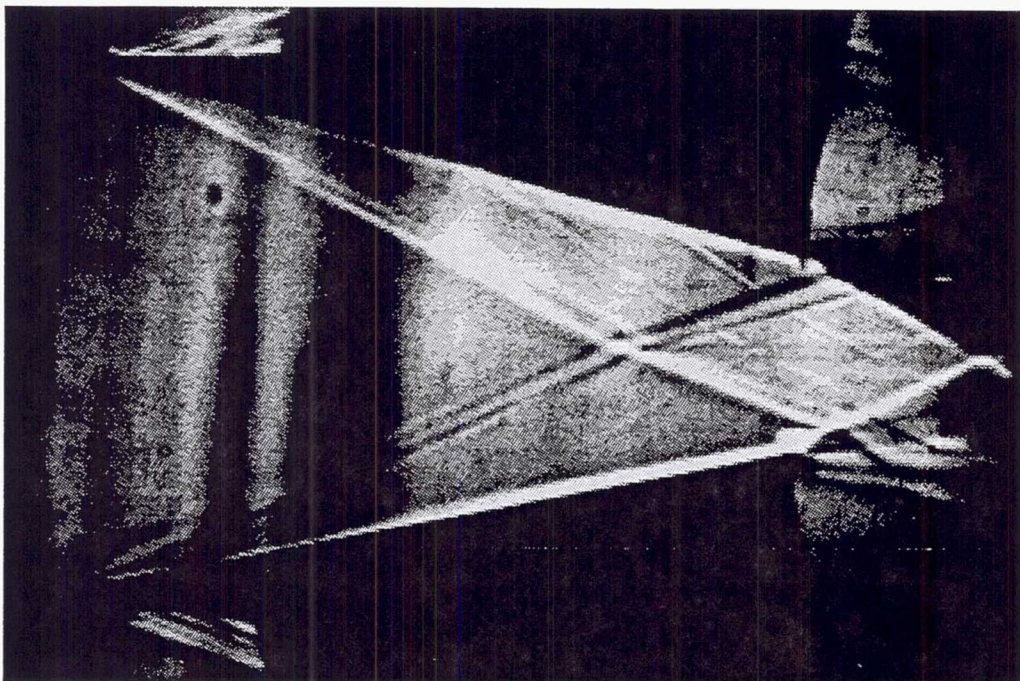


(b) Shock generator angle of 12 degrees

Figure 4. Location of static taps used



(a) 6 degree deflection



(b) 12 degree deflection

Figure 5. Schlieren results, Mach = 3.5

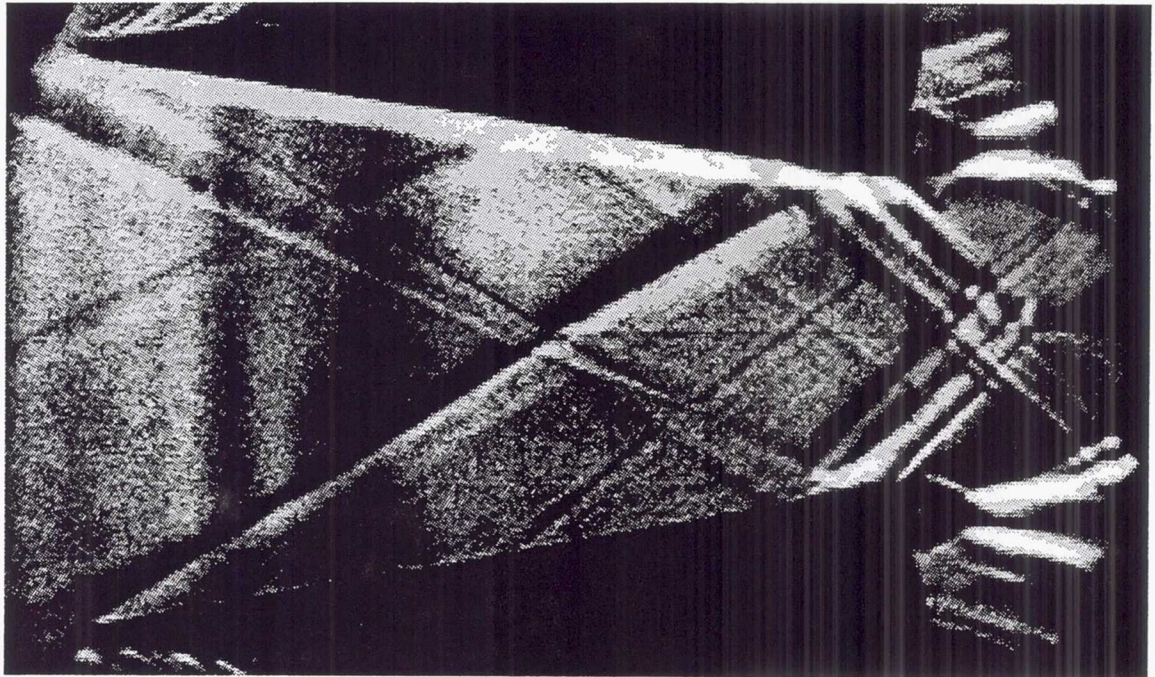
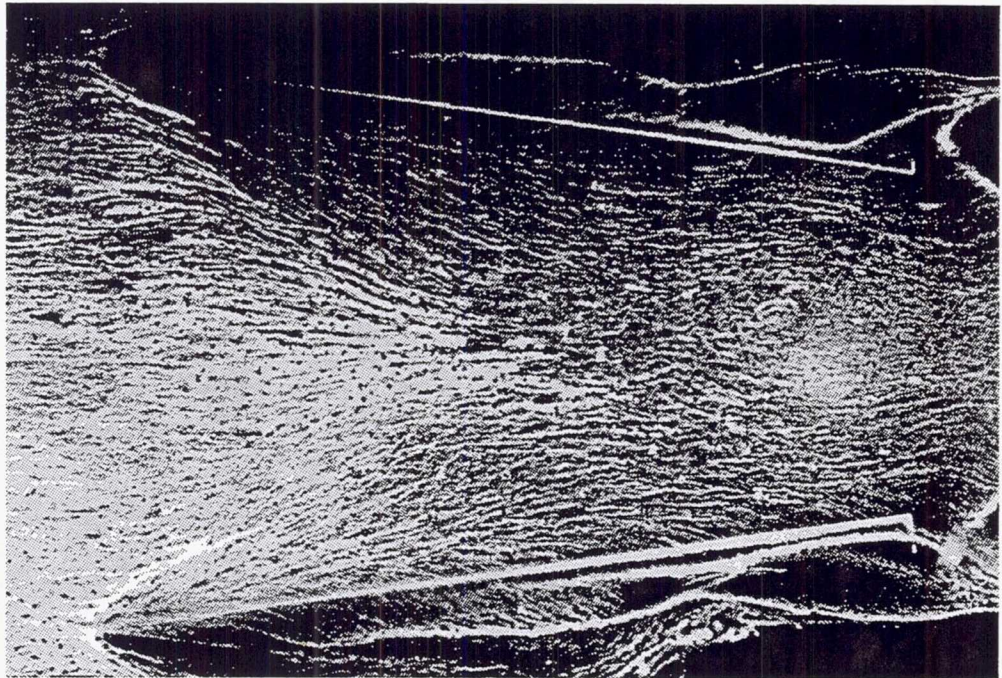
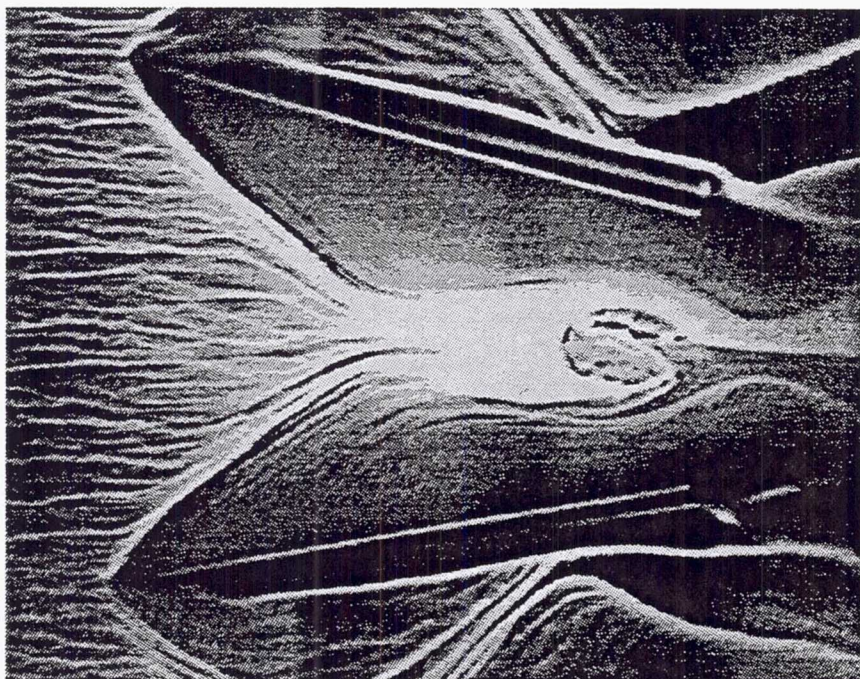


Figure 6. Schlieren results, Mach = 2.5, 9 deg deflection



(a) 6 degree deflection



(b) 10 degree deflection

Figure 7. Oil flow results, Mach 3.5

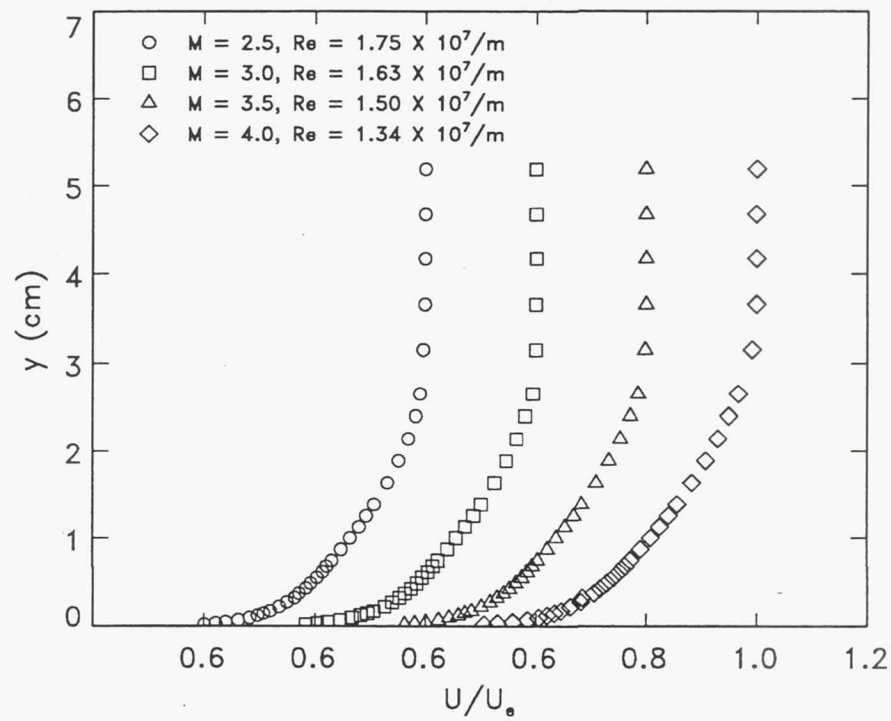
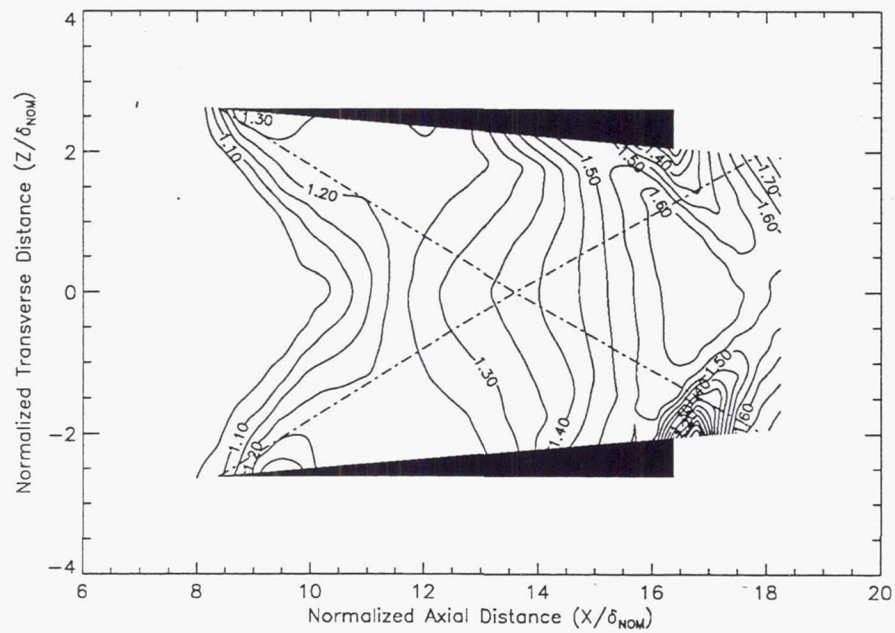
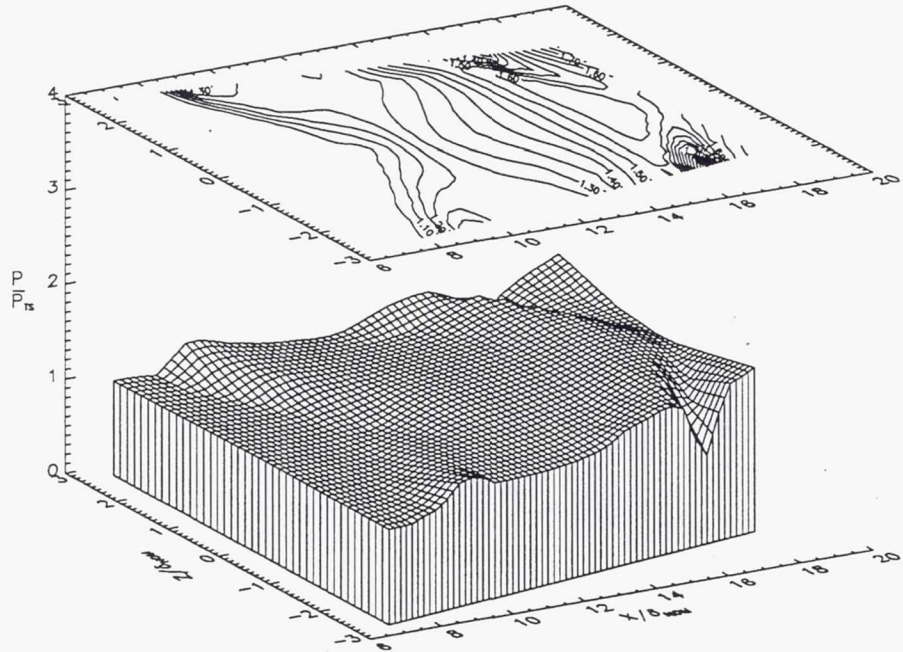


Figure 8. Boundary layer profiles, 11.43 cm downstream of the nozzle exit

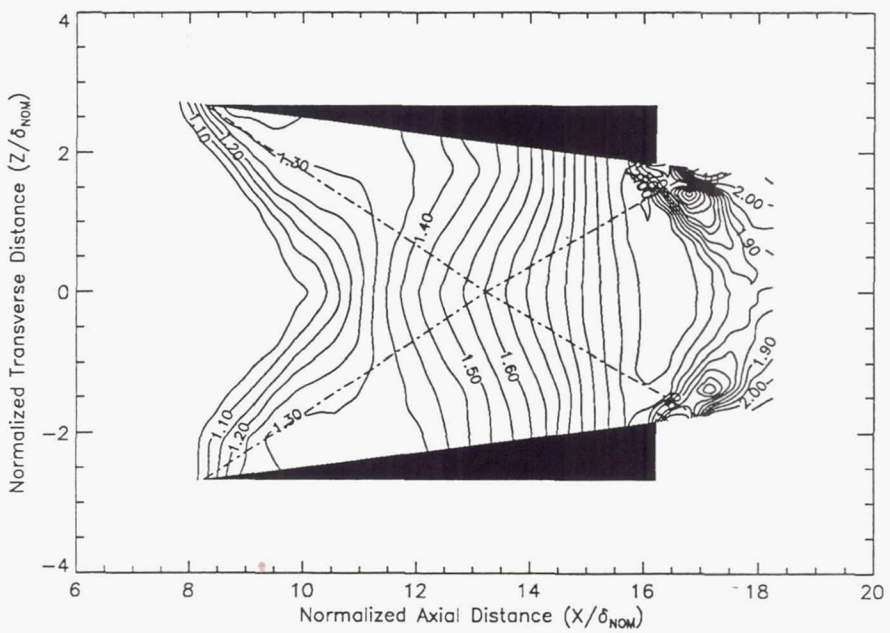


(a) Normalized pressure (P/P_{TS}) contour plot, 4 deg.

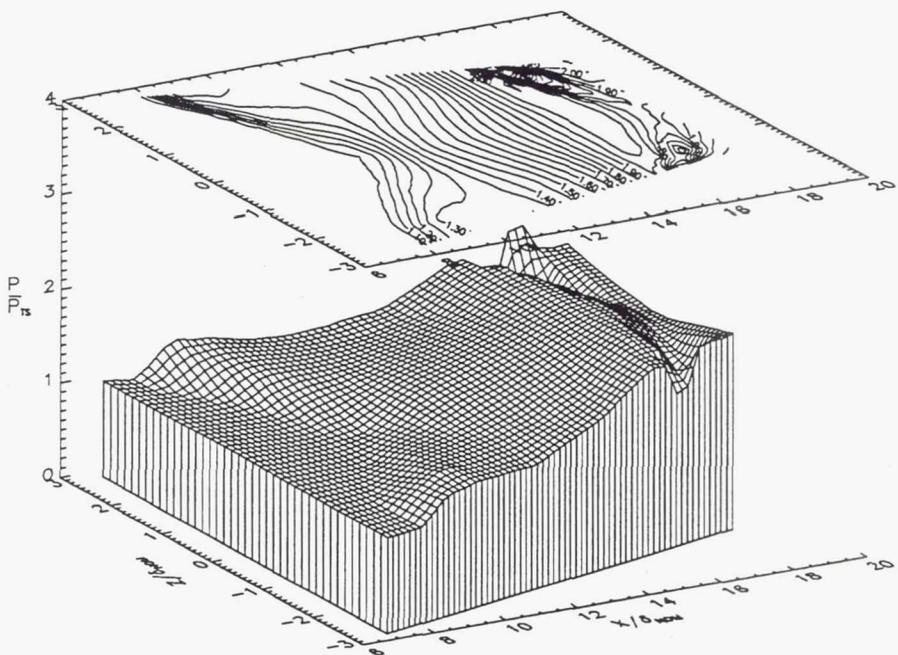


(b) Normalized pressure surface plot, 4 deg.

Figure 9. Mach 2.5

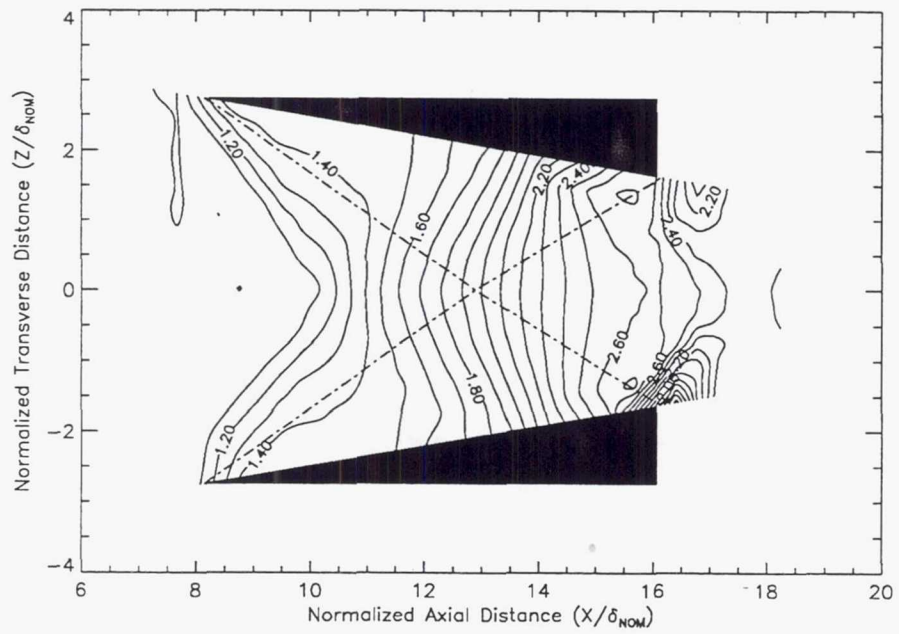


(c) Normalized pressure (P/P_{TS}) contour plot, 6 deg.

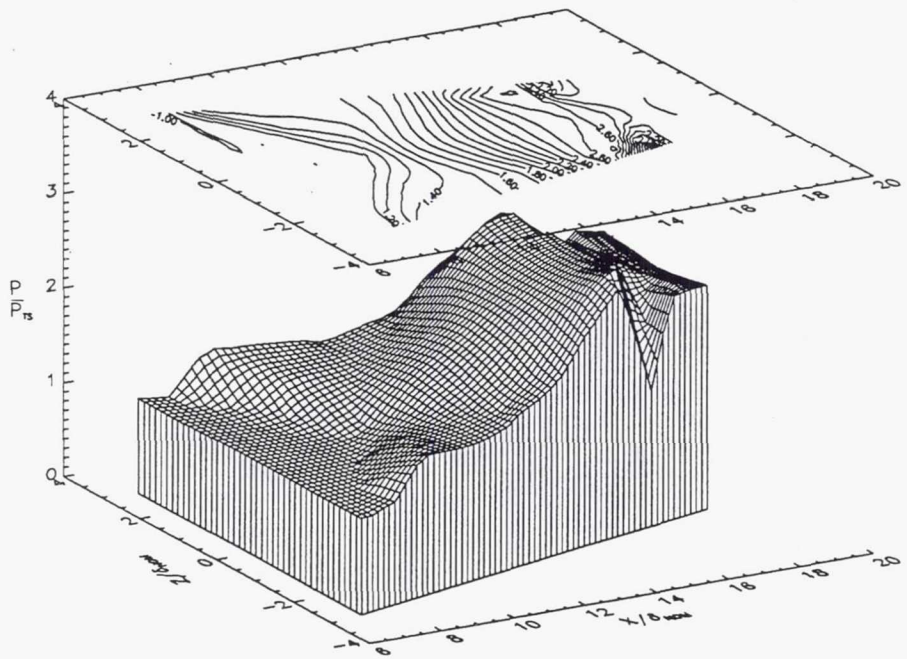


(d) Normalized pressure surface plot, 6 deg.

Figure 9 (cont.). Mach 2.5

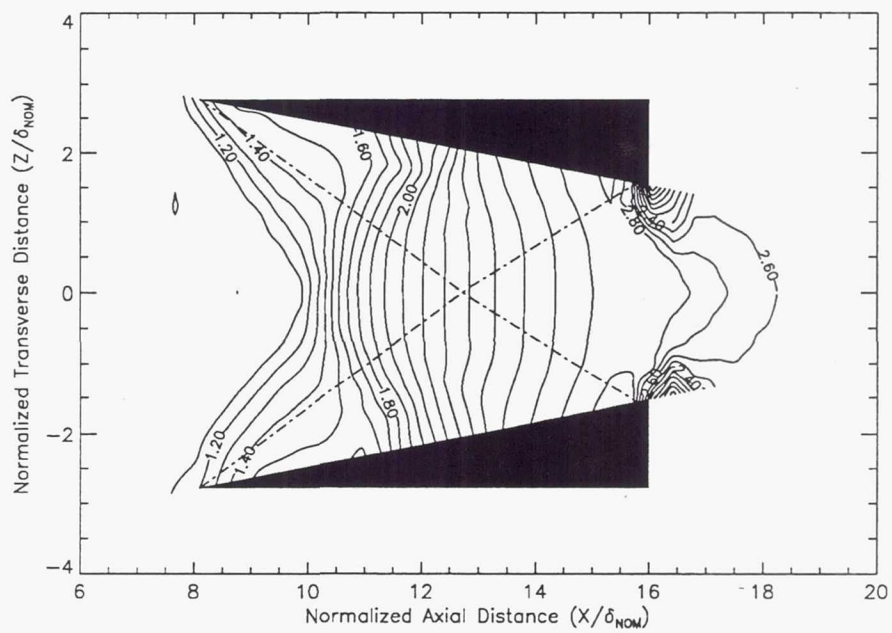


(e) Normalized pressure (P/P_{TS}) contour plot, 8 deg.

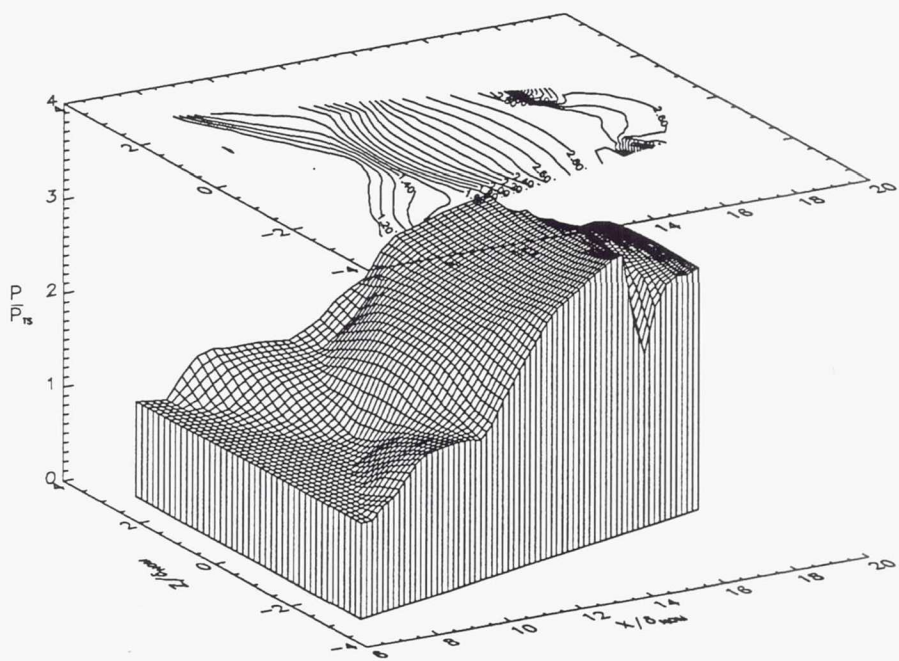


(f) Normalized pressure surface plot, 8 deg.

Figure 9 (cont.). Mach 2.5

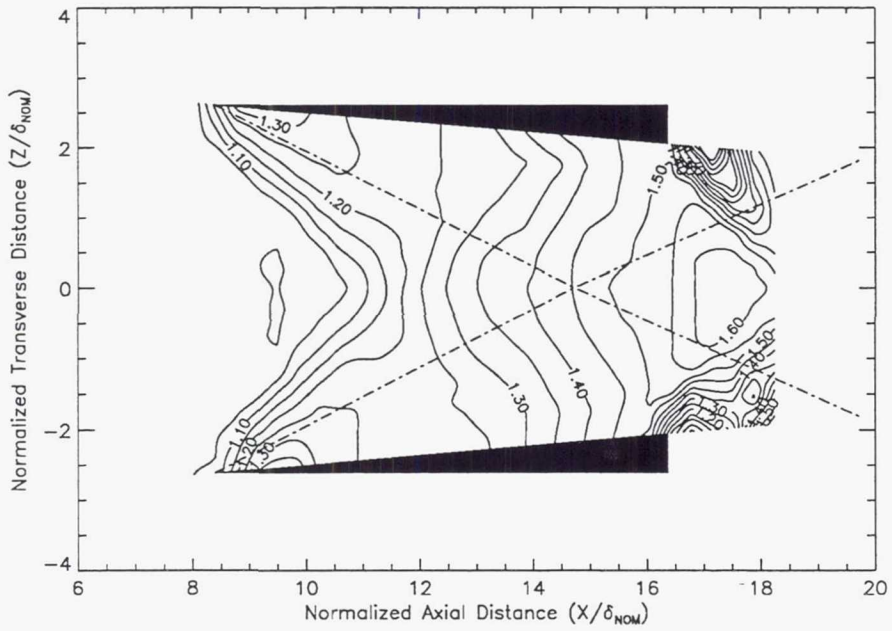


(g) Normalized pressure (P/P_{TS}) contour plot, 9 deg.

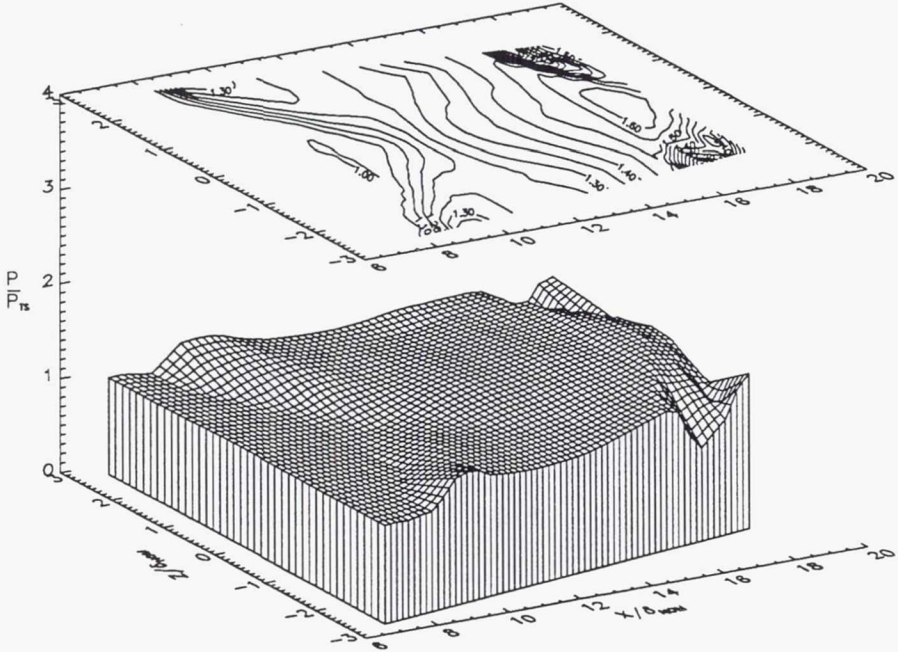


(h) Normalized pressure surface plot, 9 deg.

Figure 9 (cont.). Mach 2.5

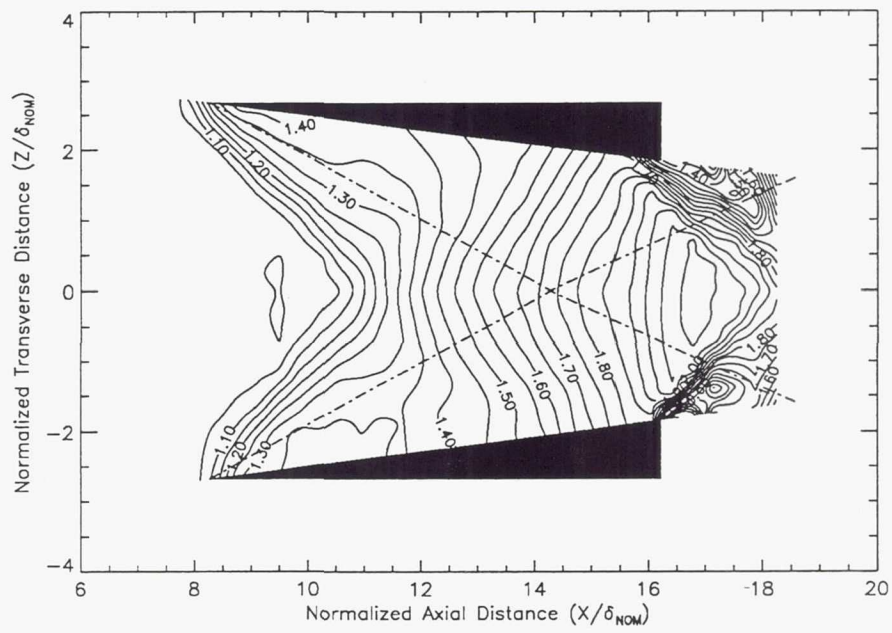


(a) Normalized pressure (P/P_{TS}) contour plot, 4 deg.

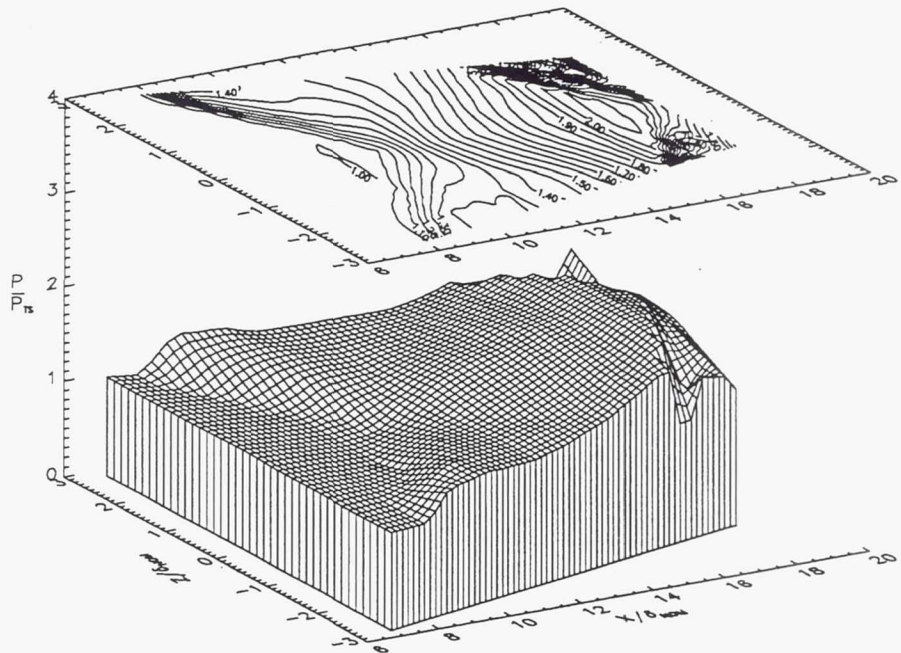


(b) Normalized pressure surface plot, 4 deg.

Figure 10. Mach 3.0

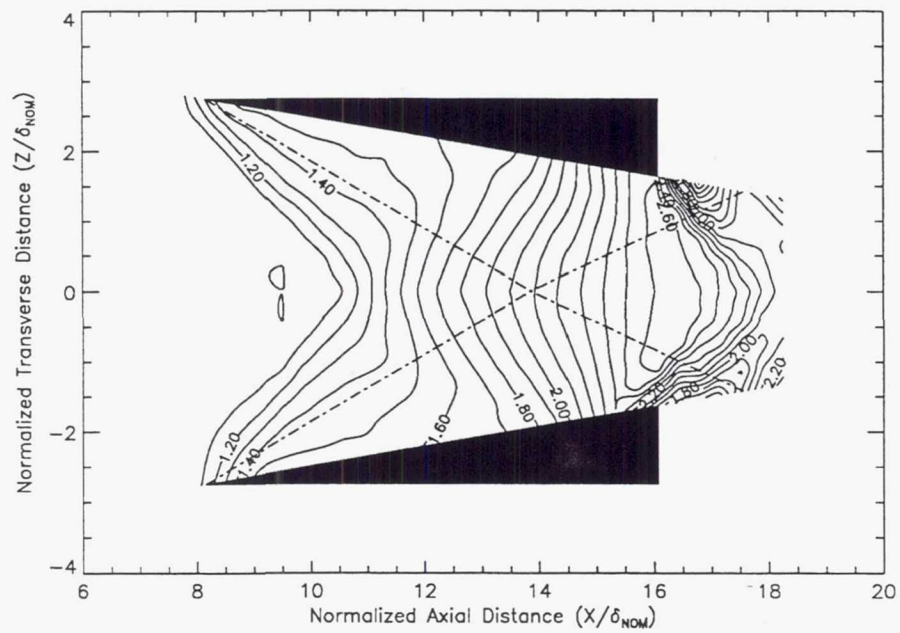


(c) Normalized pressure (P/P_{TS}) contour plot, 6 deg.

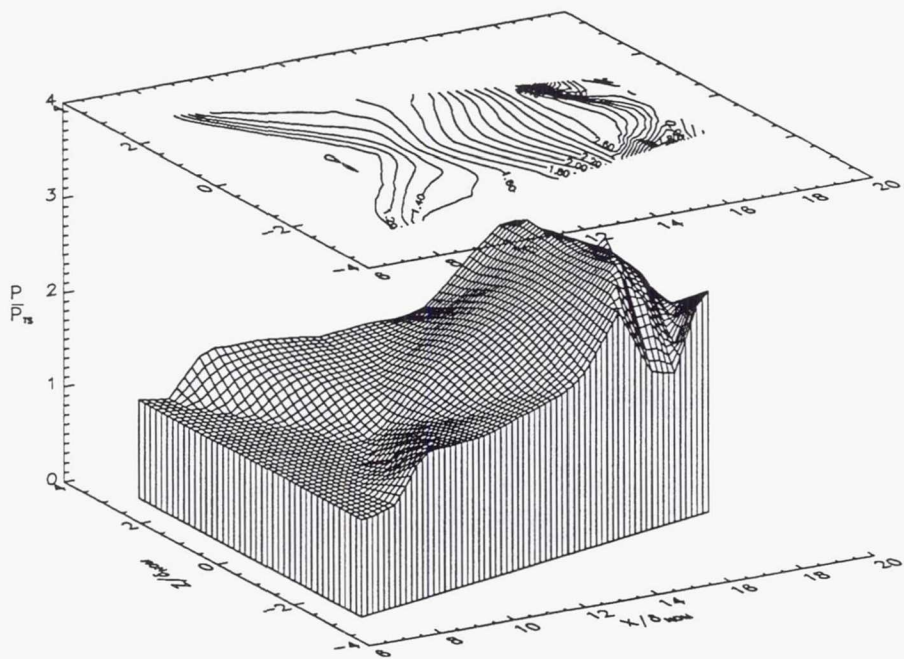


(d) Normalized pressure surface plot, 6 deg.

Figure 10 (cont.). Mach 3.0

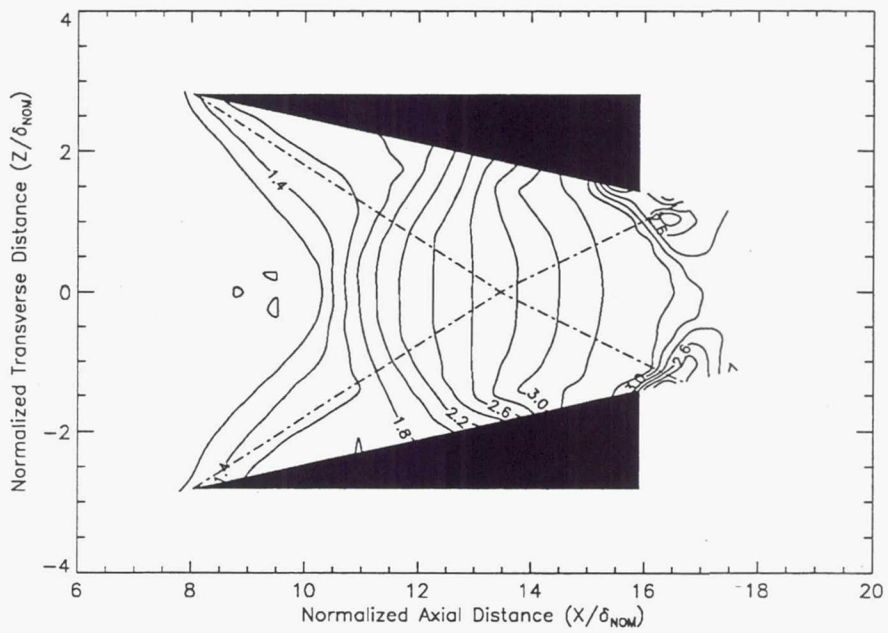


(e) Normalized pressure (P/P_{TS}) contour plot, 8 deg.

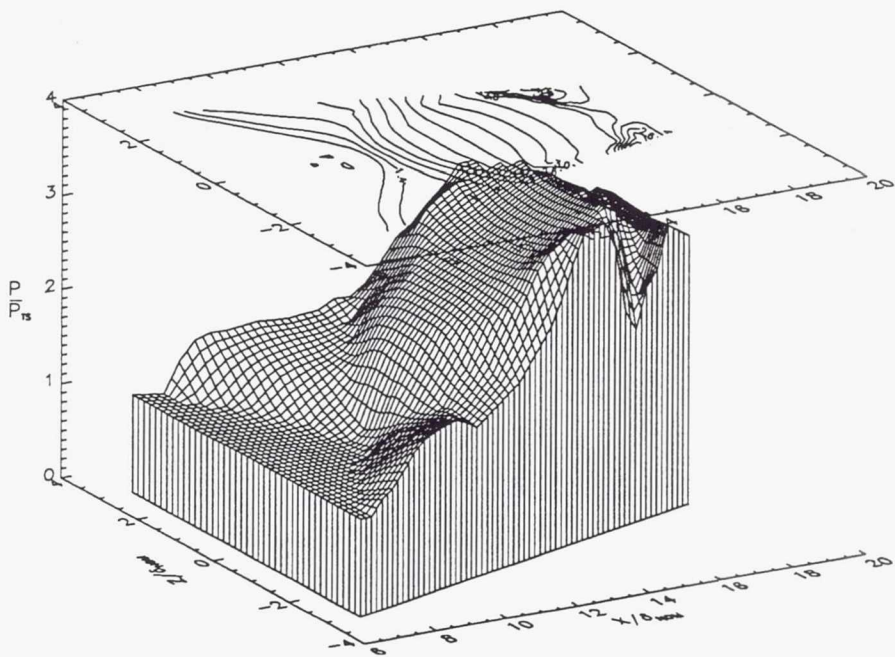


(f) Normalized pressure surface plot, 8 deg.

Figure 10 (cont.). Mach 3.0

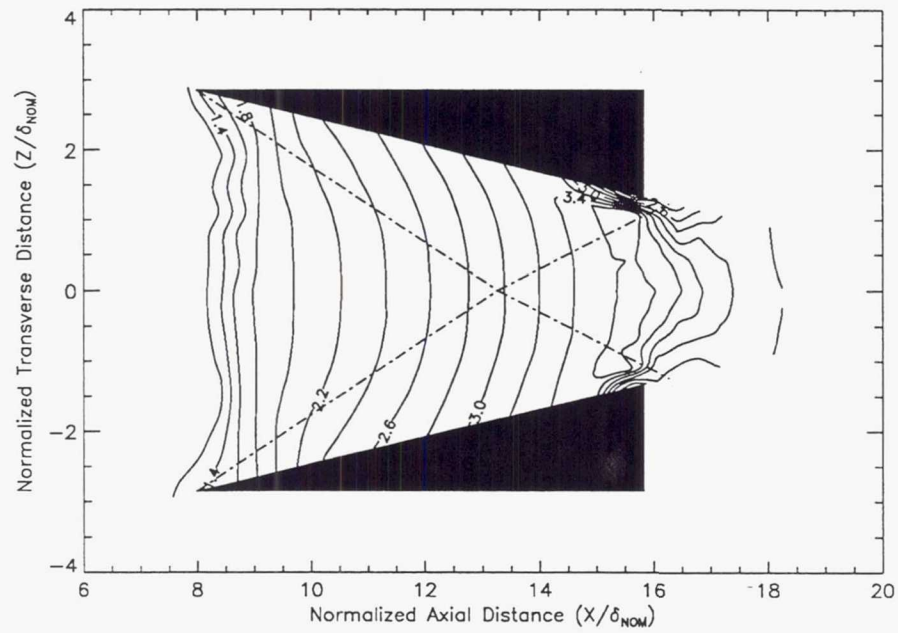


(g) Normalized pressure (P/P_{TS}) contour plot, 10 deg.

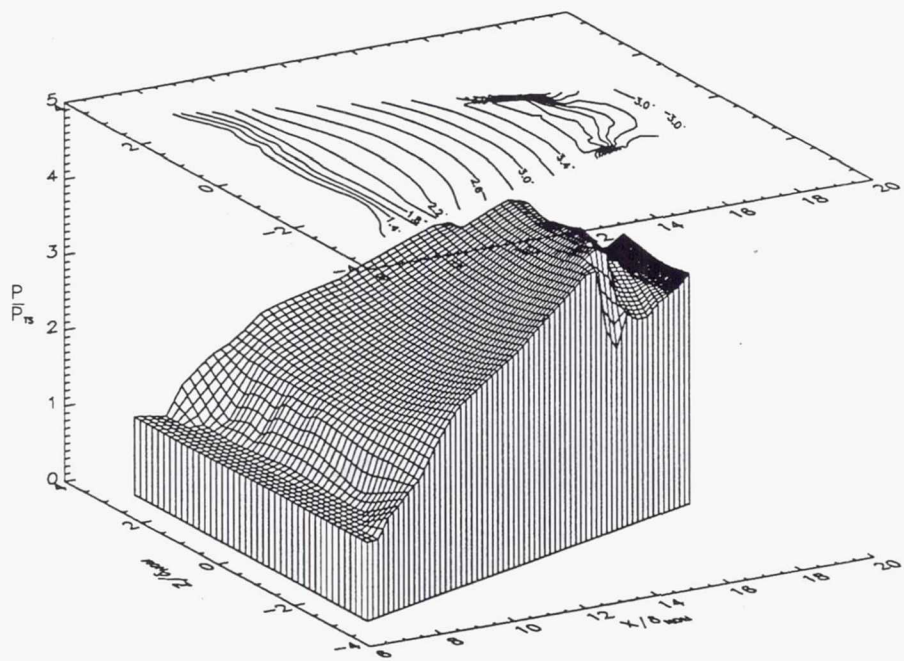


(h) Normalized pressure surface plot, 10 deg.

Figure 10 (cont). Mach 3.0

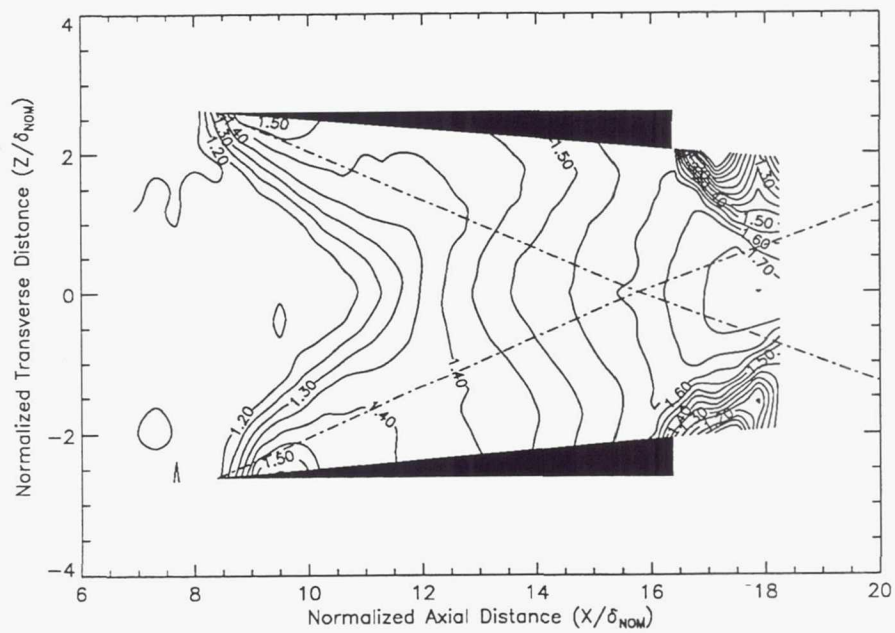


(i) Normalized pressure (P/P_{TS}) contour plot, 11 deg.

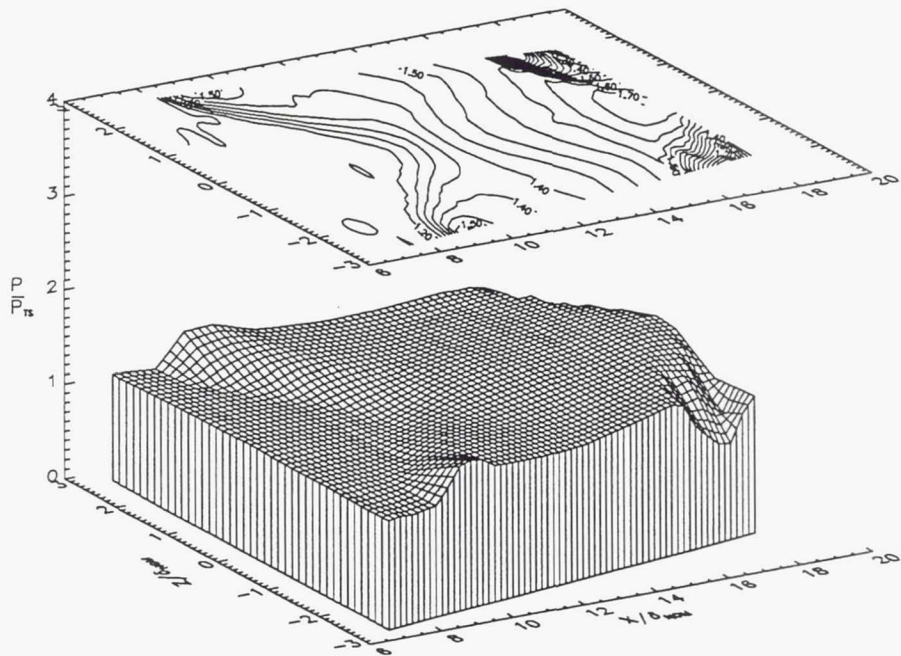


(j) Normalized pressure surface plot, 11 deg.

Figure 10 (cont). Mach 3.0

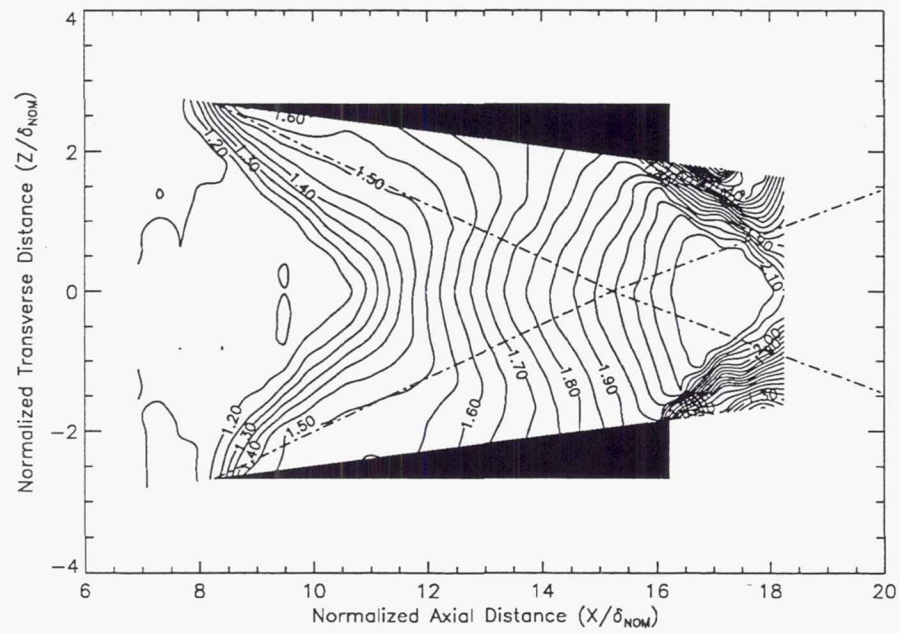


(a) Normalized pressure (P/P_{TS}) contour plot, 4 deg.

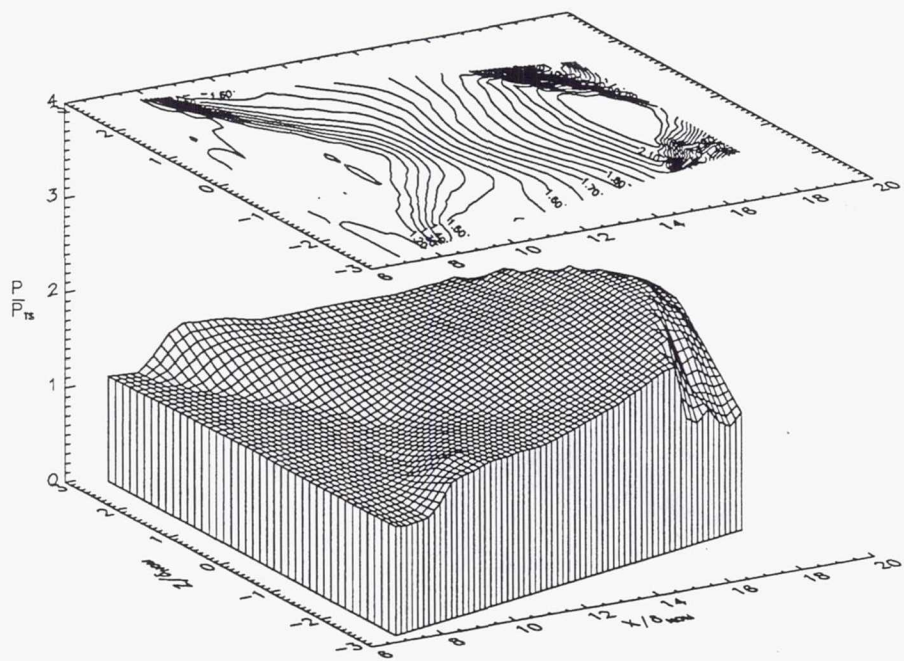


(b) Normalized pressure surface plot, 4 deg.

Figure 11. Mach 3.5

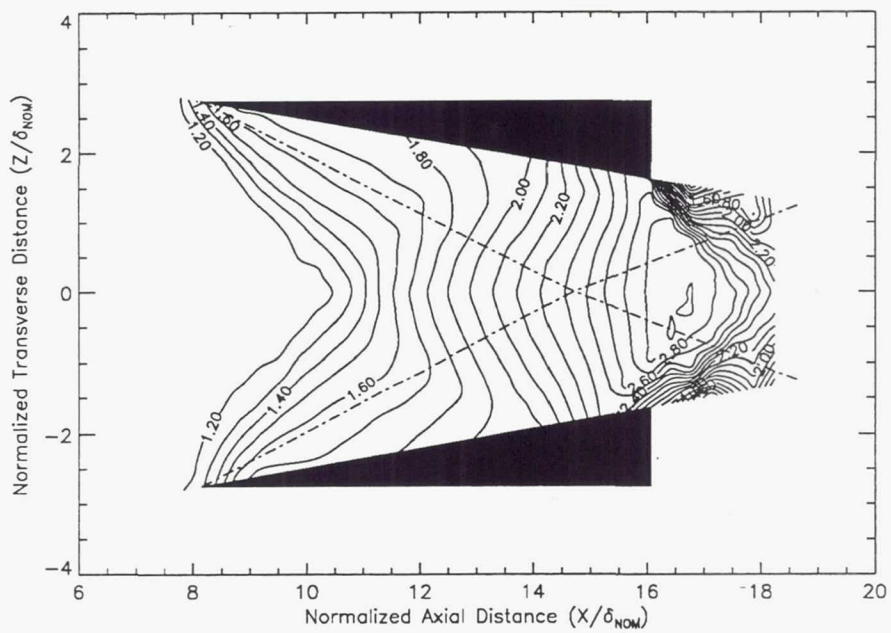


(c) Normalized pressure (P/P_{TS}) contour plot, 6 deg.

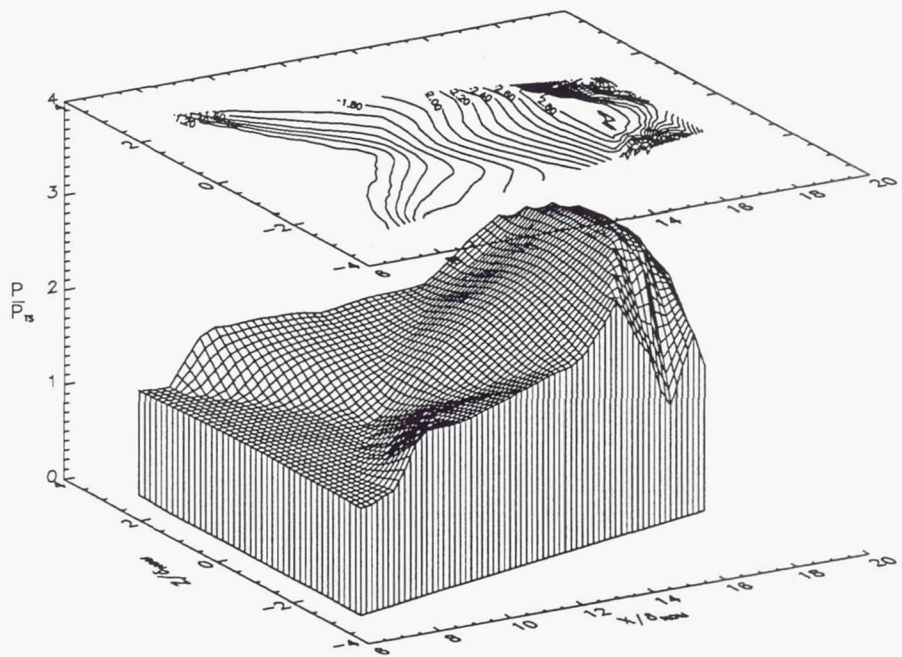


(d) Normalized pressure surface plot, 6 deg.

Figure 11 (cont.). Mach 3.5

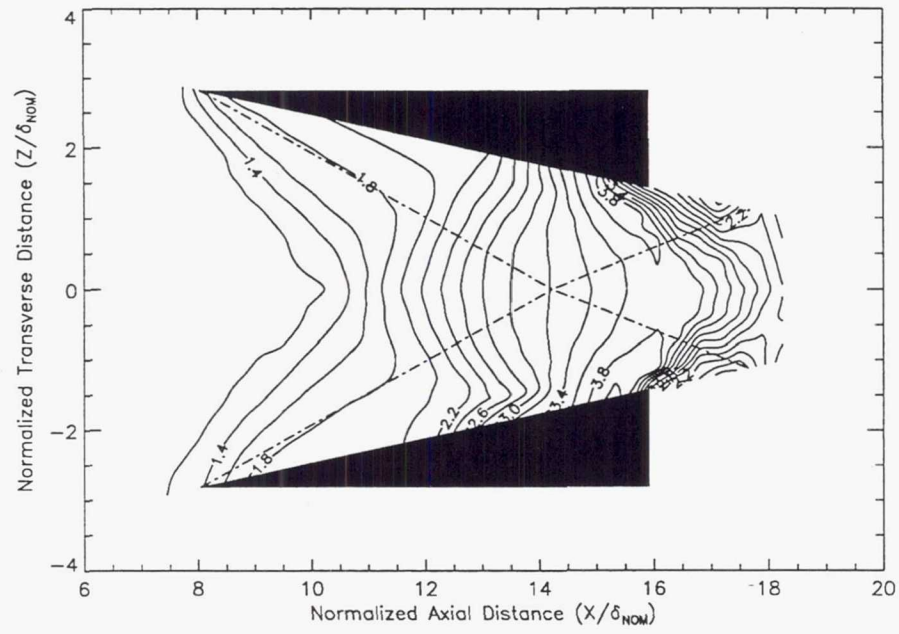


(e) Normalized pressure (P/P_{TS}) contour plot, 8 deg.

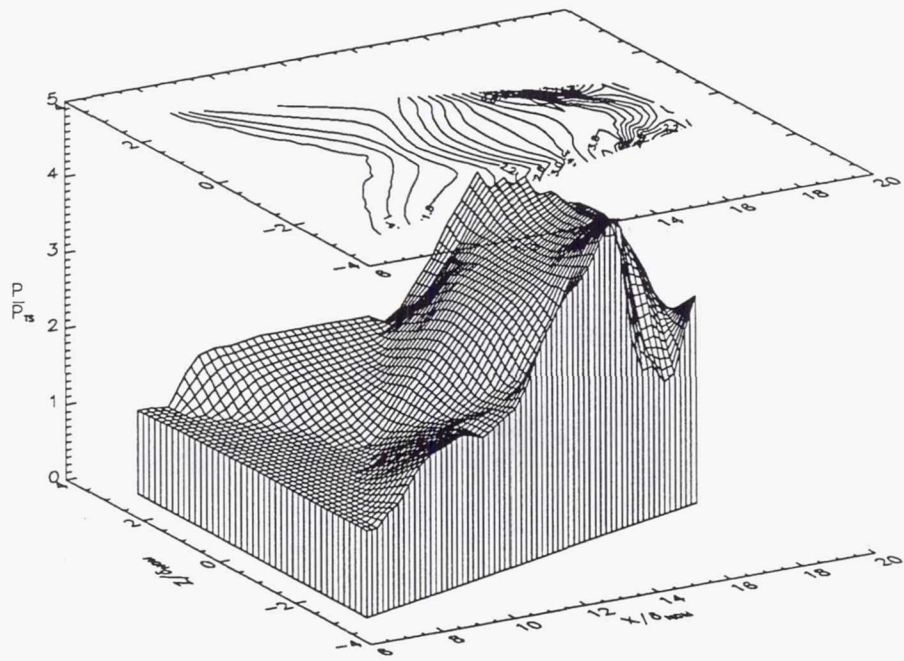


(f) Normalized pressure surface plot, 8 deg.

Figure 11 (cont.). Mach 3.5

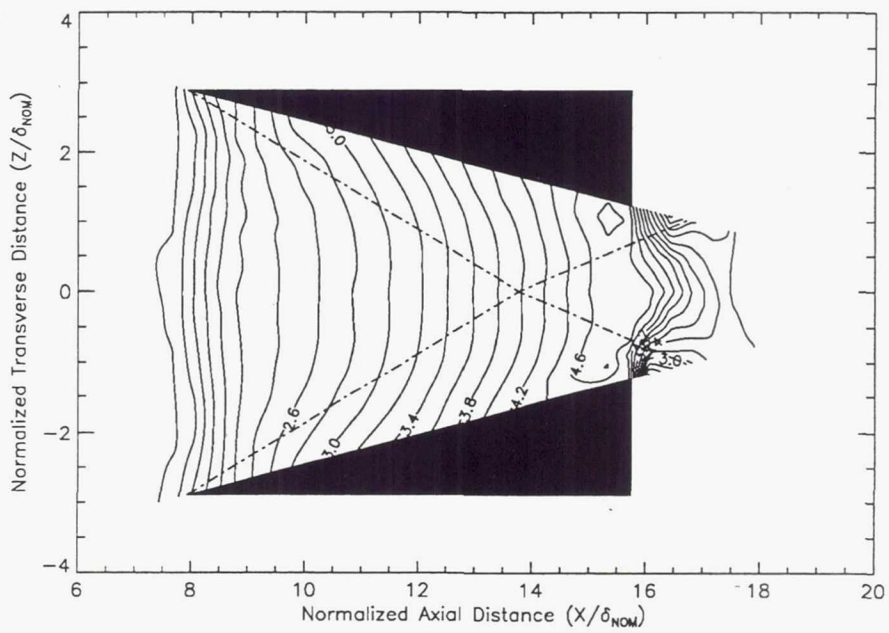


(g) Normalized pressure (P/P_{ts}) contour plot, 10 deg.

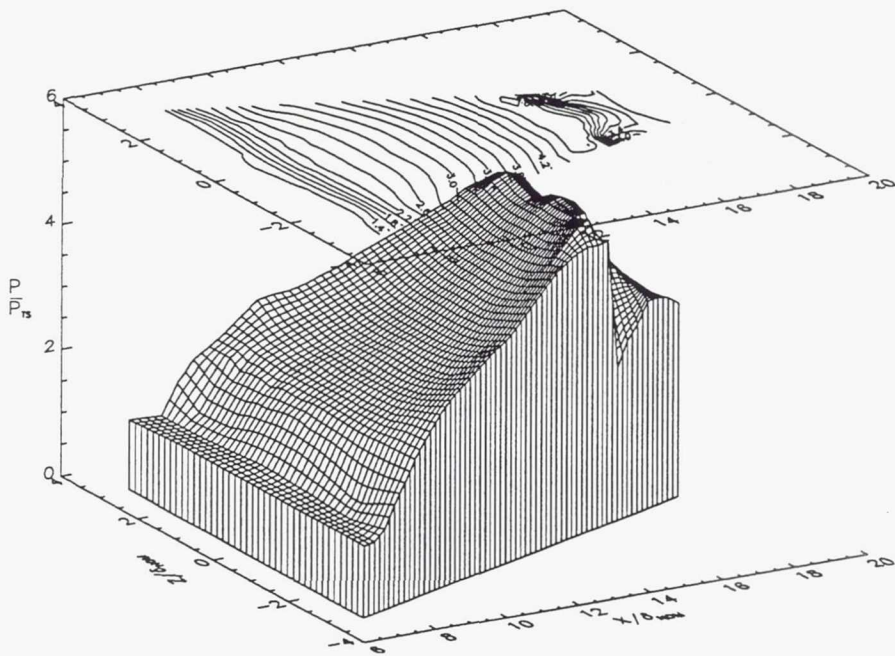


(h) Normalized pressure surface plot, 10 deg.

Figure 11 (cont.). Mach 3.5

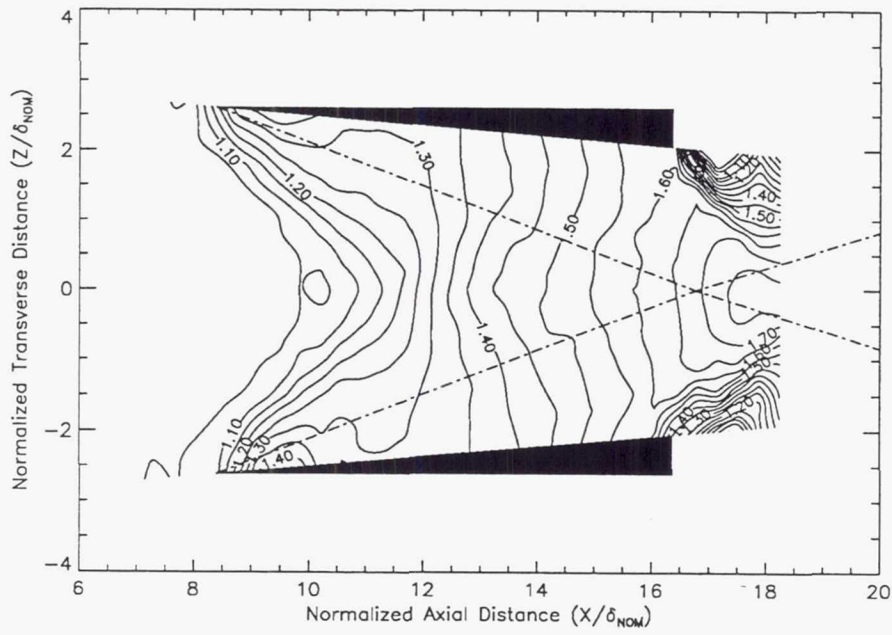


(i) Normalized pressure (P/P_{TS}) contour plot, 12 deg.

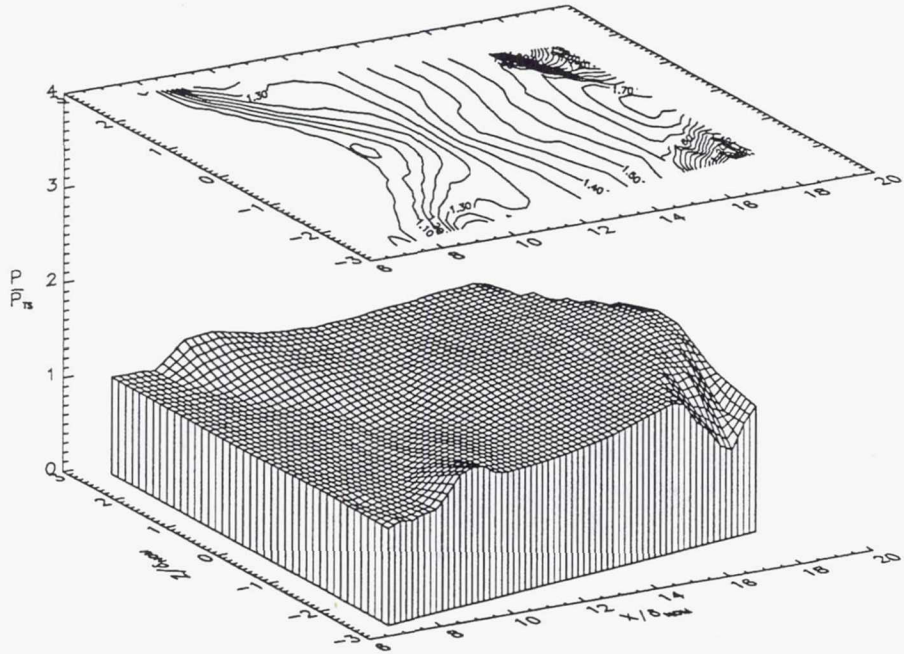


(j) Normalized pressure surface plot, 12 deg.

Figure 11 (cont.). Mach 3.5

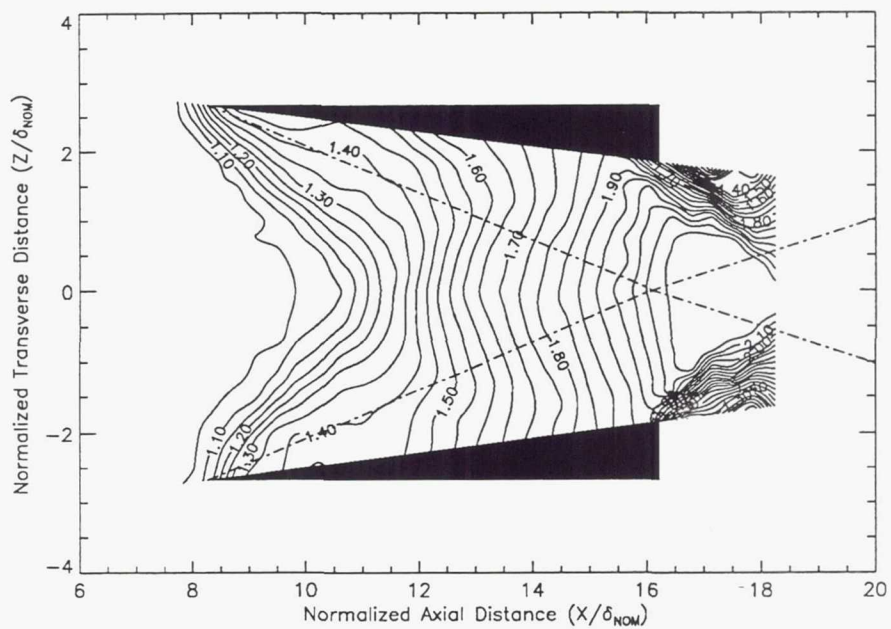


(a) Normalized pressure (P/P_{TS}) contour plot, 4 deg.

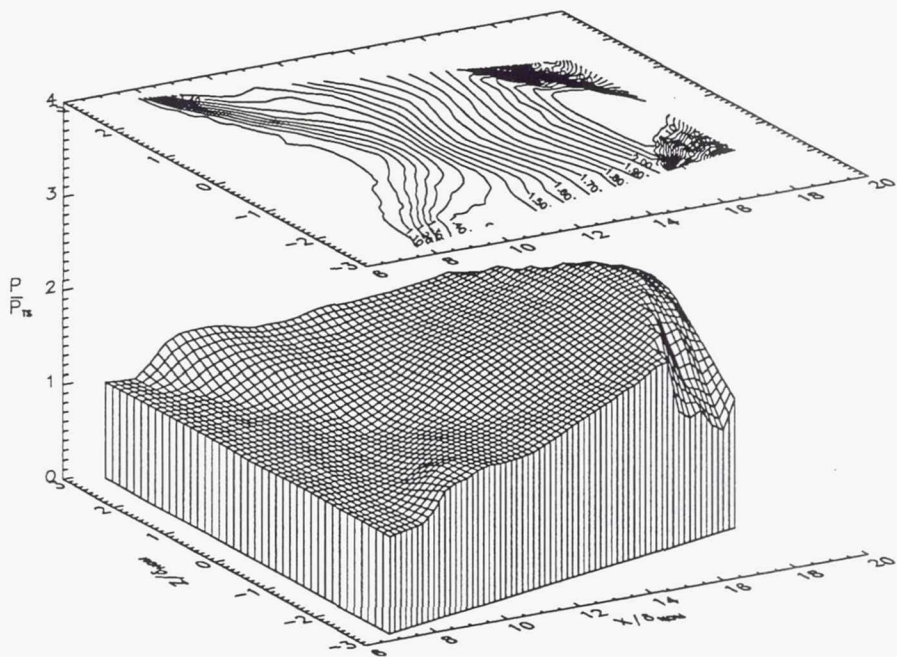


(b) Normalized pressure surface plot, 4 deg.

Figure 12. Mach 4.0

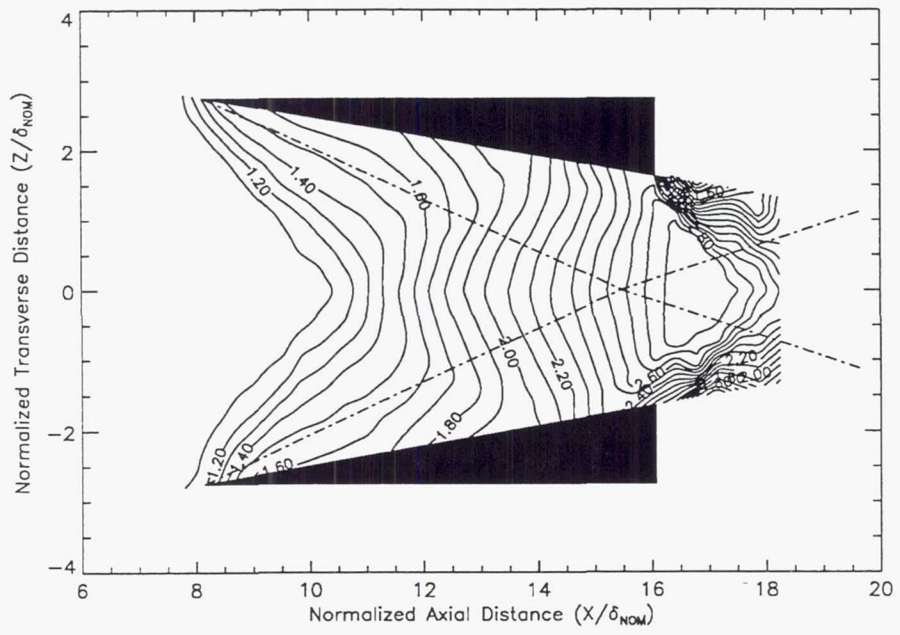


(c) Normalized pressure (P/P_{TS}) contour plot, 6 deg.

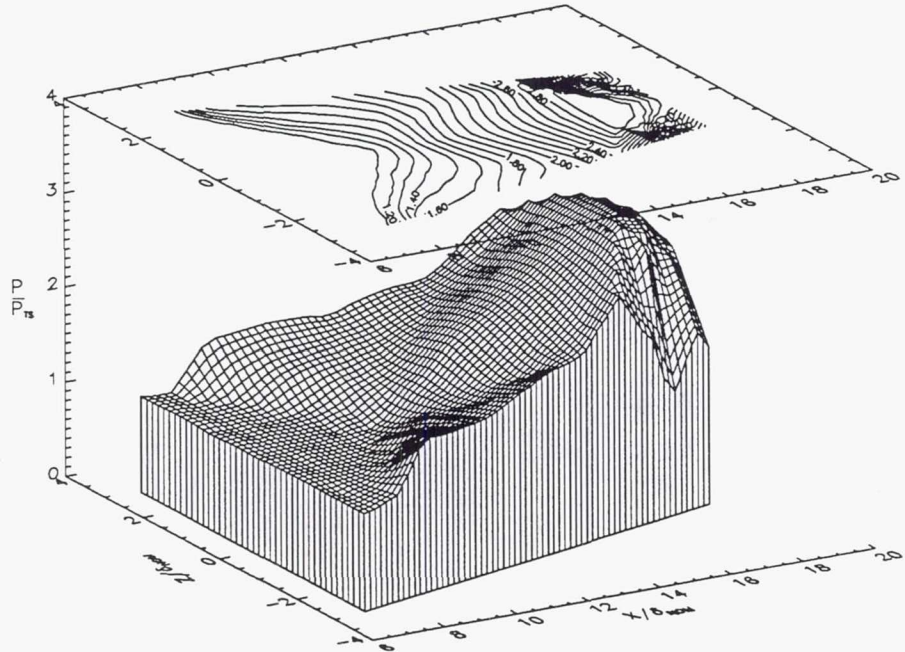


(d) Normalized pressure surface plot, 6 deg.

Figure 12 (cont.). Mach 4.0

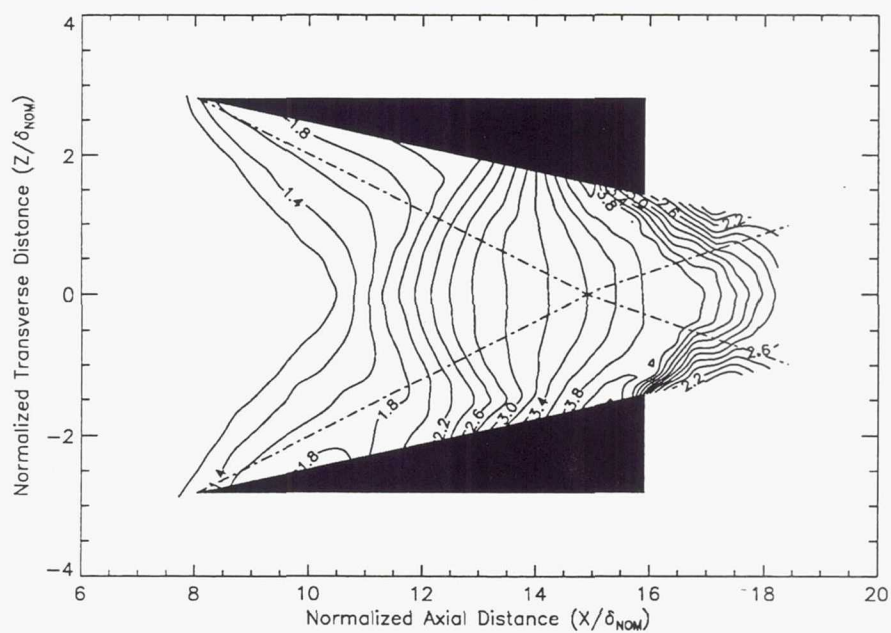


(e) Normalized pressure (P/P_{TS}) contour plot, 8 deg.

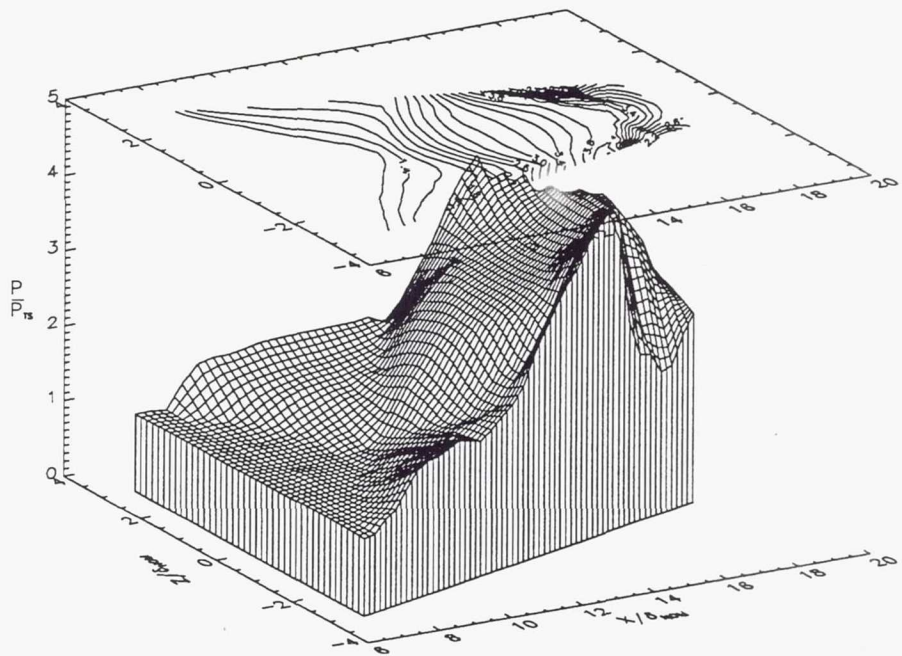


(f) Normalized pressure surface plot, 8 deg.

Figure 12 (cont.). Mach 4.0

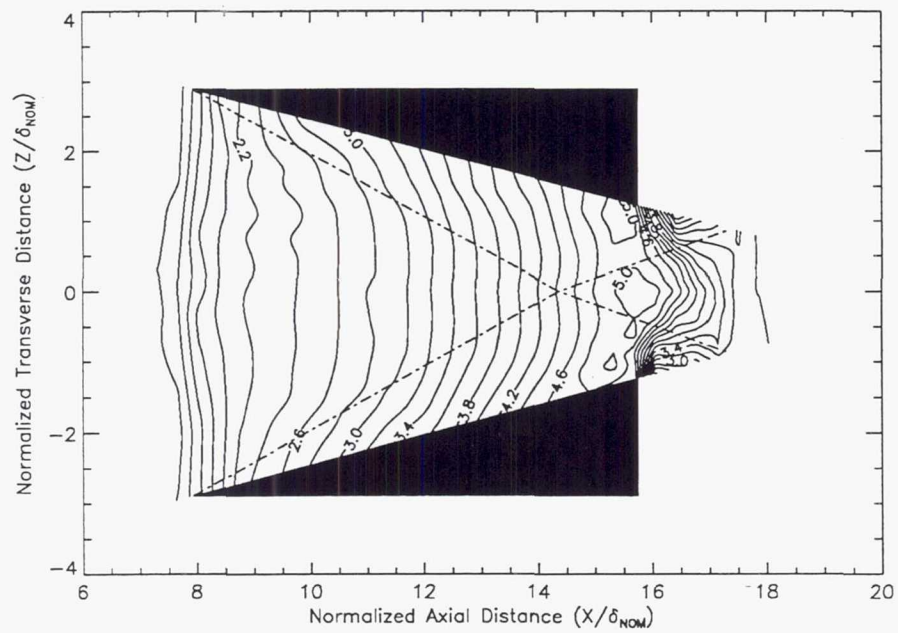


(g) Normalized pressure (P/P_{TS}) contour plot, 10 deg.

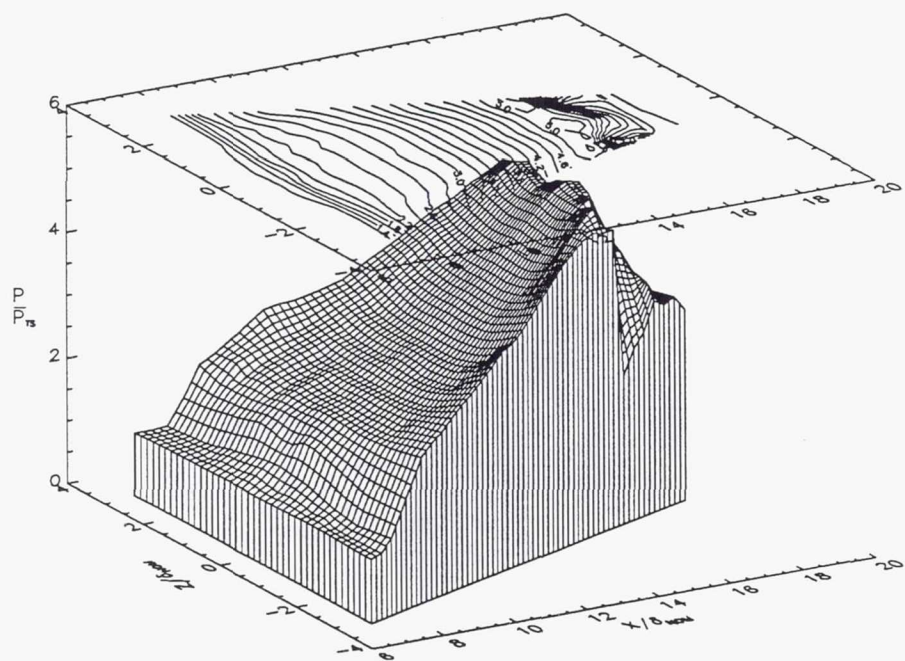


(h) Normalized pressure surface plot, 10 deg.

Figure 12 (cont.). Mach 4.0

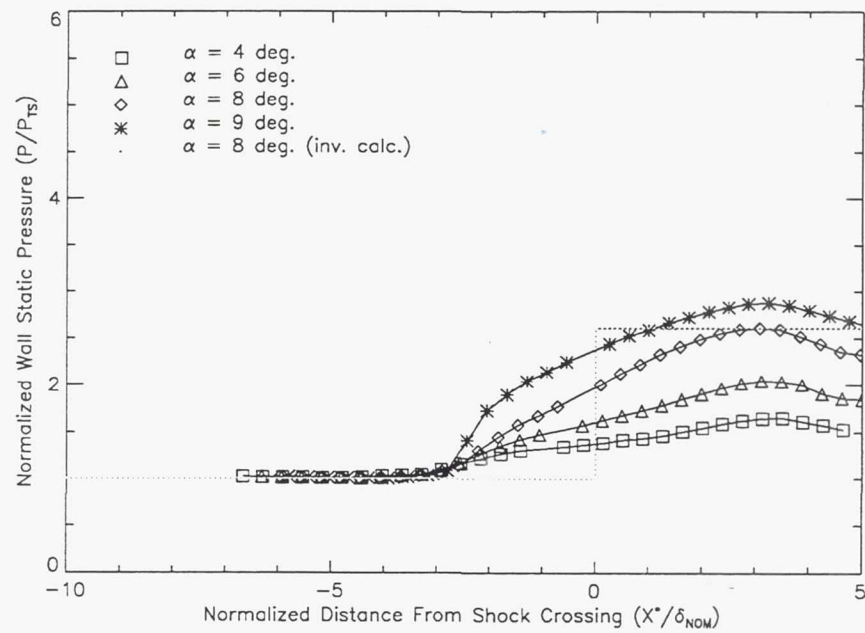


(i) Normalized pressure (P/P_{TS}) contour plot, 12 deg.

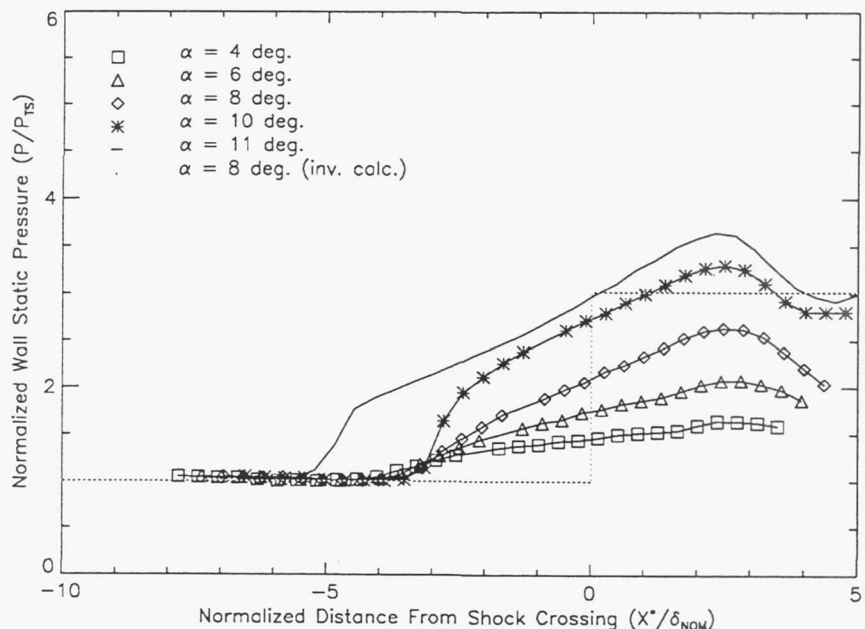


(j) Normalized pressure surface plot, 12 deg.

Figure 12 (cont.). Mach 4.0

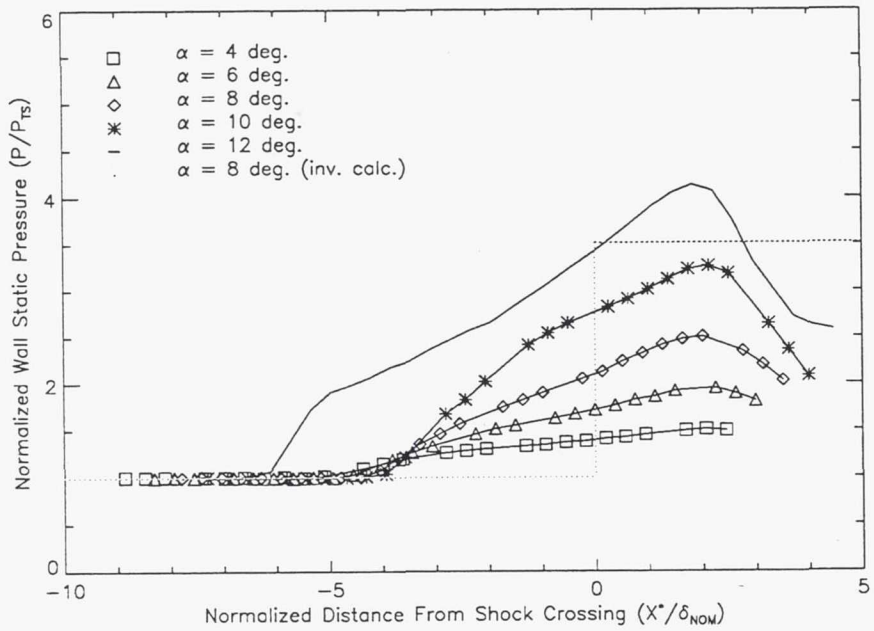


(a) Mach 2.5

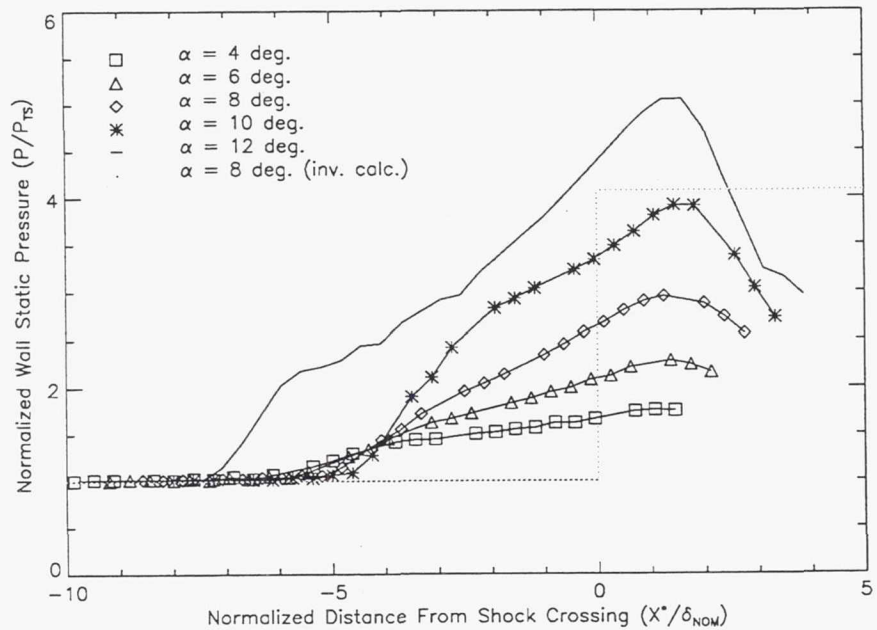


(b) Mach 3.0

Figure 13. Centerline pressures



(c) Mach 3.5



(d) Mach 4.0

Figure 13 (cont.). Centerline pressures

Table 1 Boundary Layer Profiles

Y (cm)	U/U _e (M=2.5)	U/U _e (M=3.0)	U/U _e (M=3.5)	U/U _e (M=4.0)
0.01905	0.60069	0.58375	0.56196	0.50529
0.03096	0.62111	0.60468	0.58063	0.53014
0.04524	0.63908	0.62338	0.60080	0.55781
0.06906	0.66194	0.64670	0.62341	0.58531
0.09525	0.68227	0.66692	0.64232	0.60506
0.12144	0.69641	0.68293	0.65911	0.62085
0.14526	0.70713	0.69502	0.67044	0.63386
0.17145	0.71929	0.70602	0.68259	0.64640
0.22146	0.73534	0.72559	0.70009	0.66322
0.27384	0.74938	0.73917	0.71634	0.68193
0.32385	0.76335	0.75276	0.72910	0.68456
0.37386	0.77117	0.76247	0.74096	0.70600
0.43101	0.78365	0.77328	0.75170	0.71699
0.48816	0.79191	0.78392	0.76326	0.72874
0.55245	0.80333	0.79342	0.77394	0.74123
0.61674	0.81371	0.80371	0.78427	0.75197
0.67864	0.82148	0.81344	0.79353	0.76283
0.74295	0.83121	0.82248	0.80369	0.77220
0.86914	0.84804	0.83984	0.82157	0.79057
0.99774	0.86418	0.85550	0.83765	0.80885
1.12395	0.88015	0.87145	0.85366	0.82528
1.25014	0.89309	0.88612	0.86940	0.84110
1.37874	0.90712	0.90018	0.88356	0.85597
1.63114	0.93116	0.92486	0.91007	0.88284
1.88592	0.95156	0.94634	0.93335	0.90804
2.14071	0.96928	0.96533	0.95412	0.93022

Table 1 (Continued) Boundary Layer Profiles

Y (cm)	U/U _e (M=2.5)	U/U _e (M=3.0)	U/U _e (M=3.5)	U/U _e (M=4.0)
2.39314	0.98260	0.98058	0.97219	0.94997
2.64792	0.99044	0.99460	0.98612	0.96727
3.15511	0.99602	0.99992	0.99884	0.99192
3.66471	0.99902	1.00032	1.00041	0.99956
4.17190	0.99972	1.00128	1.00054	0.99979
4.67911	0.99992	1.00051	1.00033	0.99906
5.18869	1.00000	1.00000	1.00000	1.00000
Boundary Layer Parameters for M=2.5 (cm)				
$\delta=3.0620$	$\delta^*=0.7030$	$\theta=0.1955$		
Boundary Layer Parameters for M=3.0 (cm)				
$\delta=2.6858$	$\delta^*=0.8410$	$\theta=0.1819$		
Boundary Layer Parameters for M=3.5 (cm)				
$\delta=3.0021$	$\delta^*=1.0537$	$\theta=0.1814$		
Boundary Layer Parameters for M=4.0 (cm)				
$\delta=3.3604$	$\delta^*=1.3853$	$\theta=0.1881$		

Table 2 Average Tunnel Operating Conditions

M	M _{ACT}	Re/m	T _T (K)	P _T (atm)
2.5	2.473	1.724×10^7	290.5	1.702
3.0	2.966	1.636×10^7	290.7	2.041
3.5	3.485	1.461×10^7	291.3	2.382
4.0	3.983	1.312×10^7	291.1	2.722

Table 3 Shock Generator Geometry

Geometry is symmetric about the tunnel center line. All locations are the physical dimensions divided by the nominal boundary layer thickness (2.54 cm).

Gen. Defleciton	X position of the L.E.	Z position of the L.E.	X position of the T.E.	Z position of the T.E.
4°	8.384	2.613	16.365	2.055
6°	8.267	2.676	16.224	1.840
8°	8.152	2.743	16.075	1.629
9°	8.096	2.778	15.997	1.526
10°	8.040	2.814	15.918	1.424
11°	7.985	2.851	15.838	1.324
12°	7.930	2.888	15.755	1.225

Table 4 a Data for 4 deg Deflection

X/ δ_{NOM}	Z/ δ_{NOM}	P/P _{TS} (M=2.5)	P/P _{TS} (M=3.0)	P/P _{TS} (M=3.5)	P/P _{TS} (M=4.0)
6.93500	-2.25000	1.01500	1.04200	1.01053	1.02700
6.93500	-1.50000	1.01400	1.03900	1.01053	1.03400
6.93500	-0.75000	1.01800	1.04400	1.01228	1.02700
6.93500	0.00000	1.01800	1.04700	1.02105	1.01300
6.93500	0.37500	1.01600	1.04600	1.01053	1.01300
6.93500	1.12500	1.01000	1.03200	1.01053	1.02000
6.93500	1.87500	1.00500	1.03000	0.99737	1.02400
7.31000	-1.87500	1.01300	1.03100	0.99912	1.00600
7.31000	-1.12500	1.01000	1.03200	1.01579	1.03100
7.31000	-0.37500	1.01200	1.03200	1.01754	1.01700
7.31000	0.00000	1.01200	1.03900	1.02018	1.02400

Table 4 a (Continued) Data for 4 deg Deflection

X/ δ_{NOM}	Z/ δ_{NOM}	P/P _{TS} (M=2.5)	P/P _{TS} (M=3.0)	P/P _{TS} (M=3.5)	P/P _{TS} (M=4.0)
7.31000	0.75000	1.01600	1.03600	1.02544	1.03100
7.31000	1.50000	1.00900	1.03500	1.01579	1.03100
7.31000	2.25000	1.00700	1.03500	0.99737	1.02800
7.68500	-2.25000	1.01000	1.03200	1.01053	1.04500
7.68500	-1.50000	1.00900	1.03400	1.01579	1.04500
7.68500	-0.75000	1.00700	1.03000	1.01404	1.01600
7.68500	0.00000	1.00900	1.03100	1.02105	1.02400
7.68500	0.37500	1.00600	1.03000	1.01579	1.01600
7.68500	1.12500	0.99930	1.02000	1.00614	1.01300
7.68500	1.87500	1.00000	1.02500	1.00614	1.01600
8.06000	-1.87500	1.00800	1.02300	1.01228	1.03500
8.06000	-1.12500	1.00900	1.02500	1.01754	1.03100
8.06000	-0.37500	1.00700	1.02300	1.02368	1.03500
8.06000	0.75000	1.00700	1.02400	1.01754	1.03100
8.06000	1.50000	1.00500	1.02300	1.01579	1.03500
8.06000	2.25000	1.00500	1.02000	0.99561	1.04300
8.43500	-2.25000	1.06300	1.04700	1.02895	1.07400
8.43500	-1.50000	1.01000	1.02200	1.01404	1.03800
8.43500	-0.75000	1.00700	1.01600	1.01404	1.01600
8.43500	0.00000	1.00300	1.01100	1.01930	1.02400
8.43500	0.37500	1.00300	1.01100	1.01754	1.01600
8.43500	1.12500	1.00100	1.01100	1.01404	1.01600
8.43500	1.87500	1.00300	1.01100	0.99386	1.03100
8.81000	-1.87500	1.09100	1.05200	1.05351	1.07600
8.81000	-1.12500	1.00800	1.00700	1.01754	1.02400
8.81000	-0.37500	1.00500	1.00900	1.02018	1.02400

Table 4 a (Continued) Data for 4 deg Deflection

X/ δ_{NOM}	Z/ δ_{NOM}	P/P _{TS} (M=2.5)	P/P _{TS} (M=3.0)	P/P _{TS} (M=3.5)	P/P _{TS} (M=4.0)
8.81000	0.00000	1.00300	1.00000	1.01579	1.02000
8.81000	0.75000	1.00500	1.00300	1.02018	1.02800
8.81000	1.50000	1.01200	1.00900	1.01404	1.04300
8.81000	2.25000	1.22100	1.21800	1.21228	1.24200
9.18500	-2.25000	1.24700	1.26600	1.26316	1.31600
9.18500	-1.50000	1.07800	1.03800	1.04386	1.07100
9.18500	-0.75000	1.00900	1.00600	1.01754	1.03800
9.18500	0.00000	1.00900	1.00300	1.02105	1.03800
9.18500	0.37500	1.00500	1.00100	1.02105	1.03100
9.18500	1.12500	1.00600	1.00200	1.00877	1.02400
9.18500	1.87500	1.18000	1.16800	1.14825	1.16800
9.56000	-1.87500	1.23100	1.23000	1.21930	1.27200
9.56000	-1.12500	1.08100	1.01600	1.02719	1.06800
9.56000	-0.37500	1.02600	0.99540	1.00088	1.01700
9.56000	0.00000	1.02600	0.99830	1.01053	1.03100
9.56000	0.75000	1.03500	1.00600	1.01404	1.05000
9.56000	1.50000	1.17600	1.12800	1.10702	1.16100
9.56000	2.25000	1.26800	1.28700	1.27544	1.33500
9.56000	-2.25000	1.26500	1.29100	1.27456	1.33500
9.56000	-1.50000	1.16400	1.12200	1.11053	1.13600
9.56000	-0.75000	1.02600	0.99480	1.01053	1.04200
9.56000	0.37500	1.01700	0.99240	1.00614	1.01600
9.56000	1.12500	1.07500	1.01800	1.01579	1.06300
9.56000	1.87500	1.22200	1.22700	1.21491	1.25900
9.93500	-1.87500	1.24400	1.26600	1.23947	1.30500
9.93500	-1.12500	1.14900	1.10300	1.08860	1.13500

Table 4 a (Continued) Data for 4 deg Deflection

X/ δ_{NOM}	Z/ δ_{NOM}	P/P _{TS} (M=2.5)	P/P _{TS} (M=3.0)	P/P _{TS} (M=3.5)	P/P _{TS} (M=4.0)
9.93500	-0.37500	1.04100	1.00800	1.02018	1.05700
9.93500	0.00000	1.03100	1.00900	1.02544	1.05700
9.93500	0.75000	1.08800	1.02800	1.02719	1.06800
9.93500	1.50000	1.20900	1.19800	1.17982	1.23100
9.93500	2.25000	1.24900	1.29600	1.27544	1.33800
10.31000	-2.25000	1.21700	1.27400	1.24649	1.30900
10.31000	-1.50000	1.21600	1.24400	1.21667	1.25900
10.31000	-0.75000	1.12500	1.08600	1.06228	1.08900
10.31000	0.00000	1.03900	1.01500	1.01053	1.03400
10.31000	0.37500	1.06200	1.02400	1.01579	1.04900
10.31000	1.12500	1.16900	1.16600	1.13509	1.17500
10.31000	1.87500	1.21700	1.26800	1.23947	1.27700
10.68500	-1.87500	1.21800	1.25800	1.23772	1.31200
10.68500	-1.12500	1.18800	1.21500	1.18246	1.23800
10.68500	-0.37500	1.11200	1.07500	1.05175	1.10200
10.68500	0.00000	1.09100	1.04100	1.03246	1.07900
10.68500	0.75000	1.15200	1.14400	1.10526	1.16100
10.68500	1.50000	1.21200	1.25000	1.22281	1.27200
10.68500	2.25000	1.21300	1.25100	1.23421	1.29400
11.06000	-2.25000	1.21200	1.24400	1.23684	1.29500
11.06000	-1.50000	1.21900	1.24600	1.22807	1.27300
11.06000	-0.75000	1.17900	1.17400	1.14561	1.19300
11.06000	0.37500	1.14800	1.11600	1.08684	1.14300
11.06000	1.12500	1.19300	1.21300	1.19035	1.23300
11.06000	1.87500	1.21100	1.24800	1.22456	1.26600
11.43500	-1.87500	1.22000	1.23800	1.23070	1.29000

Table 4 a (Continued) Data for 4 deg Deflection

X/ δ_{NOM}	Z/ δ_{NOM}	P/P _{TS} (M=2.5)	P/P _{TS} (M=3.0)	P/P _{TS} (M=3.5)	P/P _{TS} (M=4.0)
11.43500	-1.12500	1.22800	1.21300	1.19912	1.25300
11.43500	-0.37500	1.22000	1.16600	1.13684	1.18700
11.43500	0.00000	1.21200	1.15200	1.11491	1.16800
11.43500	0.75000	1.21400	1.19000	1.16140	1.22400
11.43500	1.50000	1.22000	1.23300	1.22456	1.28300
11.43500	2.25000	1.20300	1.23300	1.23421	1.30500
11.81000	-2.25000	1.20900	1.22400	1.22193	1.30600
11.81000	-1.50000	1.22800	1.23100	1.22193	1.28800
11.81000	-0.75000	1.24400	1.20800	1.19211	1.25100
11.81000	0.00000	1.26200	1.22000	1.16667	1.23300
11.81000	0.37500	1.25000	1.20700	1.16053	1.21500
11.81000	1.12500	1.21600	1.21500	1.20000	1.26200
11.81000	1.87500	1.20300	1.23200	1.22193	1.27300
12.18500	-1.87500	1.22600	1.24400	1.22105	1.32700
12.18500	-1.12500	1.25800	1.23400	1.20789	1.31200
12.18500	-0.37500	1.29300	1.26400	1.21754	1.31200
12.18500	0.00000	1.29800	1.27300	1.21579	1.30900
12.18500	0.75000	1.26800	1.23700	1.20263	1.29000
12.18500	1.50000	1.22900	1.24800	1.22281	1.30900
12.18500	2.25000	1.20300	1.24800	1.23772	1.32300
12.99500	-2.25000	1.23800	1.23600	1.22719	1.35500
12.99500	-1.50000	1.26700	1.25900	1.23421	1.35500
12.99500	-0.75000	1.31800	1.32000	1.25702	1.38100
12.99500	0.00000	1.34000	1.35200	1.28333	1.43700
12.99500	0.37500	1.32800	1.34700	1.27368	1.41800
12.99500	1.12500	1.28200	1.28000	1.23070	1.37000

Table 4 a (Continued) Data for 4 deg Deflection

X/ δ_{NOM}	Z/ δ_{NOM}	P/P _{TS} (M=2.5)	P/P _{TS} (M=3.0)	P/P _{TS} (M=3.5)	P/P _{TS} (M=4.0)
12.99500	1.87500	1.23700	1.25800	1.24035	1.37700
13.37000	-1.87500	1.29400	1.26973	1.23866	1.38789
13.37000	-1.12500	1.31600	1.31011	1.25726	1.39918
13.37000	-0.37500	1.35200	1.36562	1.29979	1.44636
13.37000	0.00000	1.36100	1.37571	1.30688	1.46072
13.37000	0.75000	1.33500	1.34644	1.29625	1.43918
13.37000	1.50000	1.28400	1.28891	1.25549	1.39200
13.74500	-1.50000	1.32900	1.29400	1.26053	1.42200
13.74500	-0.75000	1.35900	1.35400	1.29474	1.44500
13.74500	0.00000	1.38300	1.39100	1.32632	1.46700
13.74500	0.37500	1.37800	1.37700	1.32281	1.47100
13.74500	1.12500	1.32900	1.31900	1.27368	1.40700
13.74500	1.87500	1.29700	1.28400	1.26667	1.41100
14.12000	-1.87500	1.34700	1.31414	1.27410	1.43508
14.12000	-1.12500	1.36700	1.35754	1.29802	1.46483
14.12000	-0.37500	1.40600	1.41003	1.34410	1.51919
14.12000	0.75000	1.39100	1.38782	1.32991	1.48227
14.12000	1.50000	1.34800	1.33332	1.29625	1.45354
14.49500	-1.50000	1.37600	1.36200	1.30175	1.45600
14.49500	-0.75000	1.40500	1.41200	1.33947	1.48600
14.49500	0.00000	1.43200	1.43600	1.35702	1.52700
14.49500	0.37500	1.43000	1.43800	1.35088	1.51200
14.49500	1.12500	1.39800	1.38900	1.32105	1.48200
14.49500	1.87500	1.42300	1.33500	1.29474	1.47100
14.87000	-1.87500	1.46700	1.38379	1.31839	1.48945
14.87000	-1.12500	1.43500	1.41810	1.34232	1.51509

Table 4 a (Continued) Data for 4 deg Deflection

X/ δ_{NOM}	Z/ δ_{NOM}	P/P _{TS} (M=2.5)	P/P _{TS} (M=3.0)	P/P _{TS} (M=3.5)	P/P _{TS} (M=4.0)
14.87000	-0.37500	1.46100	1.46050	1.36802	1.54074
14.87000	0.00000	1.46000	1.46352	1.36979	1.54381
14.87000	0.75000	1.46300	1.45242	1.36802	1.54074
14.87000	1.50000	1.47200	1.41003	1.34055	1.50381
15.24500	-1.50000	1.48200	1.41900	1.34123	1.52000
15.24500	-0.75000	1.49400	1.46600	1.37544	1.55000
15.24500	0.00000	1.50400	1.49600	1.39825	1.57600
15.24500	0.37500	1.50600	1.48800	1.38860	1.56500
15.24500	1.12500	1.51500	1.44000	1.35877	1.53100
15.24500	1.87500	1.55900	1.41700	1.33947	1.52300
15.62000	-1.87500	1.55700	1.46151	1.36979	1.56638
15.62000	-1.12500	1.53700	1.46857	1.37422	1.56228
15.62000	-0.37500	1.54000	1.50793	1.39017	1.56638
15.62000	0.00000	1.54400	1.51500	1.40877	1.59100
15.62000	0.75000	1.56800	1.48977	1.40168	1.60536
15.62000	1.50000	1.58800	1.45747	1.37776	1.56946
15.62000	-1.50000	1.53300	1.44700	1.36754	1.53800
15.62000	-0.75000	1.53000	1.48000	1.39211	1.57600
15.62000	0.37500	1.54400	1.49400	1.38860	1.56800
15.62000	1.12500	1.57000	1.45600	1.37544	1.56100
15.62000	1.87500	1.60100	1.45200	1.37193	1.56100
15.99500	-1.87500	1.57200	1.49582	1.39991	1.59510
15.99500	-1.12500	1.58900	1.50087	1.40523	1.59818
15.99500	-0.37500	1.58300	1.52610	1.43092	1.63101
15.99500	0.00000	1.58700	1.52711	1.43712	1.64537
15.99500	0.75000	1.60900	1.51096	1.42029	1.62075

Table 4 a (Continued) Data for 4 deg Deflection

X/ δ_{NOM}	Z/ δ_{NOM}	P/P _{TS} (M=2.5)	P/P _{TS} (M=3.0)	P/P _{TS} (M=3.5)	P/P _{TS} (M=4.0)
15.99500	1.50000	1.61700	1.48977	1.39460	1.58382
16.37000	-1.50000	1.57800	1.52900	1.42456	1.62900
16.37000	-0.75000	1.61400	1.53900	1.44298	1.63200
16.37000	0.00000	1.62000	1.54000	1.45263	1.64400
16.37000	0.37500	1.62300	1.53700	1.44825	1.64700
16.37000	1.12500	1.62200	1.52400	1.42193	1.62100
16.37000	1.87500	1.32100	1.50800	1.40702	1.61000
16.74500	-1.87500	1.04400	1.08099	1.08095	1.27916
16.74500	-1.12500	1.58800	1.58666	1.44953	1.67511
16.74500	-0.37500	1.63600	1.59272	1.48320	1.67511
16.74500	0.00000	1.64400	1.59474	1.48143	1.68537
16.74500	0.75000	1.63500	1.59272	1.47168	1.67511
16.74500	1.50000	1.43100	1.52408	1.42738	1.63511
17.12000	-1.50000	1.29200	1.39100	1.32281	1.54600
17.12000	-0.75000	1.59300	1.62300	1.48070	1.69600
17.12000	0.37500	1.62600	1.61600	1.49561	1.72200
17.12000	1.12500	1.48700	1.54000	1.44474	1.67000
17.12000	1.87500	1.53600	0.96270	0.79561	0.87430
17.49500	-1.87500	1.60600	1.27175	0.94982	1.02220
17.49500	-1.12500	1.42900	1.51096	1.40877	1.64229
17.49500	-0.37500	1.60100	1.63814	1.52041	1.76538
17.49500	0.00000	1.61000	1.63612	1.52041	1.76846
17.49500	0.75000	1.53100	1.58464	1.49029	1.71409
17.49500	1.50000	1.55700	1.12540	1.08361	1.29044
17.87000	-1.50000	1.63500	1.20100	1.02807	1.19700
17.87000	-0.75000	1.51500	1.55000	1.46754	1.70700

Table 4 a (Continued) Data for 4 deg Deflection

X/ δ_{NOM}	Z/ δ_{NOM}	P/P _{TS} (M=2.5)	P/P _{TS} (M=3.0)	P/P _{TS} (M=3.5)	P/P _{TS} (M=4.0)
17.87000	0.00000	1.57400	1.62100	1.53684	1.78200
17.87000	0.37500	1.55000	1.59600	1.50877	1.74100
17.87000	1.12500	1.55900	1.32200	1.27982	1.49000
17.87000	1.87500	1.70200	1.46700	1.17456	1.24600
18.24500	-1.87500	1.72700	1.62804	1.26258	1.34071
18.24500	-1.12500	1.62900	1.32121	1.23511	1.46483
18.24500	-0.37500	1.53400	1.56748	1.50004	1.75102
18.24500	0.00000	1.52800	1.58666	1.52218	1.77256
18.24500	0.75000	1.57900	1.45141	1.39460	1.63819
18.24500	1.50000	1.72200	1.51096	1.12436	1.27198

Table 4 b Data for 6 deg Deflection

X/ δ_{NOM}	Z/ δ_{NOM}	P/P _{TS} (M=2.5)	P/P _{TS} (M=3.0)	P/P _{TS} (M=3.5)	P/P _{TS} (M=4.0)
6.93500	-2.25000	1.01500	1.04200	1.01404	1.03400
6.93500	-1.50000	1.01400	1.03900	1.00789	1.04200
6.93500	-0.75000	1.02000	1.04400	1.00965	1.02700
6.93500	0.00000	1.01700	1.04900	1.01579	1.01300
6.93500	0.37500	1.01800	1.04600	1.00789	1.02000
6.93500	1.12500	1.01100	1.03200	1.00439	1.02000
6.93500	1.87500	1.00500	1.03000	0.99474	1.01600
6.93500	2.62500	1.00600	1.03000	0.97807	1.01300
7.31000	-2.62500	1.01000	1.03700	0.99561	1.03500
7.31000	-1.87500	1.01300	1.03300	1.00263	1.02000
7.31000	-1.12500	1.01000	1.03200	1.01579	1.03900

Table 4 b (Continued) Data for 6 deg Deflection

X/ δ_{NOM}	Z/ δ_{NOM}	P/P _{TS} (M=2.5)	P/P _{TS} (M=3.0)	P/P _{TS} (M=3.5)	P/P _{TS} (M=4.0)
7.31000	-0.37500	1.01300	1.03400	1.01404	1.02400
7.31000	0.00000	1.01300	1.03900	1.02018	1.02400
7.31000	0.75000	1.01500	1.04000	1.02544	1.03200
7.31000	1.50000	1.01000	1.03700	1.01228	1.02800
7.31000	2.25000	1.00900	1.03400	0.99737	1.03500
7.68500	-2.25000	1.00900	1.03400	1.00789	1.04500
7.68500	-1.50000	1.00900	1.03700	1.01404	1.03800
7.68500	-0.75000	1.00700	1.03000	1.00789	1.02400
7.68500	0.00000	1.00900	1.03100	1.01579	1.02400
7.68500	0.37500	1.00500	1.02700	1.00965	1.02400
7.68500	1.12500	0.99930	1.02300	1.00439	1.01300
7.68500	1.87500	1.00000	1.02500	1.00088	1.01600
7.68500	2.62500	1.00000	1.02200	0.98596	1.02000
8.06000	-2.62500	1.01300	1.03100	1.01053	1.05400
8.06000	-1.87500	1.01000	1.02500	1.00877	1.03500
8.06000	-1.12500	1.01100	1.03000	1.01404	1.04700
8.06000	-0.37500	1.01000	1.02500	1.02368	1.05000
8.06000	0.75000	1.00800	1.02100	1.01754	1.03900
8.06000	1.50000	1.00500	1.02300	1.01053	1.04300
8.06000	2.25000	1.00600	1.01800	0.99211	1.03900
8.43500	-2.25000	1.13200	1.09000	1.06930	1.12100
8.43500	-1.50000	1.01000	1.01900	1.01140	1.03800
8.43500	-0.75000	1.00700	1.01600	1.00789	1.03100
8.43500	0.00000	1.00500	1.01100	1.01404	1.03100
8.43500	0.37500	1.00100	1.01100	1.01140	1.02400
8.43500	1.12500	1.00000	1.01100	1.01140	1.00900

Table 4 b (Continued) Data for 6 deg Deflection

X/ δ_{NOM}	Z/ δ_{NOM}	P/P _{TS} (M=2.5)	P/P _{TS} (M=3.0)	P/P _{TS} (M=3.5)	P/P _{TS} (M=4.0)
8.43500	1.87500	1.00900	1.01100	0.99474	1.03800
8.43500	2.62500	1.31300	1.34700	1.32719	1.37800
8.81000	-1.87500	1.14700	1.09400	1.09035	1.12800
8.81000	-1.12500	1.00900	1.01100	1.01404	1.02400
8.81000	-0.37500	1.00700	1.00900	1.02368	1.03200
8.81000	0.00000	1.00200	1.00400	1.01228	1.02000
8.81000	0.75000	1.00300	1.00800	1.02544	1.04300
8.81000	1.50000	1.02900	1.01600	1.01754	1.05000
8.81000	2.25000	1.28100	1.28900	1.27719	1.31500
9.18500	-2.25000	1.32300	1.33800	1.33333	1.38900
9.18500	-1.50000	1.13100	1.07200	1.06404	1.09900
9.18500	-0.75000	1.00900	1.00600	1.01579	1.04500
9.18500	0.00000	1.00900	1.00300	1.01579	1.04500
9.18500	0.37500	1.00300	1.00100	1.01579	1.03800
9.18500	1.12500	1.01900	1.00200	1.00965	1.03800
9.18500	1.87500	1.25000	1.24000	1.21404	1.24400
9.56000	-1.87500	1.30300	1.30900	1.28860	1.35900
9.56000	-1.12500	1.13100	1.04700	1.04737	1.09900
9.56000	-0.37500	1.02800	0.99480	1.00088	1.02400
9.56000	0.00000	1.02800	0.99830	1.00789	1.03100
9.56000	0.75000	1.05200	1.01000	1.02193	1.06500
9.56000	1.50000	1.24200	1.19900	1.17105	1.22900
9.56000	2.25000	1.35200	1.38100	1.36140	1.43800
9.56000	-2.25000	1.34800	1.38200	1.36053	1.42500
9.56000	-1.50000	1.23100	1.18800	1.16579	1.19700
9.56000	-0.75000	1.04000	0.99710	1.00439	1.04900

Table 4 b (Continued) Data for 6 deg Deflection

X/ δ_{NOM}	Z/ δ_{NOM}	P/P _{TS} (M=2.5)	P/P _{TS} (M=3.0)	P/P _{TS} (M=3.5)	P/P _{TS} (M=4.0)
9.56000	0.37500	1.01700	0.99240	1.00088	1.02400
9.56000	1.12500	1.12900	1.04700	1.03596	1.08500
9.56000	1.87500	1.29700	1.31100	1.28509	1.33800
9.93500	-1.87500	1.32000	1.35300	1.32018	1.38500
9.93500	-1.12500	1.21300	1.16400	1.13684	1.18100
9.93500	-0.37500	1.05600	1.01400	1.02368	1.06500
9.93500	0.00000	1.03700	1.01300	1.01754	1.05800
9.93500	0.75000	1.13500	1.05400	1.05000	1.09100
9.93500	1.50000	1.28000	1.27800	1.25263	1.31100
9.93500	2.25000	1.33100	1.39100	1.36842	1.44100
10.31000	-2.25000	1.30700	1.36500	1.34035	1.42900
10.31000	-1.50000	1.29000	1.31900	1.28684	1.33500
10.31000	-0.75000	1.18100	1.13800	1.10088	1.14300
10.31000	0.00000	1.06600	1.01900	1.01140	1.04900
10.31000	0.37500	1.10100	1.03900	1.02105	1.07400
10.31000	1.12500	1.23900	1.24000	1.20263	1.24100
10.31000	1.87500	1.30400	1.35800	1.32018	1.38200
10.68500	-1.87500	1.30900	1.35800	1.33509	1.40800
10.68500	-1.12500	1.26400	1.28900	1.25263	1.32200
10.68500	-0.37500	1.17900	1.12200	1.08509	1.13600
10.68500	0.00000	1.16100	1.06700	1.04737	1.11000
10.68500	0.75000	1.22200	1.21500	1.16491	1.21800
10.68500	1.50000	1.29500	1.33200	1.30702	1.36700
10.68500	2.25000	1.31400	1.36300	1.35702	1.42600
11.06000	-2.25000	1.31100	1.35200	1.35351	1.42100
11.06000	-1.50000	1.30800	1.32900	1.30877	1.37400

Table 4 b (Continued) Data for 6 deg Deflection

X/ δ_{NOM}	Z/ δ_{NOM}	P/P _{TS} (M=2.5)	P/P _{TS} (M=3.0)	P/P _{TS} (M=3.5)	P/P _{TS} (M=4.0)
11.06000	-0.75000	1.26700	1.24800	1.20877	1.26200
11.06000	0.37500	1.24900	1.18700	1.14211	1.20100
11.06000	1.12500	1.28100	1.29500	1.26404	1.32000
11.06000	1.87500	1.31200	1.35200	1.33684	1.38200
11.43500	-1.87500	1.33100	1.36000	1.35175	1.43000
11.43500	-1.12500	1.32400	1.30200	1.28421	1.35200
11.43500	-0.37500	1.35000	1.26800	1.22105	1.28900
11.43500	0.00000	1.34800	1.26500	1.20614	1.27700
11.43500	0.75000	1.32500	1.27300	1.24737	1.32200
11.43500	1.50000	1.32200	1.33800	1.33333	1.40400
11.43500	2.25000	1.33300	1.38100	1.39649	1.49000
11.81000	-2.25000	1.30000	1.33900	1.34561	1.43900
11.81000	-1.50000	1.34300	1.34400	1.32719	1.41000
11.81000	-0.75000	1.37400	1.31100	1.27895	1.35600
11.81000	0.00000	1.41600	1.35400	1.28509	1.35600
11.81000	0.37500	1.40100	1.33300	1.27193	1.33100
11.81000	1.12500	1.33700	1.31900	1.29737	1.37100
11.81000	1.87500	1.33800	1.38000	1.36491	1.43200
12.18500	-1.87500	1.36900	1.40100	1.37632	1.50500
12.18500	-1.12500	1.40300	1.36600	1.32018	1.42300
12.18500	-0.37500	1.46100	1.42000	1.34825	1.46700
12.18500	0.00000	1.47200	1.43800	1.35877	1.47100
12.18500	0.75000	1.43200	1.38600	1.33158	1.42300
12.18500	1.50000	1.37000	1.38800	1.36316	1.46700
12.99500	-1.50000	1.45600	1.42600	1.40175	1.54300
12.99500	-0.75000	1.52600	1.50500	1.43772	1.58400

Table 4 b (Continued) Data for 6 deg Deflection

X/ δ_{NOM}	Z/ δ_{NOM}	P/P _{TS} (M=2.5)	P/P _{TS} (M=3.0)	P/P _{TS} (M=3.5)	P/P _{TS} (M=4.0)
12.99500	0.00000	1.56900	1.56100	1.48684	1.64800
12.99500	0.37500	1.55300	1.54400	1.47368	1.62900
12.99500	1.12500	1.48100	1.45800	1.41140	1.55400
12.99500	1.87500	1.42400	1.44100	1.43596	1.61100
13.37000	-1.87500	1.50600	1.46160	1.45599	1.63196
13.37000	-1.12500	1.55000	1.51668	1.45599	1.61006
13.37000	-0.37500	1.60900	1.59725	1.53125	1.67575
13.37000	0.00000	1.62200	1.61765	1.54470	1.69035
13.37000	0.75000	1.58400	1.56053	1.51424	1.66115
13.37000	1.50000	1.50200	1.48506	1.45779	1.61006
13.74500	-1.50000	1.57100	1.51000	1.47368	1.65200
13.74500	-0.75000	1.63500	1.60000	1.53158	1.70500
13.74500	0.00000	1.67300	1.65000	1.58070	1.74700
13.74500	0.37500	1.66300	1.63200	1.56754	1.72800
13.74500	1.12500	1.58600	1.55000	1.49035	1.65200
13.74500	1.87500	1.52700	1.49100	1.48684	1.68200
14.12000	-1.87500	1.61200	1.54829	1.51603	1.71642
14.12000	-1.12500	1.65800	1.62377	1.55366	1.73832
14.12000	-0.37500	1.72100	1.71251	1.62086	1.81444
14.12000	0.75000	1.69300	1.67477	1.59129	1.77065
14.12000	1.50000	1.61900	1.57379	1.53305	1.70912
14.49500	-1.50000	1.68600	1.62900	1.55614	1.73500
14.49500	-0.75000	1.75300	1.71600	1.62193	1.80700
14.49500	0.00000	1.77800	1.76400	1.65965	1.85600
14.49500	0.37500	1.77400	1.75400	1.64649	1.84100
14.49500	1.12500	1.73000	1.67400	1.58246	1.76600

Table 4 b (Continued) Data for 6 deg Deflection

X/ δ_{NOM}	Z/ δ_{NOM}	P/P _{TS} (M=2.5)	P/P _{TS} (M=3.0)	P/P _{TS} (M=3.5)	P/P _{TS} (M=4.0)
14.49500	1.87500	1.72100	1.58600	1.54912	1.76200
14.87000	-1.87500	1.79300	1.68395	1.60473	1.81444
14.87000	-1.12500	1.80300	1.74005	1.63968	1.84781
14.87000	-0.37500	1.84100	1.81348	1.70150	1.90308
14.87000	0.00000	1.84200	1.81960	1.70418	1.90621
14.87000	0.75000	1.83700	1.77676	1.67731	1.88118
14.87000	1.50000	1.82300	1.69925	1.61727	1.81444
15.24500	-1.50000	1.86900	1.75600	1.65263	1.87500
15.24500	-0.75000	1.89000	1.82600	1.71842	1.93200
15.24500	0.00000	1.90000	1.85400	1.74912	1.97700
15.24500	0.37500	1.90400	1.83600	1.73772	1.95800
15.24500	1.12500	1.91300	1.76700	1.66754	1.89800
15.24500	1.87500	1.92700	1.70400	1.60175	1.84500
15.62000	-1.87500	1.95100	1.80022	1.68896	1.92811
15.62000	-1.12500	1.95800	1.85326	1.73375	1.95730
15.62000	-0.37500	1.95600	1.88794	1.78661	2.00527
15.62000	0.00000	1.96100	1.89100	1.79737	2.02300
15.62000	0.75000	1.98800	1.87060	1.76960	2.00527
15.62000	1.50000	2.01000	1.82572	1.71494	1.95730
15.62000	-1.50000	1.95700	1.82600	1.70702	1.92400
15.62000	-0.75000	1.94800	1.86700	1.76228	1.98500
15.62000	0.37500	1.96500	1.87400	1.76754	1.98500
15.62000	1.12500	1.99000	1.82900	1.72018	1.94000
15.62000	1.87500	1.97900	1.68200	1.57544	1.83700
15.99500	-1.12500	2.03000	1.93180	1.80096	2.03030
15.99500	-0.37500	2.01000	1.96036	1.84844	2.08557

Table 4 b (Continued) Data for 6 deg Deflection

X/ δ_{NOM}	Z/ δ_{NOM}	P/P _{TS} (M=2.5)	P/P _{TS} (M=3.0)	P/P _{TS} (M=3.5)	P/P _{TS} (M=4.0)
15.99500	0.00000	2.01200	1.95730	1.86098	2.10747
15.99500	0.75000	2.04100	1.94302	1.82783	2.06680
15.99500	1.50000	2.07500	1.90324	1.77676	2.02300
16.37000	-1.50000	1.97700	1.98400	1.83772	2.10600
16.37000	-0.75000	2.04300	2.03000	1.87719	2.13600
16.37000	0.00000	2.04000	2.02900	1.89561	2.14700
16.37000	0.37500	2.04300	2.01800	1.89035	2.15500
16.37000	1.12500	2.03800	1.98400	1.84123	2.09100
16.74500	-1.12500	1.90700	2.03277	1.89324	2.18046
16.74500	-0.37500	2.03200	2.07561	1.95148	2.23156
16.74500	0.00000	2.03400	2.07255	1.95686	2.24303
16.74500	0.75000	1.99200	2.05521	1.93446	2.20236
16.74500	1.50000	1.33600	1.46976	1.43539	1.68722
17.12000	-1.50000	1.55000	1.29100	1.23772	1.45200
17.12000	-0.75000	1.90300	2.03200	1.94298	2.25700
17.12000	0.37500	1.95900	2.05400	1.97105	2.30200
17.12000	1.12500	1.61500	1.75300	1.71491	2.02300
17.49500	-1.12500	1.73600	1.65845	1.62892	1.92498
17.49500	-0.37500	1.88800	2.02155	1.98195	2.30872
17.49500	0.00000	1.90300	2.03379	1.98732	2.31289
17.49500	0.75000	1.77800	1.88488	1.86368	2.17316
17.49500	1.50000	1.98800	1.27087	1.02682	1.23987
17.87000	-1.50000	2.01000	1.63700	1.14298	1.25100
17.87000	-0.75000	1.83900	1.80600	1.77719	2.11000
17.87000	0.00000	1.85400	1.97300	1.92807	2.27200
17.87000	0.37500	1.84300	1.91900	1.87281	2.21900

Table 4 b (Continued) Data for 6 deg Deflection

X/δ_{NOM}	Z/δ_{NOM}	P/P_{TS} (M=2.5)	P/P_{TS} (M=3.0)	P/P_{TS} (M=3.5)	P/P_{TS} (M=4.0)
17.87000	1.12500	1.97900	1.42600	1.40175	1.68200
18.24500	-1.12500	1.98400	1.59215	1.38700	1.67575
18.24500	-0.37500	1.85400	1.83184	1.81618	2.15126
18.24500	0.00000	1.84200	1.86040	1.84665	2.18776
18.24500	0.75000	1.92300	1.64009	1.63788	1.96460
18.24500	1.50000	2.04100	1.91140	1.47661	1.60276

Table 4 c Data for 8 deg Deflection

X/δ_{NOM}	Z/δ_{NOM}	P/P_{TS} (M=2.5)	P/P_{TS} (M=3.0)	P/P_{TS} (M=3.5)	P/P_{TS} (M=4.0)
6.93500	-2.25000	1.01500	1.04100	1.00614	1.03800
6.93500	-1.50000	1.01200	1.04000	1.01053	1.03800
6.93500	-0.75000	1.01800	1.04700	1.01579	1.03100
6.93500	0.00000	1.01600	1.04800	1.01404	1.02400
6.93500	0.37500	1.01600	1.04700	1.01053	1.03100
6.93500	1.12500	1.01000	1.03100	1.00614	1.00900
6.93500	1.87500	1.00300	1.02900	0.99737	1.02700
6.93500	2.62500	1.00500	1.03300	0.97632	1.01600
7.31000	-2.62500	1.00900	1.03400	1.00263	1.03900
7.31000	-1.87500	1.01200	1.03300	1.00702	1.00900
7.31000	-1.12500	1.00900	1.03200	1.02018	1.04300
7.31000	-0.37500	1.01000	1.03200	1.01754	1.03600
7.31000	0.00000	1.01000	1.03900	1.02368	1.02100
7.31000	0.75000	1.01400	1.04000	1.02018	1.04300
7.31000	1.50000	1.00900	1.03700	1.01579	1.04300

Table 4 c (Continued) Data for 8 deg Deflection

X/ δ_{NOM}	Z/ δ_{NOM}	P/P _{TS} (M=2.5)	P/P _{TS} (M=3.0)	P/P _{TS} (M=3.5)	P/P _{TS} (M=4.0)
7.31000	2.25000	1.00600	1.03700	0.99737	1.03900
7.68500	-2.25000	1.00700	1.03300	1.01053	1.04900
7.68500	-1.50000	1.00900	1.03800	1.01228	1.04200
7.68500	-0.75000	1.00500	1.03100	1.01053	1.02000
7.68500	0.00000	1.00800	1.03200	1.02105	1.02700
7.68500	0.37500	1.00300	1.02600	1.01579	1.02700
7.68500	1.12500	0.99800	1.02200	1.00614	1.01600
7.68500	1.87500	0.99870	1.02600	1.00263	1.02000
7.68500	2.62500	0.99870	1.02000	0.98772	1.02400
8.06000	-2.62500	1.07100	1.07600	1.06053	1.11400
8.06000	-1.87500	1.00800	1.02300	1.00877	1.04700
8.06000	-1.12500	1.01000	1.03000	1.01404	1.03600
8.06000	-0.37500	1.00600	1.02300	1.02368	1.05400
8.06000	0.75000	1.00700	1.02400	1.01754	1.04300
8.06000	1.50000	1.00300	1.02300	1.01053	1.03900
8.06000	2.25000	1.01300	1.02400	0.99912	1.05400
8.43500	-2.25000	1.22000	1.17100	1.13509	1.16900
8.43500	-1.50000	1.00900	1.02000	1.01404	1.04200
8.43500	-0.75000	1.00600	1.01700	1.01404	1.02700
8.43500	0.00000	1.00200	1.01000	1.01930	1.03400
8.43500	0.37500	1.00100	1.01000	1.01404	1.03100
8.43500	1.12500	0.99870	1.01200	1.01404	1.02000
8.43500	1.87500	1.03100	1.01700	1.00439	1.06400
8.43500	2.62500	1.37200	1.41500	1.40088	1.44500
8.81000	-2.62500	1.40500	1.44500	1.44825	1.55100
8.81000	-1.87500	1.22000	1.16500	1.15439	1.19300

Table 4 c (Continued) Data for 8 deg Deflection

X/ δ_{NOM}	Z/ δ_{NOM}	P/P _{TS} (M=2.5)	P/P _{TS} (M=3.0)	P/P _{TS} (M=3.5)	P/P _{TS} (M=4.0)
8.81000	-1.12500	1.01000	1.01300	1.01754	1.03600
8.81000	-0.37500	1.00600	1.00900	1.02368	1.03600
8.81000	0.00000	0.99930	1.00200	1.01228	1.03200
8.81000	0.75000	1.00100	1.00800	1.02018	1.03900
8.81000	1.50000	1.06400	1.02600	1.02544	1.07700
8.81000	2.25000	1.35500	1.36300	1.35000	1.40200
9.18500	-2.25000	1.40700	1.43000	1.41579	1.49200
9.18500	-1.50000	1.20500	1.13200	1.12018	1.15100
9.18500	-0.75000	1.01100	1.00800	1.01404	1.04200
9.18500	0.00000	1.00700	1.00400	1.01754	1.04900
9.18500	0.37500	1.00500	1.00200	1.01754	1.04200
9.18500	1.12500	1.05200	1.01200	1.01930	1.05600
9.18500	1.87500	1.32400	1.32000	1.29474	1.32500
9.56000	-1.87500	1.38300	1.39800	1.36842	1.44700
9.56000	-1.12500	1.20100	1.10100	1.09649	1.13600
9.56000	-0.37500	1.03100	0.99710	1.00088	1.02800
9.56000	0.00000	1.02700	0.99940	1.01404	1.04200
9.56000	0.75000	1.09400	1.02000	1.02719	1.08000
9.56000	1.50000	1.31700	1.28500	1.25263	1.31200
9.56000	2.25000	1.44200	1.48500	1.46579	1.54400
9.56000	-2.25000	1.43700	1.48900	1.46053	1.54300
9.56000	-1.50000	1.30700	1.27200	1.24123	1.29200
9.56000	-0.75000	1.07600	1.00600	1.01404	1.06400
9.56000	0.37500	1.02100	0.99360	1.00614	1.02000
9.56000	1.12500	1.20100	1.10700	1.08421	1.13600
9.56000	1.87500	1.37500	1.39500	1.36404	1.41900

Table 4 c (Continued) Data for 8 deg Deflection

X/ δ_{NOM}	Z/ δ_{NOM}	P/P _{TS} (M=2.5)	P/P _{TS} (M=3.0)	P/P _{TS} (M=3.5)	P/P _{TS} (M=4.0)
9.93500	-1.87500	1.40700	1.44900	1.41491	1.48800
9.93500	-1.12500	1.28600	1.25000	1.21404	1.27500
9.93500	-0.37500	1.09200	1.02100	1.02719	1.06900
9.93500	0.00000	1.05000	1.01100	1.02193	1.06900
9.93500	0.75000	1.20200	1.10100	1.08509	1.14000
9.93500	1.50000	1.35800	1.36700	1.33684	1.39400
9.93500	2.25000	1.43800	1.50600	1.49123	1.57800
10.31000	-2.25000	1.43000	1.50600	1.48246	1.58600
10.31000	-1.50000	1.37700	1.41100	1.37895	1.43000
10.31000	-0.75000	1.25600	1.22000	1.17807	1.20900
10.31000	0.00000	1.13000	1.03000	1.01754	1.06700
10.31000	0.37500	1.16800	1.08100	1.05526	1.11100
10.31000	1.12500	1.32000	1.33000	1.28772	1.32800
10.31000	1.87500	1.40500	1.46300	1.44035	1.49200
10.68500	-1.87500	1.43300	1.48600	1.47105	1.55900
10.68500	-1.12500	1.35800	1.37700	1.34211	1.41700
10.68500	-0.37500	1.29900	1.20200	1.15965	1.20000
10.68500	0.00000	1.29600	1.13600	1.09211	1.15900
10.68500	0.75000	1.32200	1.30100	1.25088	1.31200
10.68500	1.50000	1.40400	1.43500	1.41491	1.47700
10.68500	2.25000	1.46500	1.52900	1.54035	1.64100
11.06000	-2.25000	1.45500	1.51700	1.53333	1.63000
11.06000	-1.50000	1.43100	1.45100	1.43421	1.49900
11.06000	-0.75000	1.40700	1.34400	1.30965	1.37200
11.06000	0.37500	1.42200	1.30500	1.24474	1.31400
11.06000	1.12500	1.39300	1.39300	1.37105	1.42600

Table 4 c (Continued) Data for 8 deg Deflection

X/ δ_{NOM}	Z/ δ_{NOM}	P/P _{TS} (M=2.5)	P/P _{TS} (M=3.0)	P/P _{TS} (M=3.5)	P/P _{TS} (M=4.0)
11.06000	1.87500	1.44900	1.50400	1.49386	1.56400
11.43500	-1.87500	1.48800	1.52800	1.52544	1.64100
11.43500	-1.12500	1.47400	1.41900	1.39649	1.48400
11.43500	-0.37500	1.56100	1.43300	1.36842	1.45000
11.43500	0.00000	1.57300	1.45300	1.37807	1.45800
11.43500	0.75000	1.50700	1.40100	1.36667	1.43900
11.43500	1.50000	1.46300	1.47900	1.47281	1.55900
11.43500	2.25000	1.44800	1.52000	1.54561	1.68200
11.81000	-1.50000	1.51200	1.50700	1.48246	1.59000
11.81000	-0.75000	1.59500	1.49100	1.43070	1.51400
11.81000	0.00000	1.66900	1.57500	1.49035	1.57500
11.81000	0.37500	1.64700	1.54300	1.45526	1.53200
11.81000	1.12500	1.53200	1.46800	1.42895	1.52100
11.81000	1.87500	1.50000	1.56100	1.55000	1.65500
12.18500	-1.87500	1.55800	1.58600	1.57544	1.76100
12.18500	-1.12500	1.63800	1.54300	1.47632	1.61900
12.18500	-0.37500	1.75100	1.67000	1.57544	1.71200
12.18500	0.00000	1.76900	1.70100	1.59737	1.74200
12.18500	0.75000	1.69500	1.60700	1.52895	1.64100
12.18500	1.50000	1.57300	1.55500	1.52719	1.65600
12.99500	-1.50000	1.78500	1.65300	1.61140	1.78400
12.99500	-0.75000	1.93800	1.79900	1.70175	1.87500
12.99500	0.00000	1.99700	1.87900	1.78070	1.98500
12.99500	0.37500	1.98000	1.85200	1.75965	1.95100
12.99500	1.12500	1.83800	1.70700	1.63421	1.80000
12.99500	1.87500	1.68900	1.65000	1.66404	1.89400

Table 4 c (Continued) Data for 8 deg Deflection

X/ δ_{NOM}	Z/ δ_{NOM}	P/P _{TS} (M=2.5)	P/P _{TS} (M=3.0)	P/P _{TS} (M=3.5)	P/P _{TS} (M=4.0)
13.37000	-1.87500	1.86159	1.70176	1.68563	1.93403
13.37000	-1.12500	2.01388	1.82082	1.71659	1.91933
13.37000	-0.37500	2.11308	1.95425	1.83952	2.05582
13.37000	0.00000	2.11909	1.97478	1.85809	2.07052
13.37000	0.75000	2.07901	1.88445	1.79264	1.99703
13.37000	1.50000	1.90568	1.73973	1.67768	1.88258
13.74500	-1.50000	2.06800	1.81800	1.74474	1.97000
13.74500	-0.75000	2.19400	1.98700	1.86754	2.08300
13.74500	0.00000	2.22100	2.05500	1.93684	2.16600
13.74500	0.37500	2.21400	2.03400	1.91228	2.13600
13.74500	1.12500	2.13300	1.87900	1.77895	1.98500
13.74500	1.87500	1.95600	1.72400	1.71316	1.95800
14.12000	-1.87500	2.16818	1.83416	1.73869	2.01173
14.12000	-1.12500	2.29944	2.02404	1.88374	2.12617
14.12000	-0.37500	2.32649	2.15542	2.00225	2.26582
14.12000	0.75000	2.32448	2.08870	1.93415	2.19547
14.12000	1.50000	2.29643	1.91011	1.81298	2.07052
14.49500	-1.50000	2.42200	2.05300	1.91667	2.14700
14.49500	-0.75000	2.41600	2.18900	2.03684	2.29500
14.49500	0.00000	2.40800	2.24100	2.09298	2.37100
14.49500	0.37500	2.41200	2.22500	2.07456	2.34800
14.49500	1.12500	2.44600	2.09300	1.94474	2.18900
14.87000	-1.12500	2.53790	2.25601	2.06592	2.35821
14.87000	-0.37500	2.49181	2.33093	2.16409	2.46846
14.87000	0.00000	2.48680	2.33709	2.17116	2.48316
14.87000	0.75000	2.51986	2.28372	2.10837	2.42436

Table 4 c (Continued) Data for 8 deg Deflection

X/ δ_{NOM}	Z/ δ_{NOM}	P/P _{TS} (M=2.5)	P/P _{TS} (M=3.0)	P/P _{TS} (M=3.5)	P/P _{TS} (M=4.0)
14.87000	1.50000	2.62406	2.17903	2.00225	2.28787
15.24500	-1.50000	2.67600	2.36200	2.14561	2.43900
15.24500	-0.75000	2.57800	2.41800	2.23597	2.53700
15.24500	0.00000	2.54900	2.42800	2.28509	2.60900
15.24500	0.37500	2.56000	2.42200	2.26491	2.58600
15.24500	1.12500	2.64500	2.35300	2.14386	2.43900
15.62000	-1.12500	2.68117	2.55366	2.29586	2.61230
15.62000	-0.37500	2.59701	2.53621	2.35334	2.68895
15.62000	0.00000	2.59200	2.52800	2.37368	2.71100
15.62000	0.75000	2.63709	2.54134	2.33124	2.67845
15.62000	1.50000	2.77034	2.51158	2.26844	2.60495
15.62000	-1.50000	2.75400	2.54100	2.28509	2.59700
15.62000	-0.75000	2.62400	2.54000	2.33947	2.67300
15.62000	0.37500	2.60100	2.52300	2.35702	2.68400
15.62000	1.12500	2.69800	2.52100	2.27018	2.59000
15.99500	-1.12500	2.68919	2.70249	2.44620	2.79290
15.99500	-0.37500	2.61404	2.61730	2.46124	2.83700
15.99500	0.00000	2.60703	2.60395	2.46654	2.84014
15.99500	0.75000	2.63308	2.64706	2.45328	2.81495
15.99500	1.50000	2.64811	2.68504	2.40198	2.76665
16.37000	-1.50000	1.57000	1.76200	1.67368	1.98100
16.37000	-0.75000	2.56300	2.68800	2.55789	2.96800
16.37000	0.00000	2.59100	2.63400	2.52807	2.93800
16.37000	0.37500	2.58000	2.64500	2.52982	2.93400
16.37000	1.12500	2.28400	2.59100	2.50000	2.90700
16.74500	-1.12500	1.99585	2.22521	2.25695	2.74145

Table 4 c (Continued) Data for 8 deg Deflection

X/ δ_{NOM}	Z/ δ_{NOM}	P/P _{TS} (M=2.5)	P/P _{TS} (M=3.0)	P/P _{TS} (M=3.5)	P/P _{TS} (M=4.0)
16.74500	-0.37500	2.49882	2.62038	2.55763	2.98819
16.74500	0.00000	2.51786	2.62243	2.55587	2.98819
16.74500	0.75000	2.33651	2.53108	2.52049	2.97664
16.74500	1.50000	2.02791	1.35791	0.95955	1.16441
17.12000	-1.50000	2.36300	1.56900	1.02632	1.25500
17.12000	-0.75000	2.26500	2.34100	2.36404	2.84300
17.12000	0.37500	2.38500	2.49100	2.48684	2.96800
17.12000	1.12500	2.28000	1.77900	1.76930	2.14700
17.49500	-1.12500	2.39562	1.76231	1.66087	2.04427
17.49500	-0.37500	2.34352	2.34838	2.36661	2.86639
17.49500	0.00000	2.35454	2.38431	2.39579	2.91%[PrinterError: Opera
17.49500	0.75000	2.35454	2.08255	2.09953	2.56821
17.49500	1.50000	2.39762	2.04457	1.38053	1.64319
17.87000	-1.50000	2.38500	2.25700	1.60965	1.72800
17.87000	-0.75000	2.34900	1.95300	1.98421	2.45700
17.87000	0.00000	2.32800	2.20600	2.24912	2.77100
17.87000	0.37500	2.33200	2.13200	2.17807	2.68800
17.87000	1.12500	2.38800	2.01500	1.46667	1.80300
18.24500	-1.12500	2.35454	2.26730	1.48134	1.85318
18.24500	-0.37500	2.28641	1.99941	2.01551	2.55351
18.24500	0.00000	2.27839	2.03533	2.07123	2.59340
18.24500	0.75000	2.32849	1.98607	1.78380	2.25847
18.24500	1.50000	2.34853	2.42433	1.83775	2.08837

Table 4 d Data for 9 deg Deflection

X/ δ_{NOM}	Z/ δ_{NOM}	P/P _{TS} (M=2.5)
6.93500	-2.25000	1.01600
6.93500	-1.50000	1.01400
6.93500	-0.75000	1.02000
6.93500	0.00000	1.01700
6.93500	0.37500	1.01700
6.93500	1.12500	1.01100
6.93500	1.87500	1.00600
6.93500	2.62500	1.00600
7.31000	-2.62500	1.01000
7.31000	-1.87500	1.01300
7.31000	-1.12500	1.00900
7.31000	-0.37500	1.01000
7.31000	0.00000	1.01000
7.31000	0.75000	1.01400
7.31000	1.50000	1.00700
7.31000	2.25000	1.00700
7.68500	-2.25000	1.00900
7.68500	-1.50000	1.01000
7.68500	-0.75000	1.00800
7.68500	0.00000	1.00900
7.68500	0.37500	1.00600
7.68500	1.12500	0.99930
7.68500	1.87500	1.00000
7.68500	2.62500	1.00100
8.06000	-2.62500	1.15100

Table 4 d (Continued) Data for 9 deg Deflection

X/ δ_{NOM}	Z/ δ_{NOM}	P/P _{TS} (M=2.5)
8.06000	-1.87500	1.00800
8.06000	-1.12500	1.00900
8.06000	-0.37500	1.00600
8.06000	0.00000	1.00800
8.06000	0.75000	1.00700
8.06000	1.50000	1.00300
8.06000	2.25000	1.02500
8.43500	-2.25000	1.26700
8.43500	-1.50000	1.01100
8.43500	-0.75000	1.00700
8.43500	0.00000	1.00300
8.43500	0.37500	1.00300
8.43500	1.12500	1.00000
8.43500	1.87500	1.05600
8.43500	2.62500	1.41200
8.81000	-2.62500	1.44400
8.81000	-1.87500	1.26500
8.81000	-1.12500	1.01200
8.81000	-0.37500	1.00500
8.81000	0.00000	0.99930
8.81000	0.75000	1.00200
8.81000	1.50000	1.09700
8.81000	2.25000	1.39600
9.18500	-2.25000	1.45800
9.18500	-1.50000	1.25100
9.18500	-0.75000	1.01800

Table 4 d (Continued) Data for 9 deg Deflection

X/ δ_{NOM}	Z/ δ_{NOM}	P/P _{TS} (M=2.5)
9.18500	0.00000	1.01000
9.18500	0.37500	1.00500
9.18500	1.12500	1.08700
9.18500	1.87500	1.36900
9.56000	-1.87500	1.43100
9.56000	-1.12500	1.24800
9.56000	-0.37500	1.04100
9.56000	0.00000	1.03100
9.56000	0.75000	1.12800
9.56000	1.50000	1.36000
9.56000	2.25000	1.49700
9.56000	-2.25000	1.49600
9.56000	-1.50000	1.35200
9.56000	-0.75000	1.11000
9.56000	0.37500	1.02900
9.56000	1.12500	1.24600
9.56000	1.87500	1.42200
9.93500	-1.87500	1.46100
9.93500	-1.12500	1.33400
9.93500	-0.37500	1.13200
9.93500	0.00000	1.07900
9.93500	0.75000	1.25200
9.93500	1.50000	1.40400
9.93500	2.25000	1.50500
10.31000	-2.25000	1.51500
10.31000	-1.50000	1.43700

Table 4 d (Continued) Data for 9 deg Deflection

X/ δ_{NOM}	Z/ δ_{NOM}	P/P _{TS} (M=2.5)
10.31000	-0.75000	1.38800
10.31000	0.00000	1.40700
10.31000	0.37500	1.38600
10.31000	1.12500	1.39000
10.31000	1.87500	1.47600
10.68500	-1.87500	1.51400
10.68500	-1.12500	1.55000
10.68500	-0.37500	1.71600
10.68500	0.00000	1.72600
10.68500	0.75000	1.65100
10.68500	1.50000	1.49800
10.68500	2.25000	1.54500
11.06000	-2.25000	1.51000
11.06000	-1.50000	1.63500
11.06000	-0.75000	1.85400
11.06000	0.00000	1.88900
11.06000	0.37500	1.88600
11.06000	1.12500	1.74300
11.06000	1.87500	1.55600
11.43500	-1.87500	1.69000
11.43500	-1.12500	1.95900
11.43500	-0.37500	2.03500
11.43500	0.00000	2.03700
11.43500	0.75000	2.02000
11.43500	1.50000	1.82200
11.81000	-1.50000	2.00100

Table 4 d (Continued) Data for 9 deg Deflection

X/ δ_{NOM}	Z/ δ_{NOM}	P/P _{TS} (M=2.5)
11.81000	-0.75000	2.13000
11.81000	0.00000	2.13700
11.81000	0.37500	2.13600
11.81000	1.12500	2.10000
11.81000	1.87500	1.83200
12.18500	-1.87500	2.13000
12.18500	-1.12500	2.24000
12.18500	-0.37500	2.24800
12.18500	0.00000	2.24800
12.18500	0.75000	2.24500
12.18500	1.50000	2.19500
12.99500	-1.50000	2.50200
12.99500	-0.75000	2.43500
12.99500	0.00000	2.43700
12.99500	0.37500	2.43500
12.99500	1.12500	2.45500
12.99500	1.87500	2.53600
13.37000	-1.87500	2.59939
13.37000	-1.12500	2.54182
13.37000	-0.37500	2.52365
13.37000	0.00000	2.52567
13.37000	0.75000	2.52567
13.37000	1.50000	2.58626
13.74500	-1.50000	2.64500
13.74500	-0.75000	2.59000
13.74500	0.00000	2.58600

Table 4 d (Continued) Data for 9 deg Deflection

X/ δ_{NOM}	Z/ δ_{NOM}	P/P _{TS} (M=2.5)
13.74500	0.37500	2.58400
13.74500	1.12500	2.61100
14.12000	-1.12500	2.68421
14.12000	-0.37500	2.66402
14.12000	0.00000	2.66402
14.12000	0.75000	2.66806
14.12000	1.50000	2.72360
14.49500	-1.50000	2.78500
14.49500	-0.75000	2.72700
14.49500	0.00000	2.72200
14.49500	0.37500	2.72200
14.49500	1.12500	2.75100
14.87000	-1.12500	2.81550
14.87000	-0.37500	2.78520
14.87000	0.00000	2.78217
14.87000	0.75000	2.79530
14.87000	1.50000	2.86801
15.24500	-1.50000	2.92700
15.24500	-0.75000	2.84400
15.24500	0.00000	2.83100
15.24500	0.37500	2.83500
15.24500	1.12500	2.87900
15.62000	-1.12500	2.91345
15.62000	-0.37500	2.86599
15.62000	0.00000	2.86700
15.62000	0.75000	2.88013

Table 4 d (Continued) Data for 9 deg Deflection

X/ δ_{NOM}	Z/ δ_{NOM}	P/P _{TS} (M=2.5)
15.62000	1.50000	2.95486
15.62000	-1.50000	2.97800
15.62000	-0.75000	2.87500
15.62000	0.37500	2.86500
15.62000	1.12500	2.91400
15.99500	-1.12500	2.83367
15.99500	-0.37500	2.87306
15.99500	0.00000	2.87811
15.99500	0.75000	2.84983
15.99500	1.50000	1.72586
16.37000	-1.50000	1.74700
16.37000	-0.75000	2.74500
16.37000	0.00000	2.84800
16.37000	0.37500	2.82700
16.37000	1.12500	2.28800
16.74500	-1.12500	2.54687
16.74500	-0.37500	2.76803
16.74500	0.00000	2.79732
16.74500	0.75000	2.67311
16.74500	1.50000	2.48325
17.12000	-1.50000	2.46200
17.12000	-0.75000	2.64300
17.12000	0.00000	2.73900
17.12000	0.37500	2.70400
17.12000	1.12500	2.59500
17.49500	-1.12500	2.58525

Table 4 d (Continued) Data for 9 deg Deflection

X/ δ_{NOM}	Z/ δ_{NOM}	P/P _{TS} (M=2.5)
17.49500	-0.37500	2.66604
17.49500	0.00000	2.68220
17.49500	0.75000	2.62968
17.49500	1.50000	2.47315
17.87000	-1.50000	2.50600
17.87000	-0.75000	2.59400
17.87000	0.00000	2.63100
17.87000	0.37500	2.61400
17.87000	1.12500	2.56700
18.24500	-1.12500	2.57919
18.24500	-0.37500	2.59434
18.24500	0.00000	2.60040
18.24500	0.75000	2.58626
18.24500	1.50000	2.52062

Table 4 e Data for 10 deg Deflection

X/ δ_{NOM}	Z/ δ_{NOM}	P/P _{TS} (M=3.0)	P/P _{TS} (M=3.5)	P/P _{TS} (M=4.0)
6.93500	-2.25000	1.04200	1.01053	1.03400
6.93500	-1.50000	1.04200	1.01053	1.04200
6.93500	-0.75000	1.04400	1.01228	1.02700
6.93500	0.00000	1.04700	1.02105	1.02000
6.93500	0.37500	1.04400	1.01053	1.02000
6.93500	1.12500	1.03400	1.00614	1.02000
6.93500	1.87500	1.03000	0.99561	1.01600

Table 4 e (Continued) Data for 10 deg Deflection

X/ δ_{NOM}	Z/ δ_{NOM}	P/P _{TS} (M=3.0)	P/P _{TS} (M=3.5)	P/P _{TS} (M=4.0)
6.93500	2.62500	1.03200	0.98070	1.01300
7.31000	-2.62500	1.02900	0.99737	1.03200
7.31000	-1.87500	1.03000	1.00439	1.01700
7.31000	-1.12500	1.03100	1.01754	1.04300
7.31000	-0.37500	1.02900	1.01228	1.02800
7.31000	0.00000	1.03600	1.02105	1.02800
7.31000	0.75000	1.03500	1.02281	1.03600
7.31000	1.50000	1.03000	1.01404	1.03200
7.31000	2.25000	1.02900	1.00263	1.03200
7.68500	-2.25000	1.03400	1.00263	1.04500
7.68500	-1.50000	1.03400	1.01228	1.03800
7.68500	-0.75000	1.03000	1.01404	1.03100
7.68500	0.00000	1.02900	1.01754	1.03100
7.68500	0.37500	1.02700	1.01579	1.01600
7.68500	1.12500	1.02000	1.00263	1.01300
7.68500	1.87500	1.02700	1.00263	1.01600
7.68500	2.62500	1.02200	0.98772	1.03400
8.06000	-2.62500	1.20800	1.17018	1.23400
8.06000	-1.87500	1.02200	1.01228	1.05400
8.06000	-1.12500	1.02400	1.01579	1.03600
8.06000	-0.37500	1.02200	1.02544	1.06200
8.06000	0.75000	1.02100	1.01579	1.04300
8.06000	1.50000	1.02000	1.01404	1.03900
8.06000	2.25000	1.03000	1.01404	1.08000
8.43500	-2.25000	1.27700	1.23509	1.25900
8.43500	-1.50000	1.01900	1.01754	1.03800

Table 4 e (Continued) Data for 10 deg Deflection

X/ δ_{NOM}	Z/ δ_{NOM}	P/P _{TS} (M=3.0)	P/P _{TS} (M=3.5)	P/P _{TS} (M=4.0)
8.43500	-0.75000	1.01600	1.01404	1.03100
8.43500	0.00000	1.01300	1.01579	1.02400
8.43500	0.37500	1.01100	1.01404	1.02700
8.43500	1.12500	1.01300	1.01404	1.02400
8.43500	1.87500	1.04600	1.02895	1.07400
8.43500	2.62500	1.50900	1.49386	1.55900
8.81000	-2.62500	1.54300	1.54825	1.67100
8.81000	-1.87500	1.26700	1.24649	1.29000
8.81000	-1.12500	1.00800	1.01930	1.04300
8.81000	-0.37500	1.00300	1.02105	1.03600
8.81000	0.00000	0.99650	1.01404	1.02400
8.81000	0.75000	1.00500	1.02281	1.04700
8.81000	1.50000	1.05300	1.05526	1.10700
8.81000	2.25000	1.44600	1.43772	1.50300
9.18500	-2.25000	1.55000	1.52368	1.59900
9.18500	-1.50000	1.23400	1.21140	1.23700
9.18500	-0.75000	1.00900	1.01754	1.05200
9.18500	0.00000	1.00300	1.01754	1.04500
9.18500	0.37500	1.00100	1.01754	1.03800
9.18500	1.12500	1.04400	1.03772	1.08900
9.18500	1.87500	1.41700	1.39123	1.42100
9.56000	-1.87500	1.50600	1.47544	1.55500
9.56000	-1.12500	1.20300	1.18333	1.23000
9.56000	-0.37500	0.99420	1.00614	1.03600
9.56000	0.00000	1.00100	1.01404	1.03800
9.56000	0.75000	1.04200	1.05263	1.11000

Table 4 e (Continued) Data for 10 deg Deflection

X/ δ_{NOM}	Z/ δ_{NOM}	P/P _{TS} (M=3.0)	P/P _{TS} (M=3.5)	P/P _{TS} (M=4.0)
9.56000	1.50000	1.38600	1.35439	1.41300
9.56000	2.25000	1.61700	1.60000	1.67500
9.56000	-2.25000	1.62800	1.59649	1.67500
9.56000	-1.50000	1.38000	1.35088	1.38500
9.56000	-0.75000	1.03300	1.03772	1.07400
9.56000	0.37500	0.99710	1.00614	1.02400
9.56000	1.12500	1.21300	1.16667	1.22200
9.56000	1.87500	1.50400	1.46579	1.50800
9.93500	-1.87500	1.57100	1.53509	1.62200
9.93500	-1.12500	1.36000	1.31754	1.38700
9.93500	-0.37500	1.04600	1.05088	1.10300
9.93500	0.00000	1.01300	1.02719	1.07700
9.93500	0.75000	1.20200	1.15877	1.21900
9.93500	1.50000	1.46600	1.44211	1.50300
9.93500	2.25000	1.66700	1.65965	1.76400
10.31000	-2.25000	1.70400	1.70263	1.82300
10.31000	-1.50000	1.52500	1.49561	1.54400
10.31000	-0.75000	1.35000	1.28158	1.31300
10.31000	0.00000	1.14100	1.05526	1.09900
10.31000	0.37500	1.21900	1.12368	1.17500
10.31000	1.12500	1.44200	1.39737	1.43600
10.31000	1.87500	1.61300	1.58860	1.64600
10.68500	-1.87500	1.65400	1.65000	1.77200
10.68500	-1.12500	1.51200	1.46404	1.55100
10.68500	-0.37500	1.60500	1.28947	1.35000
10.68500	0.00000	1.63600	1.23684	1.29000

Table 4 e (Continued) Data for 10 deg Deflection

X/ δ_{NOM}	Z/ δ_{NOM}	P/P _{TS} (M=3.0)	P/P _{TS} (M=3.5)	P/P _{TS} (M=4.0)
10.68500	0.75000	1.51900	1.37456	1.43600
10.68500	1.50000	1.56600	1.54035	1.61900
10.68500	2.25000	1.72600	1.75088	1.89200
11.06000	-2.25000	1.57300	1.60965	1.74000
11.06000	-1.50000	1.61800	1.58684	1.66700
11.06000	-0.75000	1.79900	1.45263	1.51900
11.06000	0.37500	1.90900	1.44035	1.51500
11.06000	1.12500	1.62800	1.49211	1.55900
11.06000	1.87500	1.69200	1.68158	1.76100
11.43500	-1.87500	1.73800	1.73947	1.91400
11.43500	-1.12500	1.88900	1.54825	1.66000
11.43500	-0.37500	2.10800	1.65614	1.86900
11.43500	0.00000	2.11100	1.70439	1.92500
11.43500	0.75000	2.05700	1.56053	1.72300
11.43500	1.50000	1.72100	1.63684	1.74600
11.81000	-1.50000	1.91000	1.67807	1.79700
11.81000	-0.75000	2.25500	1.70789	1.93500
11.81000	0.00000	2.26200	1.86053	2.13400
11.81000	0.37500	2.25900	1.81053	2.08000
11.81000	1.12500	2.12900	1.60965	1.75000
11.81000	1.87500	1.80500	1.76930	1.91300
12.18500	-1.87500	1.92300	1.82544	2.08200
12.18500	-1.12500	2.31700	1.73947	2.04100
12.18500	-0.37500	2.38200	2.02018	2.41900
12.18500	0.00000	2.38300	2.06491	2.45200
12.18500	0.75000	2.37700	1.90877	2.30300

Table 4 e (Continued) Data for 10 deg Deflection

X/ δ_{NOM}	Z/ δ_{NOM}	P/P _{TS} (M=3.0)	P/P _{TS} (M=3.5)	P/P _{TS} (M=4.0)
12.18500	1.50000	2.12500	1.73421	1.91800
12.99500	-1.50000	2.59400	1.99825	2.41900
12.99500	-0.75000	2.61600	2.38947	2.84600
12.99500	0.00000	2.61200	2.46491	2.86500
12.99500	0.37500	2.60900	2.45000	2.86900
12.99500	1.12500	2.62500	2.17632	2.67000
12.99500	1.87500	2.41800	1.90351	2.21700
13.37000	-1.12500	2.78105	2.42823	2.91677
13.37000	-0.37500	2.70608	2.59661	2.96927
13.37000	0.00000	2.71327	2.59482	2.96499
13.37000	0.75000	2.72354	2.56258	3.00999
13.37000	1.50000	2.84472	2.16668	2.68960
13.74500	-1.50000	3.02800	2.41228	2.98700
13.74500	-0.75000	2.81200	2.69561	3.10500
13.74500	0.00000	2.79500	2.70526	3.07400
13.74500	0.37500	2.79100	2.70175	3.07800
13.74500	1.12500	2.89000	2.55614	3.05100
14.12000	-1.12500	2.99569	2.77396	3.24788
14.12000	-0.37500	2.90018	2.80173	3.17394
14.12000	0.75000	2.92483	2.81875	3.21145
14.12000	1.50000	3.16001	2.65215	3.32289
14.49500	-1.50000	3.20800	3.05877	3.71800
14.49500	-0.75000	3.02300	2.92456	3.33700
14.49500	0.00000	3.00000	2.88070	3.27200
14.49500	0.37500	3.00000	2.88684	3.27200
14.49500	1.12500	3.10900	2.94123	3.43600

Table 4 e (Continued) Data for 10 deg Deflection

X/ δ_{NOM}	Z/ δ_{NOM}	P/P _{TS} (M=3.0)	P/P _{TS} (M=3.5)	P/P _{TS} (M=4.0)
14.87000	-1.12500	3.18465	3.19763	3.67221
14.87000	-0.37500	3.10558	2.98355	3.38932
14.87000	0.00000	3.09839	2.97012	3.38182
14.87000	0.75000	3.13741	3.06506	3.47933
14.87000	1.50000	3.25038	3.38125	4.04833
15.24500	-1.50000	3.26100	3.57281	4.19400
15.24500	-0.75000	3.23500	3.17807	3.63000
15.24500	0.00000	3.19800	3.07544	3.53100
15.24500	0.37500	3.20400	3.09825	3.54300
15.24500	1.12500	3.28000	3.38421	3.89000
15.62000	-1.12500	3.36643	3.47618	3.95510
15.62000	-0.37500	3.27708	3.19942	3.66900
15.62000	0.00000	3.27400	3.18509	3.68400
15.62000	0.75000	3.31919	3.31944	3.78794
15.62000	-0.75000	3.30500	3.28596	3.77900
15.62000	0.37500	3.27500	3.19474	3.69100
15.62000	1.12500	3.37300	3.52544	4.03800
15.99500	-1.12500	3.37054	3.51918	4.06654
15.99500	-0.37500	3.31302	3.31048	3.86188
15.99500	0.00000	3.30378	3.29168	3.85866
15.99500	0.75000	3.31611	3.39826	3.92939
16.37000	-0.75000	3.06900	3.23070	3.90100
16.37000	0.00000	3.26000	3.32895	3.96600
16.37000	0.37500	3.22800	3.30877	3.94700
16.37000	1.12500	2.15000	2.27281	2.73900
16.74500	-1.12500	2.12584	1.79139	2.22454

Table 4 e (Continued) Data for 10 deg Deflection

X/ δ_{NOM}	Z/ δ_{NOM}	P/P _{TS} (M=3.0)	P/P _{TS} (M=3.5)	P/P _{TS} (M=4.0)
16.74500	-0.37500	3.05217	3.17703	3.86938
16.74500	0.00000	3.11071	3.24510	3.95832
16.74500	0.75000	2.66911	2.66379	3.26717
17.12000	-0.75000	2.61800	2.44825	3.01000
17.12000	0.37500	2.82900	2.90000	3.61500
17.12000	1.12500	2.70500	1.51228	1.81700
17.49500	-1.12500	3.02958	1.61762	1.93523
17.49500	-0.37500	2.81494	2.62080	3.34539
17.49500	0.00000	2.81083	2.69962	3.43004
17.49500	0.75000	2.89402	2.23207	2.83854
17.87000	-0.75000	2.89600	2.06228	2.65100
17.87000	0.00000	2.80600	2.41404	3.08200
17.87000	0.37500	2.81500	2.31404	2.96800
17.87000	1.12500	2.92500	2.09123	2.24800
18.24500	-1.12500	2.84472	2.45241	2.46672
18.24500	-0.37500	2.82829	2.06637	2.70460
18.24500	0.00000	2.80775	2.12189	2.76032
18.24500	0.75000	2.84267	1.92037	2.43671

Table 4 f Data for 11 deg Deflection

X/ δ_{NOM}	Z/ δ_{NOM}	P/P _{TS} (M=3.0)
6.93500	-2.25000	1.04100
6.93500	-1.50000	1.03800
6.93500	-0.75000	1.04500

Table 4 f (Continued) Data for 11 deg Deflection

X/ δ_{NOM}	Z/ δ_{NOM}	P/P _{TS} (M=3.0)
6.93500	0.00000	1.04400
6.93500	0.37500	1.04500
6.93500	1.12500	1.03100
6.93500	1.87500	1.02600
6.93500	2.62500	1.03300
7.31000	-2.62500	1.03300
7.31000	-1.87500	1.03400
7.31000	-1.12500	1.03300
7.31000	-0.37500	1.03300
7.31000	0.00000	1.04000
7.31000	0.75000	1.03400
7.31000	1.50000	1.03800
7.31000	2.25000	1.03800
7.68500	-2.25000	1.03300
7.68500	-1.50000	1.03600
7.68500	-0.75000	1.02900
7.68500	0.00000	1.03200
7.68500	0.37500	1.02900
7.68500	1.12500	1.02200
7.68500	1.87500	1.02600
7.68500	2.62500	1.02000
8.06000	-2.62500	1.30500
8.06000	-1.87500	1.02600
8.06000	-1.12500	1.04900
8.06000	-0.37500	1.08500
8.06000	0.00000	1.10900

Table 4 f (Continued) Data for 11 deg Deflection

X/ δ_{NOM}	Z/ δ_{NOM}	P/P _{TS} (M=3.0)
8.06000	0.75000	1.06100
8.06000	1.50000	1.03100
8.06000	2.25000	1.04900
8.43500	-2.25000	1.38500
8.43500	-1.50000	1.15900
8.43500	-0.75000	1.31400
8.43500	0.00000	1.38800
8.43500	0.37500	1.36800
8.43500	1.12500	1.22800
8.43500	1.87500	1.17200
8.43500	2.62500	1.56800
8.81000	-2.62500	1.66000
8.81000	-1.87500	1.68900
8.81000	-1.12500	1.69800
8.81000	-0.37500	1.75700
8.81000	0.00000	1.76600
8.81000	0.75000	1.73200
8.81000	1.50000	1.66800
8.81000	2.25000	1.65400
9.18500	-2.25000	1.90100
9.18500	-1.50000	1.89600
9.18500	-0.75000	1.87300
9.18500	0.00000	1.87900
9.18500	0.37500	1.87800
9.18500	1.12500	1.86800
9.18500	1.87500	1.90700

Table 4 f (Continued) Data for 11 deg Deflection

X/ δ_{NOM}	Z/ δ_{NOM}	P/P _{TS} (M=3.0)
9.56000	-1.87500	2.09100
9.56000	-1.12500	1.99000
9.56000	-0.37500	1.97200
9.56000	0.00000	1.96700
9.56000	0.75000	1.97800
9.56000	1.50000	2.03500
9.56000	2.25000	2.11400
9.56000	-2.25000	2.11800
9.56000	-1.50000	2.03000
9.56000	-0.75000	1.97100
9.56000	0.37500	1.96500
9.56000	1.12500	1.98000
9.56000	1.87500	2.06500
9.93500	-1.87500	2.21000
9.93500	-1.12500	2.09300
9.93500	-0.37500	2.06000
9.93500	0.00000	2.06000
9.93500	0.75000	2.06700
9.93500	1.50000	2.14000
9.93500	2.25000	2.28400
10.31000	-2.25000	2.40000
10.31000	-1.50000	2.23900
10.31000	-0.75000	2.15700
10.31000	0.00000	2.14300
10.31000	0.37500	2.14200
10.31000	1.12500	2.18200

Table 4 f (Continued) Data for 11 deg Deflection

X/ δ_{NOM}	Z/ δ_{NOM}	P/P _{TS} (M=3.0)
10.31000	1.87500	2.29800
10.68500	-1.87500	2.41400
10.68500	-1.12500	2.28700
10.68500	-0.37500	2.24500
10.68500	0.00000	2.23800
10.68500	0.75000	2.25400
10.68500	1.50000	2.33900
10.68500	2.25000	2.48800
11.06000	-1.50000	2.43800
11.06000	-0.75000	2.34400
11.06000	0.00000	2.34000
11.06000	0.37500	2.33500
11.06000	1.12500	2.37500
11.06000	1.87500	2.50600
11.43500	-1.87500	2.60900
11.43500	-1.12500	2.48300
11.43500	-0.37500	2.42700
11.43500	0.00000	2.42900
11.43500	0.75000	2.44200
11.43500	1.50000	2.53600
11.81000	-1.50000	2.63000
11.81000	-0.75000	2.53900
11.81000	0.00000	2.51800
11.81000	0.37500	2.52300
11.81000	1.12500	2.57200
11.81000	1.87500	2.68800

Table 4 f (Continued) Data for 11 deg Deflection

X/ δ_{NOM}	Z/ δ_{NOM}	P/P _{TS} (M=3.0)
12.18500	-1.87500	2.80400
12.18500	-1.12500	2.68400
12.18500	-0.37500	2.62900
12.18500	0.00000	2.62400
12.18500	0.75000	2.64200
12.18500	1.50000	2.73600
12.99500	-1.50000	2.99200
12.99500	-0.75000	2.88800
12.99500	0.00000	2.87100
12.99500	0.37500	2.87500
12.99500	1.12500	2.93000
13.37000	-1.12500	3.07135
13.37000	-0.37500	2.99734
13.37000	0.00000	3.00557
13.37000	0.75000	3.02201
13.37000	1.50000	3.12891
13.74500	-1.50000	3.24300
13.74500	-0.75000	3.13100
13.74500	0.00000	3.10600
13.74500	0.37500	3.10600
13.74500	1.12500	3.17100
14.12000	-1.12500	3.31907
14.12000	-0.37500	3.25123
14.12000	0.00000	3.25637
14.12000	0.75000	3.27179
14.12000	1.50000	3.38075

Table 4 f (Continued) Data for 11 deg Deflection

X/ δ_{NOM}	Z/ δ_{NOM}	P/P _{TS} (M=3.0)
14.49500	-1.50000	3.47800
14.49500	-0.75000	3.38200
14.49500	0.00000	3.36300
14.49500	0.37500	3.36400
14.49500	1.12500	3.43900
14.87000	-1.12500	3.58735
14.87000	-0.37500	3.48970
14.87000	0.00000	3.49176
14.87000	0.75000	3.51951
15.24500	-0.75000	3.61300
15.24500	0.00000	3.58200
15.24500	0.37500	3.58000
15.24500	1.12500	3.69500
15.62000	-1.12500	3.76312
15.62000	-0.37500	3.63978
15.62000	0.00000	3.64800
15.62000	0.75000	3.67884
15.62000	-0.75000	3.64800
15.62000	0.37500	3.63000
15.62000	1.12500	3.77400
15.99500	-1.12500	2.84110
15.99500	-0.37500	3.59558
15.99500	0.00000	3.62127
15.99500	0.75000	3.43728
16.37000	-0.75000	3.02600
16.37000	0.00000	3.46500

Table 4 f (Continued) Data for 11 deg Deflection

X/ δ_{NOM}	Z/ δ_{NOM}	P/P _{TS} (M=3.0)
16.37000	0.37500	3.38500
16.37000	1.12500	2.40600
16.74500	-1.12500	2.67253
16.74500	-0.37500	3.20498
16.74500	0.00000	3.25740
16.74500	0.75000	3.02201
17.12000	-0.75000	2.97100
17.12000	0.00000	3.06700
17.12000	0.37500	3.02700
17.12000	1.12500	2.76000
17.49500	-1.12500	2.84830
17.49500	-0.37500	2.97781
17.49500	0.00000	2.97062
17.49500	0.75000	2.97576
17.87000	-0.75000	2.89100
17.87000	0.00000	2.91900
17.87000	0.37500	2.92900
17.87000	1.12500	2.92700
18.24500	-1.12500	3.07752
18.24500	-0.37500	3.00351
18.24500	0.00000	2.99426
18.24500	0.75000	3.08163

Table 4 g Data for 12 deg Deflection

X/ δ_{NOM}	Z/ δ_{NOM}	P/P _{TS} (M=3.5)	P/P _{TS} (M=4.0)
6.93500	-2.25000	1.01053	1.03100
6.93500	-1.50000	1.01404	1.04500
6.93500	-0.75000	1.00877	1.03100
6.93500	0.00000	1.01404	1.02400
6.93500	0.37500	1.01053	1.03100
6.93500	1.12500	1.00263	1.02400
6.93500	1.87500	1.00088	1.02000
6.93500	2.62500	0.97632	1.00900
7.31000	-2.62500	1.00526	1.04300
7.31000	-1.87500	1.00175	1.02800
7.31000	-1.12500	1.02193	1.08400
7.31000	-0.37500	1.02368	1.12600
7.31000	0.00000	1.03333	1.15600
7.31000	0.75000	1.03509	1.13300
7.31000	1.50000	1.01491	1.06900
7.31000	2.25000	1.00000	1.04300
7.68500	-2.25000	1.01404	1.11400
7.68500	-1.50000	1.02895	1.19400
7.68500	-0.75000	1.05877	1.34700
7.68500	0.00000	1.09035	1.42300
7.68500	0.37500	1.08684	1.40800
7.68500	1.12500	1.03596	1.28500
7.68500	1.87500	1.00614	1.14000
7.68500	2.62500	0.99912	1.10300
8.06000	-2.62500	1.37895	1.60200

Table 4 g (Continued) Data for 12 deg Deflection

X/ δ_{NOM}	Z/ δ_{NOM}	P/P _{TS} (M=3.5)	P/P _{TS} (M=4.0)
8.06000	-1.87500	1.17368	1.58000
8.06000	-1.12500	1.30614	1.76400
8.06000	-0.37500	1.43158	1.89900
8.06000	0.75000	1.40088	1.85400
8.06000	1.50000	1.24649	1.70700
8.06000	2.25000	1.20877	1.59500
8.43500	-2.25000	1.64474	1.96700
8.43500	-1.50000	1.62632	1.95600
8.43500	-0.75000	1.71491	2.00400
8.43500	0.00000	1.75614	2.05400
8.43500	0.37500	1.75439	2.04400
8.43500	1.12500	1.67632	1.98500
8.43500	1.87500	1.60702	1.94900
8.43500	2.62500	1.73421	2.03300
8.81000	-2.62500	1.96579	2.35300
8.81000	-1.87500	1.94649	2.22900
8.81000	-1.12500	1.91667	2.17600
8.81000	-0.37500	1.94298	2.21400
8.81000	0.00000	1.94649	2.20600
8.81000	0.75000	1.93596	2.20300
8.81000	1.50000	1.92982	2.19500
8.81000	2.25000	1.97895	2.29300
9.18500	-2.25000	2.15614	2.42800
9.18500	-1.50000	2.03860	2.25400
9.18500	-0.75000	2.01140	2.23600
9.18500	0.00000	2.02018	2.25000

Table 4 g (Continued) Data for 12 deg Deflection

X/ δ_{NOM}	Z/ δ_{NOM}	P/P _{TS} (M=3.5)	P/P _{TS} (M=4.0)
9.18500	0.37500	2.02193	2.23600
9.18500	1.12500	2.01842	2.22500
9.18500	1.87500	2.08333	2.29800
9.56000	-1.87500	2.24561	2.51800
9.56000	-1.12500	2.12982	2.36800
9.56000	-0.37500	2.11667	2.36000
9.56000	0.00000	2.10789	2.31900
9.56000	0.75000	2.12982	2.38300
9.56000	1.50000	2.17105	2.41300
9.56000	2.25000	2.33947	2.60800
9.56000	-2.25000	2.32719	2.57400
9.56000	-1.50000	2.15088	2.35600
9.56000	-0.75000	2.10614	2.31900
9.56000	0.37500	2.10439	2.29800
9.56000	1.12500	2.10789	2.30100
9.56000	1.87500	2.21404	2.42500
9.93500	-1.87500	2.35789	2.61900
9.93500	-1.12500	2.23684	2.48400
9.93500	-0.37500	2.22368	2.47300
9.93500	0.00000	2.21754	2.47300
9.93500	0.75000	2.22544	2.46900
9.93500	1.50000	2.28158	2.51800
9.93500	2.25000	2.48860	2.76900
10.31000	-2.25000	2.59386	2.87100
10.31000	-1.50000	2.37018	2.59200
10.31000	-0.75000	2.29561	2.49700

Table 4 g (Continued) Data for 12 deg Deflection

X/ δ_{NOM}	Z/ δ_{NOM}	P/P _{TS} (M=3.5)	P/P _{TS} (M=4.0)
10.31000	0.00000	2.29035	2.49400
10.31000	0.37500	2.28860	2.50800
10.31000	1.12500	2.31667	2.51500
10.31000	1.87500	2.43860	2.65700
10.68500	-1.87500	2.59123	2.90800
10.68500	-1.12500	2.44386	2.71700
10.68500	-0.37500	2.41228	2.68700
10.68500	0.00000	2.41579	2.69400
10.68500	0.75000	2.41228	2.68300
10.68500	1.50000	2.49649	2.76200
10.68500	2.25000	2.67368	3.00200
11.06000	-1.50000	2.58246	2.84200
11.06000	-0.75000	2.49825	2.74800
11.06000	0.37500	2.48772	2.73300
11.06000	1.12500	2.51930	2.75900
11.06000	1.87500	2.68070	2.96600
11.43500	-1.87500	2.84912	3.25300
11.43500	-1.12500	2.66404	2.97600
11.43500	-0.37500	2.62105	2.94200
11.43500	0.00000	2.62719	2.95300
11.43500	0.75000	2.62281	2.94600
11.43500	1.50000	2.72018	3.06600
11.81000	-1.50000	2.83860	3.15100
11.81000	-0.75000	2.72193	3.00200
11.81000	0.00000	2.70877	3.00200
11.81000	0.37500	2.70877	2.98700

Table 4 g (Continued) Data for 12 deg Deflection

X/ δ_{NOM}	Z/ δ_{NOM}	P/P _{TS} (M=3.5)	P/P _{TS} (M=4.0)
11.81000	1.12500	2.75526	3.02700
11.81000	1.87500	2.94649	3.28100
12.18500	-1.87500	3.10351	3.56800
12.18500	-1.12500	2.90702	3.29100
12.18500	-0.37500	2.85526	3.22700
12.18500	0.00000	2.85526	3.24600
12.18500	0.75000	2.85877	3.23100
12.18500	1.50000	2.98947	3.40300
12.99500	-1.50000	3.34649	3.87900
12.99500	-0.75000	3.16579	3.62800
12.99500	0.00000	3.16754	3.64700
12.99500	0.37500	3.15614	3.63200
12.99500	1.12500	3.23509	3.70400
13.37000	-1.12500	3.40088	3.92371
13.37000	-0.37500	3.31462	3.81616
13.37000	0.00000	3.32361	3.83107
13.37000	0.75000	3.33709	3.83107
13.37000	1.50000	3.52308	4.10259
13.74500	-1.50000	3.68246	4.34900
13.74500	-0.75000	3.47281	4.01900
13.74500	0.00000	3.47456	4.04600
13.74500	0.37500	3.45439	4.01900
13.74500	1.12500	3.54474	4.10600
14.12000	-1.12500	3.73872	4.38156
14.12000	-0.37500	3.63898	4.24421
14.12000	0.75000	3.65067	4.24421

Table 4 g (Continued) Data for 12 deg Deflection

X/ δ_{NOM}	Z/ δ_{NOM}	P/P _{TS} (M=3.5)	P/P _{TS} (M=4.0)
14.12000	1.50000	3.75220	4.40073
14.49500	-0.75000	3.81053	4.46300
14.49500	0.00000	3.81053	4.50500
14.49500	0.37500	3.78772	4.45900
14.49500	1.12500	3.91842	4.61900
14.87000	-1.12500	4.12329	4.88094
14.87000	-0.37500	3.95796	4.66905
14.87000	0.00000	3.98851	4.73933
14.87000	0.75000	3.99749	4.70206
15.24500	-0.75000	4.13158	4.92200
15.24500	0.00000	4.12982	4.95600
15.24500	0.37500	4.09561	4.89600
15.24500	1.12500	4.28070	5.10100
15.62000	-1.12500	4.30568	5.21635
15.62000	-0.37500	4.16282	5.00339
15.62000	0.00000	4.21404	5.11200
15.62000	0.75000	4.23290	5.09709
15.62000	-0.75000	4.18947	5.07000
15.62000	0.37500	4.15175	5.00900
15.62000	1.12500	4.34298	5.23300
15.99500	-1.12500	2.22293	2.51714
15.99500	-0.37500	4.04871	4.97784
15.99500	0.00000	4.15024	5.11945
15.99500	0.75000	3.62640	4.54234
16.37000	-0.75000	2.92544	3.62000
16.37000	0.00000	3.82719	4.81600

Table 4 g (Continued) Data for 12 deg Deflection

X/ δ_{NOM}	Z/ δ_{NOM}	P/P _{TS} (M=3.5)	P/P _{TS} (M=4.0)
16.37000	0.37500	3.61667	4.53900
16.37000	1.12500	2.15614	2.28100
16.74500	-1.12500	2.47900	2.70241
16.74500	-0.37500	3.25262	4.06213
16.74500	0.00000	3.37841	4.26976
16.74500	0.75000	2.92916	3.38386
17.12000	-0.75000	2.97105	3.62800
17.12000	0.37500	2.94298	3.58600
17.12000	1.12500	2.65789	3.05500
17.49500	-1.12500	2.89322	3.19753
17.49500	-0.37500	2.84470	3.32424
17.49500	0.00000	2.78270	3.27952
17.49500	0.75000	2.82942	3.43284
17.87000	-0.75000	2.81228	3.31300
17.87000	0.00000	2.67895	3.19200
17.87000	0.37500	2.66140	3.16900
17.87000	1.12500	2.68421	3.13100
18.24500	-1.12500	2.71532	3.07508
18.24500	-0.37500	2.66679	3.02716
18.24500	0.00000	2.63625	3.00480
18.24500	0.75000	2.68296	3.04952

REPORT DOCUMENTATION PAGE

*Form Approved
OMB No. 0704-0188*

Public reporting burden for this collection of information is estimated to average 1 hour per response, including the time for reviewing instructions, searching existing data sources, gathering and maintaining the data needed, and completing and reviewing the collection of information. Send comments regarding this burden estimate or any other aspect of this collection of information, including suggestions for reducing this burden, to Washington Headquarters Services, Directorate for Information Operations and Reports, 1215 Jefferson Davis Highway, Suite 1204, Arlington, VA 22202-4302, and to the Office of Management and Budget, Paperwork Reduction Project (0704-0188), Washington, DC 20503.

1. AGENCY USE ONLY (Leave blank)	2. REPORT DATE	3. REPORT TYPE AND DATES COVERED
	September 1991	Technical Memorandum
4. TITLE AND SUBTITLE		5. FUNDING NUMBERS
Interaction of Two Glancing, Crossing Shock Waves With a Turbulent Boundary-Layer at Various Mach Numbers		
6. AUTHOR(S)		WU - 505 - 62 - 31
Warren R. Hingst and Kevin E. Williams		
7. PERFORMING ORGANIZATION NAME(S) AND ADDRESS(ES)		8. PERFORMING ORGANIZATION REPORT NUMBER
National Aeronautics and Space Administration Lewis Research Center Cleveland, Ohio 44135 - 3191		E - 6566
9. SPONSORING/MONITORING AGENCY NAMES(S) AND ADDRESS(ES)		10. SPONSORING/MONITORING AGENCY REPORT NUMBER
National Aeronautics and Space Administration Washington, D.C. 20546 - 0001		NASA TM - 103740
11. SUPPLEMENTARY NOTES		
Warren R. Hingst, NASA Lewis Research Center; Kevin E. Williams, University of Washington, Seattle, Washington 98195. Responsible person, Warren R. Hingst, (216) 433 - 5923.		
12a. DISTRIBUTION/AVAILABILITY STATEMENT		12b. DISTRIBUTION CODE
Unclassified - Unlimited Subject Category 02		

13. ABSTRACT (*Maximum 200 words*)

A preliminary experimental investigation was conducted to study two crossing, glancing shock waves of equal strengths, interacting with the boundary-layer developed on a supersonic wind tunnel wall. This study was performed at several Mach numbers between 2.5 and 4.0. The shock waves were created by fins (shock generators), spanning the tunnel test section, that were set at angles varying from 4 to 12 degrees. The data acquired in this investigation are wall static pressure measurements, and qualitative information in the form of oil flow and schlieren visualizations. The principle aim of this study is two-fold. First, a fundamental understanding of the physics underlying this flow phenomena is desired. Also, a comprehensive data set is needed for computational fluid dynamic code validation. Results of this study indicate that for small shock generator angles, the boundary-layer remains attached throughout the flow field. However, with increasing shock strengths (increasing generator angles), boundary-layer separation does occur and becomes progressively more severe as the generator angles are increased further. The location of the separation, which starts well downstream of the shock crossing point, moves upstream as shock strengths are increased. At the highest generator angles, the separation appears to begin coincident with the generator leading edges and engulfs most of the area between the generators. This phenomena occurs very near the 'unstart' limit for the generators. The wall pressures at the lower generator angles are nominally consistent with the flow geometries (i.e. shock patterns) although significantly affected by the boundary-layer upstream influence. As separation occurs, the wall pressures exhibit a gradient that is mainly axial in direction in the vicinity of the separation. At the limiting conditions the wall pressure gradients are primarily in the axial direction throughout.

14. SUBJECT TERMS		15. NUMBER OF PAGES	
Shock wave interaction; Turbulent boundary layer		96	
		16. PRICE CODE	
		A05	
17. SECURITY CLASSIFICATION OF REPORT	18. SECURITY CLASSIFICATION OF THIS PAGE	19. SECURITY CLASSIFICATION OF ABSTRACT	20. LIMITATION OF ABSTRACT
Unclassified	Unclassified	Unclassified	